AE-153
UDC 536.24
621.039.534

AE-153

Measurements of Burnout Conditions for Flow of Boiling Water in Vertical 3-Rod and 7-Rod Clusters

K. M. Becker, G. Hernborg
and J. E. Flinta

AKTIEBOLAGET ATOMENERGI
STOCKHOLM, SWEDEN 1964

MEASUREMENTS OF BURNOUT CONDITIONS FOR FLOW OF BOILING WATER IN VERTICAL 3-ROD AND 7-ROD CLUSTERS

Kurt M Becker, Gunnar Hernborg and Jan E Flinta

Summary

The present report deals with measurements of burnout conditions for flow of boiling water in vertical 3-rod and 7-rod clusters.

Data were obtained in respect of heating the rods only, as well as for simultaneous uniform and non-uniform heating of the rods and the shroud. Totally, 520 runs were performed.

In the case of equal heat fluxes on all surfaces of the channels, burnout always occurred on the rods, and the data were low by a factor of about 1.3 compared with round duct data.

When only the rods were heated, the data showed very low burnout values in comparison with the results for total uniform heating and round ducts. This disagreement was explained by considering the climbing film flow model and the fact that only a fraction of the channel perimeter was heated.

For simultaneous and non-uniform heating of the rods and the shroud it was found that the shroud could be overloaded up to 50 per cent without reducing the margin of safety in respect of burnout for the rod cluster.

Finally, a correlation for predicting burnout conditions in round ducts, annuli and rod clusters has been presented. This correlation predicts the burnout heat fluxes for the present measurements and previously obtained annuli measurements within $\pm$ 5 per cent.

Printed and distributed in August 1964

List of Contents

1.0 Introduction

In recent years a research program intended to establish a method which predicts the burnout conditions for flow of boiling water in vertical channels has been in progress at the Heat Engineering Laboratory of AB Atomenergi in Sweden. The method of dealing with the problem has been to simulate the reactor fuel elements by means of test sections which are electrically heated. The first phase of the program dealt with test sections of the simplest possible geometry such as round ducts, (1, 2), and it was found that for duct diameters between 4 and 13 mm, the burnout conditions could be correlated within $\pm$ 5 per cent (3) in terms of the local values of enthalpy, heat flux, mass velocity and pressure. In order to interpret the round duct results, which were obtained at relatively high steam qualities $0.1 < x < 1.00$, the climbing film flow model was adopted.

Later, a 3-rod cluster was also studied at pressures up to 10 kg/cm^2 (4). The most important observation made during the rod cluster study was that burnout occurred at a much lower burnout steam quality compared with the round duct results of approximately the same heat flux, pressure and mass velocity. This difference was explained by considering that in the case of the round duct the total perimeter of the cross-section was heated, while as far as the rod cluster was concerned only a part of the perimeter was heated, and furthermore, that the liquid in the film flowing on the unheated shroud of the rod cluster escapes through the channel without participating in the cooling of the heated rods. It was also suggested that if the total perimeter of a channel of any cross-section is heated, burnout values of the same order of magnitude as for round ducts may be expected, except for a relatively small reduction owing to the higher shear stress in certain parts of the perimeter compared with round ducts where the wall shear stress is constant.

This assumption was verified by the experiments with an annulus reported in reference (5). The annulus was designed so that both cylinders could be heated simultaneously and also either the inner or the outer cylinder could be heated separately. It was found that in the case of equal heat fluxes on both walls, burnout always occurred

on the inner wall, and the data were slightly lower than the corresponding round duct data. However, when the annulus was heated internally only, the data showed very low burnout values in comparison with the results for dual uniform heating of the annulus and for round ducts. It was further observed that for dual non-uniform heating, the outer surface of the annulus could be overloaded from 30 to 70 per cent compared with the inner surface without reducing the margin of safety in respect of burnout for the annulus, and the highest burnout values were observed when burnout occurred simultaneously on both cylinders.

The purpose of the present paper is to extend our earlier low pressure 3-rod cluster data to pressures up to 40 kg/cm^2, and also to study the effects of heating the outer shroud of the rod clusters. Data from three different 3-rod cluster geometries will be presented as well as data obtained with a 7-rod cluster.

2.0 Apparatus

A simplified flowsheet of the loop is shown in figure 1. From the electrically heated test section the fluid passes through an aircooled condenser before entering the circulating pump, which delivers a head of 8.5 kg/cm^2 at flow rates up to 1500 liter/min. After going through the circulating pump the fluid passes through an electric 20 kW preheater and a flowmeter before it enters the test section. Between the flowmeter and the test section a throttle valve was inserted to control the mass flow rate. The major portion of the available pressure head was used between the pump and the test section inlet, which made it possible to avoid flow oscillations in the loop even at the highest exit steam qualities which during the present investigation were about 80 per cent.

The loop was designed for a maximum pressure of 50 kg/cm^2, and all parts of the loop in contact with the fluid were made of stainless steel.

The desired static pressure during operations was obtained with the help of the feed pump and the automatically controlled valve located after the condenser and a blow-off valve placed on a duct connected to the loop between the feed pump and the circulating pump.

2.1 Test Sections

The cross-sections of the rod clusters employed during the present investigation are shown in figure 2, and the most important dimensions are given in the table below.

No of Rods	Rod Diameter	Rod Clearance	Heated Length	Shroud Diameter
3	10.06 mm	6.4 mm	835 mm	40.04 mm
3	10.06 mm	6.4 mm	835 mm	35.03 mm
3	10.06 mm	6.4 mm	1670 mm	35.03 mm
7	10.06 mm	6.0 mm	1670 mm	49.95 mm

The heated length of the rods were adjusted to the correct dimensions by inserting copper cylinders in the rods and silver soldering the copper to the stainless steel. The rods penetrated to the exterior through seals filled in the flanges at the ends of the test section, as shown in figure 3, which shows the details of the downstream end of the 7-rod cluster. The power was supplied to the rods by means of heavy copper electrodes attached to the ends of the copper cylinders. Close to the seals, electrical insulators were placed between the rods and the flange. The insulators also helped to keep the rods in the correct position. For further positioning of the rods, a 1 mm x 1 mm ring and three pins were welded to the rods at two axial positions, as shown in figure 4. Three glass spacers were also used to fix the distance between the cluster and the shroud. Since burnout always occurred at the end of the heated section, and the distance between the spacer arrangement and the end was 557 mm, the influence on burnout of the spacers was negligible.

The water was supplied to the test section through two ducts of 20 mm inside diameter, 180 deg apart, which were welded to the shroud 100 mm below the heated section.

The steam water mixture left the test section through three similar ducts, 120 deg apart, welded to the shroud 100 mm above the heated section. This arrangement secured angular symmetry in the flow through the heated part of the test section.

2.2 Power Supply

The power was supplied by two direct current generators. The maximum available current from each generator was 6000 amps, and voltages ranging from 0 to 140 volts could be obtained.

2.3 Instrumentation

The flowmeter consisted of 4, 6, 10 and 12 mm ducts of 1300 mm length. The flow rate measurements were based on measuring the pressure drop over one of these ducts with a U-tube mercury manometer. The accuracy of this flowmeter system was better than 0.5 per cent in the whole range of application. A detailed description of the flowmeter with the establishment of calibration charts is given in a report by Becker and Hernborg (6).

The static pressure in the loop was measured with a precision calibrated manometer connected to the inlet of the test section. The pressure drop between the inlet and the outlet of the test section was measured with a U-tube mercury manometer.

The fluid temperature was measured before the flowmeter, before the test section and after the test section. This was accomplished by means of copper constantan thermocouples mounted in wells 150 mm deep and of 3 mm inside diameter. A precision Cambridge potentiometer was used for measuring the voltages.

The power input was determined by measuring the currents through and the voltages over the rods and the shroud.

The voltages were measured with a Goerz precision voltmeter of 1/4 per cent rated accuracy, and the currents were obtained by measuring the voltages over calibrated shunts. For these measurements a millivoltmeter with a rated accuracy of 1/4 per cent was used.

In order to protect the heated parts of the test section burnout detectors were attached to all the rods and the outer shroud. If on one of the rods an imbalance in average temperature appeared between the last two 100 mm sections below the upper electrode, the burnout detector

attached to this rod reacted and the power was shut off. This temperature imbalance appeared suddenly and indicated that burnout conditions had been reached on the cylinder to which the reacting detector was attached. It should be noted that burnout always occurred just below the end of the heated section.

For the outer shroud one of the burnout detector leads was silver soldered to the upper electrode and the other two to the outside wall of the test section. For the inner rods two of the leads were silver soldered to the inside wall of the inner cylinder and taken to the exterior through a channel drilled in one of the cylindrical copper bars elongating the inner cylinder. The third wire was attached to the upper electrode.

In order to check the accuracy of the instrumentation, heat balances for one-phase flow relating the electric heat input to the enthalpy increase of water, were taken every day before starting ordinary runs. The error of the heat balances was always less than $\pm$ 1 per cent. On the basis of the heat balances, which included measurements of heat input, inlet and outlet temperature and mass flow rate, we conclude the apparatus and instruments employed should yield satisfactory results for burnout conditions.

3.0 Method of Testing and Burnout Position

Burnout conditions in the annulus may be approached in two different ways. The most common method described in published works on the subject was during the course of a particular run, to keep the mass flow rate, pressure and inlet temperature constant, while the surface heat flux was gradually increased until burnout occurred. In the other method the surface heat flux is kept constant, but instead the mass flow rate is gradually decreased until burnout conditions are reached, as indicated by one of the burnout detectors.

During our earlier round duct measurements (1) some data were taken with both methods and identical results were obtained. Throughout the present study the constant heat flux method was employed.

Keeping pressure, inlet temperature and surface heat fluxes constant, burnout conditions were approached by decreasing the mass flow rate by small steps. Just before burnout these steps amounted to about one per cent of the flow, and one set of data was taken after each step. The last set of data obtained before the burnout detectors reacted was used to evaluate the burnout conditions. For the three-rod clusters burnout appeared simultaneously on the three rods at the circumferential positions shown in figure 4. For the seven rod cluster, the burnout detectors connected to the outer 6 rods reacted simultaneously while the seventh detector connected to the central rod remained steady, indicating that burnout occurred on the outer rods. Visual inspection of the cluster after the completion of the experimental programme revealed that burnout occurred in the areas of the cross-section indicated in figure 5.

4.0 Parameters Influencing Burnout Conditions

For a given geometry of the rod cluster, the burnout conditions are defined by the function

$$f(x,\ p,\ t_{in},\ q/A,\ \eta) = 0 \qquad (1)$$

The mass velocity, $\dot{m}/F$, is omitted since this quantity is a dependent variable determined from the heat balance below when the other quantities in equation 1 are fixed

$$\dot{m}/F = \frac{q/A \cdot L \cdot P_H}{(h_{sat} - h_{in} + x_{BO}\, h_{fg})\, F} \qquad (2)$$

The effects of mass velocity can be studied either by employing test sections of different lengths or by varying the inlet temperature. In the present report the former method has been used for the 3-rod cluster studies. In the parameter ranges which have been covered by this study, only negligible mass velocity effects can be obtained by varying the inlet temperature, and since according to the burnout correlation of Becker and Persson (2), the inlet temperature in it-

self has negligible effects, equation 1 reduces to

$$f(x, p, \dot{q}/A, \eta) = 0 \qquad (3)$$

It should be observed that equation 3 applies only to the case where equal heat fluxes are applied to the rods and the shroud and to the cases where either the rods or the shroud is heated. If different heat fluxes are applied to the rods and the shroud, equation 3 may be modified to read

$$f\left[x, p, (q/A)_i, (q/A)_o\right] \qquad (4)$$

5.0 Research Programme and Range of Variables

The maximum possible pressure at the burnout positions was 45 kg/cm^2, and the minimum pressure used during this study was 10 kg/cm^2.

The power supply system limited the maximum heat flux on the rods to 225 W/cm^2 for the 7-rod cluster. In the case of the 3-rod clusters, the seals at the ends of the test sections permitted only heat fluxes below 300 W/cm^2 to be used without being damaged by overheating.

The power supply system permitted heat fluxes up to 200 W/cm^2 to be applied on the shrouds of the 3-rod clusters. For the 7-rod cluster this value was only 100 W/cm^2, and it was therefore decided in this case to omit the measurements where also the shroud was heated.

The highest inlet sub-cooling temperature attainable with the present cooler in the loop was 180 °C for a heat flux of 100 W/cm^2. When the heat flux increased, this value decreased. In the case of the 7-rod cluster, for instance, the highest sub-cooling temperature attainable was 80 °C when the heat flux was 225 W/cm^2.

In order to avoid cavitation in the pump the lowest inlet sub-cooling temperature applied was approximately 30 °C. For an

appreciable portion of the present study only small mass velocity variations could therefore be achieved by controlling the inlet temperature.

Considering the mentioned limitations the experimental program comprised the ranges of variables given in table I.

Table I Ranges of Variables

No of Rods	Heated Length mm	Shroud Diameter mm	Pressure kg/cm^2	Rod Heat Flux W/cm^2	Shroud Heat Flux W/cm^2	Inlet Sub-Cooling ^oC	Mass Velocity kg/m^2s
3	835	40.42	10-46	88-306	0-130	59-163	48-544
3	835	35.03	16-38	100-304	0-200	34-184	86-497
3	1670	35.03	16-44	98-300	0-150	58-151	186-1330
7	1670	49.95	11-41	86-227	0	27-126	181-882

6.0 Computations

For each run the following quantities were evaluated at the burnout position, which was defined as the end of the heated surface.

1. Surface heat flux on the rods, $(q/A)_i$, W/cm^2
2. Surface heat flux on the shroud, $(q/A)_o$, W/cm^2
3. Mass velocity, $\dot{m}/F$, kg/m^2s
4. Static pressure at the burnout position, p, kg/cm^2
5. Steam quality at the burnout position, x_{BO}.

In all, 520 runs were made and the results are given in tables II and III.

7.0 Experimental Results for 3-Rod Cluster with a 40 mm Diameter Shroud

The first 3-rod cluster studied consisted of 10 mm diameter rods of 835 mm heated length mounted in a 40 mm inside diameter shroud. The relatively large shroud diameter caused the mass velocities to be rather low, so that values as low as 50 kg/m^2s were encountered when

the surface heat flux was 100 W/cm^2. At the lowest mass velocities much higher burnout values were obtained than one would expect in the light of our earlier measurements with annular geometries (5). This disagreement may be explained by assuming that a change of flow pattern takes place below a certain mass velocity, where the interfacial shear becomes too small to support a climbing liquid film on the walls.

Since the main purpose of the present study is to provide burnout data applicable to boiling water reactors operating in the film flow regime, the shroud was later on replaced by a 35 mm diameter shroud in order to increase the mass velocity.

In the present section the data obtained with the 40 mm diameter shroud will briefly be discussed. These data included measurements with internal heating, total uniform and total non-uniform heating.

7.1 Internal Heating

The results when only the rods were heated are shown in figure 6, where the burnout steam qualities are plotted versus the pressure. It can be observed that for a given pressure the burnout steam quality increases quite rapidly as the surface heat flux decreases. Especially at the lowest heat fluxes this increase is extremely large, and the burnout steam qualities obtained at 100 and 125 W/cm^2 are much higher than one would predict from our earlier measurements with annuli (5). As an explanation of this disagreement we refer to the earlier suggestion that a change of flow pattern takes place at the low mass velocities encountered during these runs. It seems that this change occurs at a mass velocity of approximately 100 kg/m^2 sec. We have no suggestion as to the model of this flow pattern, but we may refer to it as the low velocity regime.

7.2 Total Uniform Heating

Two series of runs were performed when also the outer shroud was heated. The heat fluxes employed were 100 and 125 W/cm^2, and the results are shown in figure 7 together with curves indicating the

burnout conditions for round ducts at the same heat fluxes and mass velocities. The round duct curves were obtained by means of the data in reference (1, 2). It will be observed that although the total perimeter of the rod cluster is heated, the rod cluster data are low by a factor of ≈ 1.30 compared with the round duct data. This difference is a geometrical effect caused by the influence of the cross-section geometry on the velocity and shearstress distribution in the channel.

It should also be emphasized that burnout always occurred on the rods just below the end of the heated section at the positions indicated in figure 4.

7.3 Total Non-Uniform Heating

Having observed that burnout always occurred on the rods when the channel was totally, uniformly heated, the question arose as to how much the outer shroud may be overloaded as compared with the rods before burnout occurs on the shroud.

In order to answer this question, one series of experiments was performed where the heat flux on the shroud was kept constant at 125 W/cm^2, while the heat flux of the inner rods was varied from run to run. The pressure was 31 kg/cm^2, and the results are shown in figure 8. For a rod heat flux of 83 W/cm^2, burnout occurred simultaneously on the rods and the shroud, indicating an overload ratio, $(q/A)_o/(q/A)_i$, of 1.50. When $(q/A)_i < 83$ W/cm^2 burnout occurred on the shroud only, and when $(q/A)_i > 83$ W/cm^2 the rods experienced burnout. One should also observe that the highest burnout steam qualities were obtained when burnout occurred simultaneously on all surfaces. This is in agreement with our earlier measurements with annular test sections (5).

The effects of varying the heat flux on the shroud was also studied. Figure 9 shows the results obtained when the rod heat flux was 196 W/cm^2. For all the runs in this figure burnout occurred on the inner rods. It will be observed that as the heat flux on the shroud increases the burnout conditions for the rod cluster improves.

Comparing the shape of the curve for zero heat flux on the shroud with the other curves, one observes that up to a pressure of 30 kg/cm^2 the agreement is good. At 30 kg/cm^2, however, the burnout steam quality starts to increase quite rapidly, indicating that a change of flow pattern has taken place and that we now are in the low velocity regime.

8.0 Experimental Results for 3-Rod Clusters with 35 mm Shrouds

Since it also was desirable to establish burnout measurements at higher mass velocities than at the values which were possible with the test section reported in the previous paragraph, two test sections were built, where the diameter of the outer shroud was reduced to 35 mm. The heated lengths of these clusters were 835 mm and 1670 mm, and the rod diameter and the rod clearance were as before, 10 mm and 6 mm respectively.

Experiments were performed for both test sections in respect of internal heating only as well as in respect of total uniform and total non-uniform heating. In the following paragraphs examples of the results will be shown. As regards the remaining data we refer to table II.

8.1 Internal Heating

Figure 10 shows the results obtained with the 835 mm long test section when only the inner rods were heated. It is interesting to compare these data with the previous results for the 40 mm outer shroud test section. For the highest heat fluxes of 250 and 300 W/cm^2 the agreement is excellent. However, as the heat flux decreases, and therefore likewise the mass velocity, a difference between the two sets of results appears, and for 100 W/cm^2 the burnout steam qualities obtained with the 40 mm diameter shroud are twice the values obtained with the 35 mm shroud. This large difference is considered to be a verification of the earlier discussed assumption that a change of flow pattern occurs at certain low mass velocities, where the vapour shear is too small to support the liquid film on the unheated wall.

Figure 11 shows the results for internal heating of the 1670 mm long test section, and in figure 12 a comparison between the 835 and 1670 mm test sections is given for a pressure of 30 kg/cm^2. The burnout steam quality is here plotted versus the surface heat flux. The mass velocities are also indicated in the figure. One observes that for mass velocities below $\approx$ 500 kg/m^{2}s the burnout steam quality and heat flux are independent of the mass velocity. However, above this value an increasing and inverse mass velocity effect appears. This is consistent with our earlier round duct measurements (1) where we found that for $\dot{m}/F < 500$ kg/m^{2}s the burnout steam quality is independent of the mass velocity, and that above this value the inverse mass velocity effect followed the relation $q/A \approx (\dot{m}/F)^{-0.5}$. In the present case the data are too meagre for the exponent for the mass velocity effect to be accurately determined.

The results of our efforts to study the mass velocity effect by altering the inlet temperature are shown in figure 13, where the burnout steam quality is plotted versus the mass velocity. One observes that although the mass velocity varied between 210 and 430 kg/m^{2}s no effect is visible, which is in agreement with the previous discussion. It would have been desirable to perform similar measurements at higher mass velocities. However, then the total power would also be larger and then, unfortunately, the cooler in the loop would not be able to deliver a sufficient range of sub-cooling temperatures.

One should also note that the results in figures 10 and 11, owing to the unheated shroud are rather low compared with round duct data. In figure 14 this comparison is given for the shortest rod cluster at a pressure of 30 kg/cm^2. The round duct burnout qualities were obtained by means of the correlation by Becker and Persson (2) at the same heat fluxes and mass velocities as the corresponding rod cluster points. It is observed that the round duct data are high by a factor 2 - 4 compared with the rod cluster data.

8.2 Total Uniform Heating

Figure 15 shows the results obtained for total uniform heating of the 835 mm long cluster, and a comparison with corresponding

round duct data at a pressure of 30 kg/cm^2 is given in figure 16, which indicates that the round duct data are high by a factor of about 1.3 compared with the rod cluster results. This difference can be considered to be the true effect of the cross section geometry.

8.3 Total Non-Uniform Heating

Measurements were also made with the present rod clusters using different heat fluxes on the rods and the shroud.

For the 835 mm long test section three series of runs were performed where the inner surface heat flux was kept at a certain value while different values for the heat flux on the shroud were chosen. The heat flux on the rods for these series were 100, 145 and 189 W/cm^2 respectively. The results for the last two series are given in figure 17 and 18. It will be observed that as the heat flux on the shroud increases, the burnout values for the cluster improve rapidly, and also that a significant overload of the shroud is possible. For the highest shroud heat flux the overload ratio ($q/A_o/q/A_i$) was ~ 1.25, and it should be emphasized that even at this overload of the shroud burnout occurred on the rods.

The effect of the shroud heat flux on burnout quality is more clearly demonstrated in figure 19, where the burnout quality for a pressure of 30 kg/cm^2, is plotted versus the outer surface heat flux with the inner surface heat flux as the parameter.

9.0 Results for a 7-Rod Cluster

The 7-Rod cluster consisted of 10 mm rods of 1670 mm heated length mounted in a 50 mm inside diameter tube. The rod clearance was 6 mm.

The measurements were performed in respect of heating the rods only, and heat fluxes from 88 to 227 W/cm^2 were used.

The results are shown in figure 20 and a comparison with burnout in round ducts is given in figure 21 for a pressure of 40 kg/cm^2.

Since only one 7-rod cluster geometry was studied, the influence of mass velocity could only be investigated by varying the inlet temperature. However, as previously mentioned this procedure permitted in the present case only relatively small mass velocity variations to take place. For a series of runs performed at a pressure of 30 kg/cm^2 and at a heat flux of 125 W/cm^2, a mass velocity variation from 263 to 390 kg/m^2 s was obtained when the inlet subcooling temperature changed from 35 ^{o}C to 126 ^{o}C. The results of these measurements, which are given in figure 12, show that the effect of mass velocity in the range studied is negligible.

10.0 Burnout Correlation for Rod Clusters

In the previously mentioned paper (5) concerning burnout in annuli we suggested that burnout for internally heated rod clusters could be correlated by an expression on the form

$$x_{BO} = x_{RD} \cdot f_1(\eta, q/A) \qquad (5)$$

where x_{RD} is the burnout steam quality for flow in a round duct obtained at the same mass velocity and surface heat flux, and $f_1(\eta, q/A)$ is a factor which is a function of the heat flux and the perimeter ratio, $\eta = P_H/P$. Further, it was also proposed that for accurate computations another correction factor η_2 (geometry) should be included in order to account for the fact that totally heated annuli and rod clusters may show lower values than round duct values obtained under corresponding conditions. Equation 5 then becomes

$$x_{BO} = x_{RD} \cdot f_1(\eta, q/A) \cdot \eta_2 \text{ (geometry)} \qquad (6)$$

In the present derivation it is assumed that $f_1(\eta, q/A)$ can be written $\eta \cdot \eta_1(q/A)$, where $\eta_1(q/A)$ is a function of q/A only. One then obtains

$$x_{BO} = x_{RD} \cdot \eta \cdot \eta_1 \cdot \eta_2$$

The geometrical correction factor, η_2 was determined from the burnout data obtained for totally heated annuli and rod clusters, plotting $\eta_2 = x_{BO}/x_{RD}$ versus the surface heat flux. Figure 22 shows a plot of the data obtained at a pressure of 30 kg/cm^2. Although a slight heat flux effect is visible, the data can quite accurately be correlated by putting $\eta_2 = 0.80$ for the annuli and $\eta_2 = 0.68$ for the 3-rod clusters. Unfortunately no data are available for total heating of the 7-rod cluster, but we assume that the value 0.68 is also applicable then.

Further, it is assumed that the effect of geometry is the same for internally heated test sections as for totally heated test sections, so that the values for η_2 are also valid in the former case.

The function η_1 (q/A) was now established from the experimental data by plotting η_1 (q/A) = $x_{BO}/x_{RD} \cdot \eta \cdot \eta_2$ versus the heat flux. Figure 23 shows a plot of the data obtained at a pressure of 30 kg/cm^2 and mass velocities, $\dot{m}/F > 80$ kg/m^{2}s.

Similar plots were also made for the data obtained at the pressures 20 and 35 kg/cm^2 and figure 24 shows a summary of the η_1 (q/A) functions.

The final correlation then becomes

$$x_{BO} = x_{RD} \cdot \eta \cdot \eta_1 \cdot \eta_2 \qquad (7)$$

where η_2 is equal to 0.8 for annuli and 0.68 for 3 and 7-rod clusters, η_1 should be taken from the curves in figure 24 and η is the ratio of heated to total perimeter. For the evaluation of x_{RD} we recommend the correlation by Becker and Persson (2) be used.

However, one should note that the solution obtained from equation 7 must satisfy the heat balance equation for the test section, which was written

$$\dot{m}/F = \frac{q/A \cdot L \cdot P_H}{(h_{sat} - h_{in} + x_{BO}\, h_{fg})\, F} \qquad (2)$$

Predicting burnout conditions therefore involves to find a set of values, which satisfies equations 2 and 7. This is in general only possible by leaving two of the variables unspecified and determining these variables simultaneously. For the present data the burnout steam quality, x_{BO}, and the burnout heat flux, q/A , were predicted in this manner.

In figure 25 the predicted burnout steam qualities for the measurements obtained at pressures of 30 $\pm$ 2.5 kg/cm^2 are plotted versus the measured values, and in figure 26 the same comparison is given in terms of the surface heat fluxes. Our data for annular geometries (5, 7) are also included in the figures. Tables IV, V and VI give the data together with the predicted values. One should observe that the rather limited space in certain areas of figure 26 permitted only about 50 per cent of the points to be included. The agreement between predictions and measurements is excellent, the scatter in terms of q/A being less than $\pm$ 5 per cent and the RMS error is equal to 3.15 per cent.

The correlation was also tested by means of the data obtained at the pressures of 20 and 35 kg/cm^2. All runs for pressures 20 $\pm$ 2.5 kg/cm^2 and 35 $\pm$ 2.5 kg/cm^2 obtained with annuli and rod clusters were included, and it appeared that in terms of the burnout heat flux, q/A, the data were correlated within $\pm$ 5 per cent, taking η_1 from figure 23 and using the same values for η_2 as were earlier used for correlating the 30 kg/cm^2 data.

Figure 27 shows the comparison for the data obtained at the pressure of 20 kg/cm^2.

The correlation was finally checked by means of data obtained at the Atomic Power Division of ASEA in Västerås, Sweden (8). These measurements were obtained in an annulus with an inner diameter of 13.9 mm, an outside diameter of 34.5 mm and a heated length of 4220 mm. One should observe that this geometry differs considerably from the geometries employed for the establishment of the present correlation.

In table VII the ASEA data are given together with the predicted values for burnout steam quality, enthalpy and burnout heat flux, and in figure 28 the measured burnout heat fluxes are plotted versus the predicted values. The agreement between predictions and measure-

ments is excellent, as the RMS error is 2.53 per cent and the maximum scatter is except for a few points within $\pm$ 5 per cent.

One should observe that the correlation is also applicable in the case of totally and uniformly heated channels, where $\eta \cdot \eta_1 = 1.0$ and for round ducts were $\eta \cdot \eta_1 \cdot \eta_2 = 1.0$. In the latter case equation 7 reduces to the round duct correlation. Considering the fact that also our round duct measurements were correlated within $\pm$ 5 per cent (3), we conclude that a correlation has been derived, which predicts within $\pm$ 5 per cent *all* our burnout measurements, or more than 5000 data points. These points cover the geometries of round ducts, annuli, 3-rod and 7-rod clusters, and the cases of internal as well as total uniform heating are included.

Nomenclature

Symbol	Definition	Units
d_i	Diameter of Rods	m
d_o	Diameter of Shroud	m
F	Channel cross-section	m^2
h_{BO}	Burnout Enthalpy	KJ/kg
h_{fg}	Latent heat of evaporation	KJ/kg
h_{in}	Inlet enthalpy	KJ/kg
h_{sat}	Saturation enthalpy	KJ/kg
L	Heated length	m
$\dot{m}$	Mass flow rate	kg/s
$\dot{m}/F$	Mass velocity	kg/m^2s
$(q/A)_i$	Surface heat flux on rods	W/cm^2
$(q/A)_o$	Surface heat flux on shroud	W/cm^2
p	Pressure	kg/cm^2
P	Perimeter	m
P_H	Heated perimeter	m
t	Temperature	^oC
t_{in}	Inlet temperature	^oC
Δt_{sub}	Inlet sub-cooling temperature	^oC
x_{BO}	Burnout steam quality	Dimensionless
x_{RD}	Burnout quality for round duct	Dimensionless
η	Perimeter ratio	Dimensionless
η_1	Correction factor	Dimensionless
η_2	Correction factor	Dimensionless

References

1. Becker K M,
Measurements of Burnout Conditions for Flow of Boiling Water in Vertical Round Ducts (Part 1 and 2), Reports AE-87 and AE-114, Aktiebolaget Atomenergi, Studsvik, Sweden, 1962 and 1963

2. Becker K M and Persson P,
An Analysis of Burnout Conditions for Flow of Boiling Water in Vertical Round Ducts, ASME-Paper No. 63-WA-51

3. Becker K M and Persson P,
Authors Closure for ASME-Paper No. 63-WA-51. To be published in the Journal of Heat Transfer.

4. Becker K M,
Burnout Conditions for Flow of Boiling Water in Vertical Rod Clusters, AICHE-Journal, March 1963

5. Becker K M and Hernborg G,
Measurements of Burnout Conditions for Flow of Boiling Water in a Vertical Annulus, ASME-Paper No. 63-HT-25

6. Becker K M and Hernborg G,
Development and Description of a Novel Method for Accurate Measurements of Fluid Flow Rates, Report RPL-102, Aktiebolaget Atomenergi, Studsvik, Sweden, Internal report 1961

7. Becker K M and Hernborg G,
Measurements of Burnout Conditions for Flow of Boiling Water in Vertical Annuli (Part 2), Report in Progress, Aktiebolaget Atomenergi, Studsvik, Sweden

8. Becker K M, Bengtsson J and Hernborg G,
Static Burnout Measurements in a Vertical Annulus, Report in Progress, AB Atomenergi, Studsvik, Sweden, and Atomic Power Division, ASEA, Västerås, Sweden.

Table II. Burnout in 3-Rod Clusters

Run	d_i	d_o	s	L	p	Δt_{sub}	$\dot{m}/F$	$(q/A)_i$	$(q/A)_o$	x_{BO}	h_{BO}
No	mm	mm	mm	mm	kg/cm^2	°C	kg/m^{2}s	W/cm^2	W/cm^2		kJ/kg
1	10.01	40.42	6	835	30.0	131.0	97.4	97.0	102.0	0.683	2226
2	10.01	40.42	6	835	31.0	142.0	96.4	95.6	102.0	0.664	2196
3	10.01	40.42	6	835	35.0	140.0	102.2	95.8	103.5	0.627	2145
4	10.01	40.42	6	835	35.0	144.0	96.4	95.8	103.5	0.677	2233
5	10.01	40.42	6	835	35.0	150.0	97.4	95.8	102.5	0.647	2179
6	10.01	40.42	6	835	41.0	151.0	95.5	97.2	104.4	0.694	2280
7	10.01	40.42	6	835	41.0	149.0	96.4	97.3	104.4	0.689	2272
8	10.01	40.42	6	835	26.0	98.0	114.6	97.0	105.0	0.614	2085
9	10.01	40.42	6	835	26.0	98.0	114.6	97.0	105.0	0.614	2085
10	10.01	40.42	6	835	21.0	94.0	115.5	97.2	104.0	0.601	2035
11	10.01	40.42	6	835	21.0	93.0	115.5	97.2	103.5	0.601	2035
12	10.01	40.42	6	835	16.0	77.0	118.4	97.0	103.0	0.600	2002
13	10.01	40.42	6	835	16.0	75.0	120.3	97.0	103.0	0.592	1987
14	10.01	40.42	6	835	31.0	116.0	99.3	94.9	100.2	0.681	2226
15	10.01	40.42	6	835	31.0	110.0	103.1	100.5	107.6	0.723	2301
16	10.01	40.42	6	835	21.0	92.0	110.8	95.6	104.9	0.639	2107
17	10.01	40.42	6	835	21.0	98.0	111.7	95.6	104.5	0.617	2065
18	10.01	40.42	6	835	15.5	86.0	113.6	95.1	104.5	0.612	2022
19	10.01	40.42	6	835	16.5	85.0	116.5	95.1	104.5	0.597	2000
20	10.01	40.42	6	835	36.0	129.0	100.3	98.0	106.4	0.700	2276
21	10.01	40.42	6	835	36.0	134.0	102.2	98.0	105.5	0.664	2213
22	10.01	40.42	6	835	22.0	125.0	102.2	97.7	107.0	0.660	2152
23	10.01	40.42	6	835	23.0	126.0	99.3	97.7	106.4	0.685	2203
24	10.01	40.42	6	835	21.0	122.0	101.2	97.3	105.5	0.664	2154
25	10.01	40.42	6	835	30.5	103.0	132.3	122.0	125.9	0.664	2194
26	10.01	40.42	6	835	30.5	103.0	133.7	122.0	129.1	0.668	2201
27	10.01	40.42	6	835	35.5	130.0	127.8	121.4	125.2	0.638	2166
28	10.01	40.42	6	835	35.5	128.0	127.8	120.8	126.4	0.646	2180
29	10.01	40.42	6	835	26.0	111.0	136.4	120.6	130.0	0.620	2097
30	10.01	40.42	6	835	26.0	115.0	136.4	120.6	128.5	0.605	2069
31	10.01	40.42	6	835	21.0	100.0	137.3	119.8	128.9	0.621	2073
32	10.01	40.42	6	835	20.0	99.0	140.2	119.8	125.7	0.591	2010
33	10.01	40.42	6	835	20.0	95.0	138.5	119.8	124.8	0.606	2039
34	10.01	40.42	6	835	41.0	143.0	125.1	121.2	127.0	0.646	2197
35	10.01	40.42	6	835	41.0	148.0	128.0	121.2	128.0	0.615	2145
36	10.01	40.42	6	835	31.0	104.0	139.4	125.5	129.5	0.641	2154
37	10.01	40.42	6	835	31.0	85.0	135.6	124.5	129.7	0.709	2276
38	10.01	40.42	6	835	11.0	128.0	48.0	88.2	0	0.422	1607
39	10.01	40.42	6	835	10.5	134.0	66.0	100.5	0	0.291	1338
40	10.01	40.42	6	835	14.7	143.0	57.2	102.0	0	0.378	1560
41	10.01	40.42	6	835	18.1	152.0	61.4	102.0	0	0.315	1472
42	10.01	40.42	6	835	22.2	163.0	42.9	100.9	0	0.573	1989
43	10.01	40.42	6	835	25.7	160.0	38.4	101.6	0	0.707	2254
44	10.01	40.42	6	835	29.5	161.0	34.1	101.3	0	0.850	2525
45	10.01	40.42	6	835	10.3	124.0	68.8	99.4	0	0.282	1316
46	10.01	40.42	6	835	14.0	137.0	61.1	101.4	0	0.342	1482
47	10.01	40.42	6	835	17.8	146.0	47.8	100.9	0	0.504	1831
48	10.01	40.42	6	835	22.8	158.0	34.4	100.5	0	0.815	2444
49	10.01	40.42	6	835	17.5	63.0	112.8	127.3	0	0.297	1431
50	10.01	40.42	6	835	17.0	76.0	105.2	128.4	0	0.304	1440
51	10.01	40.42	6	835	23.0	97.0	87.0	128.4	0	0.365	1608
52	10.01	40.42	6	835	22.0	101.0	88.5	128.4	0	0.345	1563
53	10.01	40.42	6	835	26.0	110.0	76.5	129.2	0	0.426	1741
54	10.01	40.42	6	835	27.0	112.0	71.7	129.2	0	0.470	1826
55	10.01	40.42	6	835	33.0	136.0	66.9	129.2	0	0.476	1870
56	10.01	40.42	6	835	36.5	151.0	61.2	127.5	0	0.510	1947
57	10.01	40.42	6	835	37.5	153.0	47.9	125.3	0	0.738	2346
58	10.01	40.42	6	835	37.0	145.0	51.3	124.3	0	0.672	2230
59	10.01	40.42	6	835	39.0	148.0	50.3	124.3	0	0.690	2267
60	10.01	40.42	6	835	44.0	155.0	48.0	123.9	0	0.731	2350

Table II. Burnout in 3-Rod Clusters

Run No	d_i mm	d_o mm	s mm	L mm	p kg/cm^2	Δt_{sub} °C	$\dot{m}/F$ kg/m^{2}s	$(q/A)_i$ W/cm^2	$(q/A)_o$ W/cm^2	x_{BO}	h_{BO} kJ/kg
61	10.01	40.42	6	835	41.0	151.0	48.5	123.9	0	0.723	2329
62	10.01	40.42	6	835	43.0	154.0	48.2	123.2	0	0.720	2330
63	10.01	40.42	6	835	36.0	143.0	55.5	122.0	0	0.578	2063
64	10.01	40.42	6	835	36.0	143.0	55.4	123.9	0	0.594	2092
65	10.01	40.42	6	835	31.0	135.0	60.4	123.2	0	0.522	1942
66	10.01	40.42	6	835	25.0	85.0	185.0	193.2	0	0.218	1352
67	10.01	40.42	6	835	24.5	90.0	188.3	193.2	0	0.199	1313
68	10.01	40.42	6	835	21.5	94.0	180.0	193.2	0	0.209	1303
69	10.01	40.42	6	835	21.5	98.0	180.0	193.2	0	0.200	1286
70	10.01	40.42	6	835	26.5	113.0	158.3	193.2	0	0.227	1381
71	10.01	40.42	6	835	26.5	109.0	159.5	193.2	0	0.232	1390
72	10.01	40.42	6	835	31.5	119.0	145.5	195.4	0	0.265	1487
73	10.01	40.42	6	835	32.0	116.0	144.5	195.2	0	0.276	1509
74	10.01	40.42	6	835	36.0	125.0	134.3	195.2	0	0.299	1577
75	10.01	40.42	6	835	36.5	129.0	134.3	194.4	0	0.287	1559
76	10.01	40.42	6	835	42.0	139.0	120.0	192.7	0	0.334	1671
77	10 01	40.42	6	835	39.0	140.0	122.2	192.2	0	0.316	1624
78	10.01	40.42	6	835	42.5	145.0	115.0	192.2	0	0.348	1698
79	10.01	40.42	6	835	45.0	151.0	103.0	192.2	0	0.422	1834
80	10.01	40.42	6	835	43.0	149.0	109.0	191.7	0	0.378	1751
81	10.01	40.42	6	835	38.5	142.0	118.0	191.2	0	0.332	1648
82	10.01	40.42	6	835	24.5	59.0	275.2	246.8	0	0.219	1348
83	10.01	40.42	6	835	19.5	60.0	329.0	250.2	0	0.160	1190
84	10.01	40.42	6	835	22.5	80.0	279.3	249.3	0	0.168	1236
85	10.01	40.42	6	835	20.0	73.0	320.1	249.3	0	0.138	1154
86	10.01	40.42	6	835	26.0	91.0	256.0	249.3	0	0.176	1283
87	10.01	40.42	6	835	28.5	95.0	242.0	249.3	0	0.190	1329
88	10.01	40.42	6	835	35.0	106.0	212.0	249.3	0	0.225	1441
89	10.01	40.42	6	835	31.0	102.0	223.0	250.4	0	0.212	1389
90	10.01	40.42	6	835	37.0	117.0	210.0	252.1	0	0.209	1427
91	10.01	40.42	6	835	41.5	122.	194.0	251.0	0	0.237	1504
92	10.01	40.42	6	835	40.0	122.0	186.3	251.0	0	0.261	1535
93	10.01	40.42	6	835	46.5	131.0	172.0	249.9	0	0.286	1615
94	10.01	40.42	6	835	44.0	130.0	176.0	249.9	0	0.274	1580
95	10.01	40.42	6	835	21.5	64.0	338.0	244.8	0	0.136	1167
96	10.01	40.42	6	835	26.0	81.0	268.5	246.2	0	0.176	1282
97	10.01	40.42	6	835	33.0	103.0	231.5	248.2	0	0.188	1361
98	10.01	40.42	6	835	33.0	103.0	236.2	248.2	0	0.179	1345
99	10.01	40.42	6	835	35.5	117.0	223.0	256.1	0	0.187	1378
100	10.01	40.42	6	835	37.0	118.0	210.0	252.1	0	0.207	1423
101	10.01	40.42	6	835	35.0	107.0	216.0	249.3	0	0.214	1420
102	10.01	40.42	6	835	19.5	67.0	497.3	298.3	0	0.080	1039
103	10.01	40.42	6	835	25.5	89.0	340.1	298.3	0	0.141	1214
104	10.01	40.42	6	835	27.5	76.0	379.0	300.1	0	0.136	1223
105	10.01	40.42	6	835	32.5	86.0	331.0	300.8	0	0.160	1307
106	10.01	40.42	6	835	31.0	88.0	351.7	301.4	0	0.134	1248
107	10.01	40.42	6	835	36.5	97.0	310.2	299.8	0	0.157	1332
108	10.01	40.42	6	835	41.0	108.0	277.1	299.2	0	0.178	1399
109	10.01	40.42	6	835	46.0	114.0	252.5	299.8	0	0.209	1484
110	10.01	40.42	6	835	44.5	113.0	269.3	299.8	0	0.179	1424
111	10.01	40.42	6	835	38.0	103.0	301.0	298.2	0	0.152	1335
112	10.01	40.42	6	835	44.5	113.0	270.3	297.7	0	0.174	1415
113	10.01	40.42	6	835	37.8	103.0	313.6	298.6	0	0.136	1304
114	10.01	40.42	6	835	39.0	103.	298.1	299.8	0	0.158	1352
115	10.01	40.42	6	835	34.0	94.0	326.0	301.4	0	0.147	1296
116	10.01	40.42	6	835	30.5	87.0	359.2	302.6	0	0.130	1238
117	10.01	40.42	6	835	29.5	82.0	376.4	302.0	0	0.125	1221
118	10.01	40.42	6	835	26.5	74.0	418.0	303.2	0	0.113	1172
119	10.01	40.42	6	835	27.5	75.0	372.1	303.2	0	0.148	1244
120	10.01	40.42	6	835	24.0	66.0	432.9	304.5	0	0.123	1168

Table II. Burnout in 3-Rod Clusters

Run	d_i	d_o	s	L	p	Δt_{sub}	$\dot{m}/F$	$(q/A)_i$	$(q/A)_o$	x_{BO}	h_{BO}
No	mm	mm	mm	mm	kg/cm^2	°C	kg/m^{2}s	W/cm^2	W/cm^2		kJ/kg
121	10.01	40.42	6	835	20.0	55.0	523.5	306.3	0	0.101	1085
122	10.01	40.42	6	835	19.5	53.0	544.1	305.1	0	0.096	1070
123	10.01	40.42	6	835	19.5	67.0	497.1	298.3	0	0.080	1040
124	10.01	40.42	6	835	27.5	76.0	388.8	300.1	0	0.127	1208
125	10.01	40.42	6	835	32.5	89.0	338.3	300.8	0	0.144	1280
126	10.01	40.42	6	835	31.0	89.0	358.6	301.4	0	0.124	1232
127	10.01	40.42	6	835	27.5	73.0	382.0	303.2	0	0.144	1237
128	10.01	40.42	6	835	31.0	125.0	162.3	195.6	37.4	0.324	1588
129	10.01	40.42	6	835	31.0	136.0	161.4	192.7	37.3	0.294	1535
130	10.01	40.42	6	835	31.0	140.0	160.4	192.6	36.6	0.286	1521
131	10.01	40.42	6	835	36.0	137.0	160.4	199.1	36.0	0.310	1595
132	10.01	40.42	6	835	36.0	139.0	162.3	198.6	36.2	0.297	1572
133	10.01	40.42	6	835	41.0	150.0	156.6	198.6	36.0	0.295	1598
134	10.01	40.42	6	835	41.0	149.0	157.4	198.6	35.4	0.291	1593
135	10.01	40.42	6	835	26.0	110.0	188.3	200.7	36.2	0.277	1467
136	10.01	40.42	6	835	26.0	110.0	189.7	201.2	36.7	0.275	1464
137	10.01	40.42	6	835	21.0	90.0	219.8	201.2	37.4	0.246	1368
138	10.01	40.42	6	835	21.0	92.0	220.6	201.2	36.2	0.237	1351
139	10.01	40.42	6	835	16.0	75.0	245.4	201.2	37.4	0.229	1284
140	10.01	40.42	6	835	16.0	81.0	237.8	200.7	38.1	0.229	1285
141	10.01	40.42	6	835	30.0	98.0	205.3	197.6	74.3	0.359	1644
142	10.01	40.42	6	835	30.0	104.0	208.2	193.1	78.1	0.337	1606
143	10.01	40.42	6	835	35.0	123.0	188.1	194.1	79.4	0.367	1689
144	10.01	40.42	6	835	35.0	116.0	189.1	195.4	80.3	0.386	1722
145	10.01	40.42	6	835	41.0	138.0	175.7	194.1	81.1	0.389	1760
146	10.01	40.42	6	835	41.0	137.0	175.7	195.4	80.9	0.394	1768
147	10.01	40.42	6	835	26.0	99.0	218.7	193.1	81.7	0.327	1559
148	10.01	40.42	6	835	26.0	108.0	206.3	193.1	81.1	0.339	1581
149	10.01	40.42	6	835	26.0	110.0	205.3	195.6	81.7	0.344	1590
150	10.01	40.42	6	835	21.0	96.0	220.6	195.6	78.9	0.322	1511
151	10.01	40.42	6	835	21.0	91.0	226.3	199.7	78.9	0.327	1520
152	10.01	40.42	6	835	30.0	109.0	218.7	197.6	120.0	0.414	1743
153	10.01	40.42	6	835	31.0	124.0	100.3	78.2	125.9*	0.728	2310
154	10.01	40.42	6	835	31.0	122.0	102.2	78.7	125.9*	0.715	2288
155	10.01	40.42	6	835	31.0	125.0	101.2	83.1*	125.9*	0.737	2326
156	10.01	40.42	6	835	31.0	124.0	101.2	83.1*	125.9*	0.739	2330
157	10.01	40.42	6	835	31.0	124.0	101.2	88.7	125.3	0.759	2366
158	10.01	40.42	6	835	31.0	119.0	105.0	88.7	125.3	0.732	2317
159	10.01	40.42	6	835	29.0	117.0	115.4	96.6	125.3	0.668	2195
160	10.01	40.42	6	835	35.0	134.0	111.7	96.3	125.3	0.672	2224
161	10.06	35.03	6	835	28.5	90.0	149.6	104.3	102.9	0.676	2208
162	10.06	35.03	6	835	26.0	83.0	151.0	105.2	101.8	0.676	2198
163	10.06	35.03	6	835	31.0	97.0	146.9	105.0	101.8	0.680	2224
164	10.06	35.03	6	835	31.0	91.0	149.6	102.7	103.0	0.673	2212
165	10.06	35.03	6	835	31.0	88.0	151.0	104.1	104.7	0.686	2235
166	10.06	35.03	6	835	37.5	100.0	144.3	105.0	102.7	0.708	2295
167	10.06	35.03	6	835	36.0	96.0	155.4	105.0	103.1	0.647	2184
168	10.06	35.03	6	835	21.5	59.0	167.9	103.6	104.1	0.636	2103
169	10.06	35.03	6	835	21.0	61.0	163.8	105.1	103.9	0.653	2134
170	10.06	35.03	6	835	16.0	49.0	167.9	103.2	102.5	0.634	2068
171	10.06	35.03	6	835	16.0	49.0	162.4	102.9	103.1	0.660	2119
172	10.06	35.03	6	835	26.0	78.0	238.1	143.0	143.6	0.581	2025
173	10.06	35.03	6	835	26.0	85.0	235.4	142.2	143.6	0.572	2008
174	10.06	35.03	6	835	31.0	96.0	229.9	141.3	147.4	0.584	2053
175	10.06	35.03	6	835	31.0	98.0	225.7	140.9	146.5	0.591	2065
176	10.06	35.03	6	835	36.0	105.0	221.6	141.7	149.6	0.611	2121
177	10.06	35.03	6	835	36.0	108.0	223.0	141.3	148.4	0.593	2090
178	10.06	35.03	6	835	21.0	66.0	256.0	143.9	145.0	0.550	1940
179	10.06	35.03	6	835	21.0	62.0	256.0	143.5	147.6	0.565	1968
180	10.06	35.03	6	835	16.0	51.0	267.0	142.2	148.3	0.547	1900

Table II. Burnout in 3-Rod Clusters

Run	d_i	d_o	s	L	p	Δt_{sub}	$\dot{m}/F$	$(q/A)_i$	$(q/A)_o$	x_{BO}	h_{BO}
No	mm	mm	mm	mm	kg/cm^2	°C	kg/m^{2}s	W/cm^2	W/cm^2		kJ/kg
181	10.06	35.03	6	835	16.0	58.0	269.8	142.2	150.9	0.531	1869
182	10.06	35.03	6	835	32.5	104.0	91.9	103.6	0	0.425	1778
183	10.06	35.03	6	835	29.0	96.0	101.9	103.2	0	0.371	1659
184	10.06	35.03	6	835	28.0	92.0	104.5	102.1	0	0.358	1629
185	10.06	35.03	6	835	25.5	81.0	109.3	101.6	0	0.352	1603
186	10.06	35.03	6	835	22.6	69.0	117.7	101.6	0	0.338	1554
187	10.06	35.03	6	835	21.8	62.0	124.3	101.2	0	0.325	1523
188	10.06	35.03	6	835	27.0	84.0	104.9	100.5	0	0.364	1634
189	10.06	35.03	6	835	30.5	83.0	105.4	100.0	0	0.364	1657
190	10.06	35.03	6	835	31.8	89.0	99.2	100.0	0	0.387	1706
191	10.06	35.03	6	835	36.5	97.0	91.8	100.0	0	0.422	1794
192	10.06	35.03	6	835	35.5	92.0	92.5	100.0	0	0.428	1799
193	10.06	35.03	6	835	36.0	99.0	88.4	100.3	0	0.445	1831
194	10.06	35.03	6	835	37.0	100.0	86.4	100.3	0	0.460	1863
195	10.06	35.03	6	835	22.0	58.0	217.5	150.4	0	0.262	1408
196	10.06	35.03	6	835	20.8	37.0	251.9	151.2	0	0.257	1388
197	10.06	35.03	6	835	26.0	72.0	203.0	151.7	0	0.265	1447
198	10.06	35.03	6	835	26.0	62.0	192.0	151.7	0	0.315	1537
199	10.06	35.03	6	835	31.0	88.0	181.7	151.9	0	0.283	1516
200	10.06	35.03	6	835	31.0	83.0	185.8	151.7	0	0.284	1516
201	10.06	35.03	6	835	34.5	101.0	166.6	150.6	0	0.296	1561
202	10.06	35.03	6	835	37.5	104.0	169.3	151.0	0	0.282	1555
203	10.06	35.03	6	835	36.0	96.0	169.3	151.5	0	0.303	1583
204	10.06	35.03	6	835	31.0	91.0	181.7	152.6	0	0.279	1508
205	10.06	35.03	6	835	26.0	70.0	212.7	152.6	0	0.252	1423
206	10.06	35.03	6	835	26.0	62.0	222.5	151.7	0	0.250	1418
207	10.06	35.03	6	835	16.0	72.0	220.2	150.4	0	0.222	1271
208	10.06	35.03	6	835	22.0	73.0	291.8	194.8	0	0.214	1318
209	10.06	35.03	6	835	22.0	84.0	279.4	194.8	0	0.206	1303
210	10.06	35.03	6	835	25.0	86.0	269.8	194.8	0	0.217	1350
211	10.06	35.03	6	835	28.0	89.0	273.9	196.3	0	0.222	1383
212	10.06	35.03	6	835	31.0	81.0	273.9	196.3	0	0.227	1416
213	10.06	35.03	6	835	32.5	96.0	245.0	195.7	0	0.242	1453
214	10.06	35.03	6	835	38.0	108.0	228.5	195.7	0	0.250	1503
215	10.06	35.03	6	835	35.5	102.0	235.4	195.7	0	0.248	1484
216	10.06	35.03	6	835	30.0	100.0	249.1	195.7	0	0.224	1403
217	10.06	35.03	6	835	37.5	119.0	213.3	196.7	0	0.264	1525
218	10.06	35.03	6	835	36.0	109.0	224.4	197.2	0	0.261	1510
219	10.06	35.03	6	835	34.5	109.0	228.5	197.2	0	0.251	1482
220	10.06	35.03	6	835	17.0	79.0	340.0	198.8	0	0.152	1147
221	10.06	35.03	6	835	17.0	83.0	333.1	197.3	0	0.147	1139
222	10.06	35.03	6	835	31.0	111.0	301.0	234.0	0	0.193	1355
223	10.06	35.03	6	835	31.0	117.0	297.0	234.0	0	0.186	1341
224	10.06	35.03	6	835	31.0	127.0	301.0	234.0	0	0.179	1330
225	10.06	35.03	6	835	31.0	110.0	325.0	240.9	0	0.174	1320
226	10.06	35.03	6	835	31.0	104.0	331.0	242.5	0	0.182	1336
227	10.06	35.03	6	835	31.0	184.0	213.0	234.1	0	0.223	1407
228	10.06	35.03	6	835	31.0	171.0	240.0	240.0	0	0.191	1352
229	10.06	35.03	6	835	31.0	154.0	261.0	242.1	0	0.186	1342
230	10.06	35.03	6	835	31.0	140.0	264.0	242.1	0	0.211	1387
231	10.06	35.03	6	835	31.0	126.0	285.0	238.2	0	0.194	1356
232	10.06	35.03	6	835	31.0	121.0	287.0	240.2	0	0.206	1378
233	10.06	35.03	6	835	31.0	63.0	406.0	245.2	0	0.202	1371
234	10.06	35.03	6	835	31.0	57.0	420.0	245.2	0	0.205	1376
235	10.06	35.03	6	835	31.0	58.0	424.0	242.8	0	0.208	1382
236	10.06	35.03	6	835	31.0	101.0	468.0	304.0	0	0.139	1258
237	10.06	35.03	6	835	29.5	92.0	497.0	303.0	0	0.136	1240
238	10.06	35.03	6	835	31.0	93.0	492.0	297.9	0	0.131	1243
239	10.06	35.03	6	835	21.5	67.0	165.2	100.0	123.2	0.695	2215
240	10.06	35.03	6	835	21.5	65.0	150.0	99.6	121.7	0.778	2371

Table II. Burnout in 3-Rod Clusters

Run	d_i	d_o	s	L	p	Δt_{sub}	$\dot{m}/F$	$(q/A)_i$	$(q/A)_o$	x_{BO}	h_{BO}
No	mm	mm	mm	mm	kg/cm^2	°C	kg/m^{2}s	W/cm^2	W/cm^2		kJ/kg
241	10.06	35.03	6	835	26.5	76.0	150.0	102.0	121.4	0.778	2386
242	10.06	35.03	6	835	26.5	78.0	150.0	101.2	120.2	0.764	2361
243	10.06	35.03	6	835	32.0	89.0	152.5	100.7	122.3	0.745	2344
244	10.06	35.03	6	835	31.0	88.0	151.0	100.7	122.7	0.757	2361
245	10.06	35.03	6	835	36.0	100.0	152.5	102.5	123.2	0.740	2346
246	10.06	35.03	6	835	36.0	98.0	151.0	103.2	123.2	0.758	2377
247	10.06	35.03	6	835	16.0	59.0	165.2	100.7	122.3	0.694	2184
248	10.06	35.03	6	835	16.0	58.0	167.9	100.7	122.8	0.685	2166
249	10.06	35.03	6	835	31.0	68.0	201.0	144.5	48.1	0.430	1778
250	10.06	35.03	6	835	31.0	80.0	192.7	147.1	47.2	0.432	1782
251	10.06	35.03	6	835	36.0	91.0	187.2	146.9	48.1	0.433	1809
252	10.06	35.03	6	835	36.0	97.0	181.7	146.9	47.9	0.438	1818
253	10.06	35.03	6	835	26.0	74.0	199.6	146.0	49.0	0.421	1732
254	10.06	35.03	6	835	26.0	72.0	203.7	147.8	47.9	0.415	1721
255	10.06	35.03	6	835	21.0	61.0	220.2	148.6	46.8	0.388	1636
256	10.06	35.03	6	835	21.0	61.0	224.4	148.6	46.8	0.378	1617
257	10.06	35.03	6	835	16.0	34.0	260.1	147.8	46.8	0.359	1537
258	10.06	35.03	6	835	15.5	36.0	260.1	148.2	47.4	0.356	1526
259	10.06	35.03	6	835	26.0	75.0	221.6	145.4	102.2	0.523	1919
260	10.06	35.03	6	835	26.0	81.0	216.1	144.3	102.2	0.524	1920
261	10.06	35.03	6	835	31.0	95.0	205.1	142.2	101.1	0.529	1955
262	10.06	35.03	6	835	31.0	94.0	207.8	141.3	101.4	0.520	1939
263	10.06	35.03	6	835	35.5	107.0	201.0	144.7	99.6	0.525	1969
264	10.06	35.03	6	835	35.5	108.0	201.0	144.7	100.7	0.527	1972
265	10.06	35.03	6	835	21.0	78.0	220.2	143.9	99.9	0.500	1846
266	10.06	35.03	6	835	21.0	78.0	224.4	143.0	99.9	0.485	1817
267	10.06	35.03	6	835	16.0	57.0	238.1	141.8	100.7	0.482	1775
268	10.06	35.03	6	835	16.5	62.0	240.9	141.3	100.7	0.464	1744
269	10.06	35.03	6	835	26.0	80.0	230.6	143.5	175.0	0.697	2237
270	10.06	35.03	6	835	26.0	81.0	230.1	143.0	174.3	0.694	2230
271	10.06	35.03	6	835	31.0	91.0	236.1	142.2	176.7	0.664	2196
272	10.06	35.03	6	835	31.0	96.0	235.9	143.9	177.4	0.660	2188
273	10.06	35.03	6	835	36.5	110.0	226.7	141.7	178.5	0.673	2230
274	10.06	35.03	6	835	36.5	111.0	226.4	141.5	178.9	0.672	2229
275	10.06	35.03	6	835	21.0	69.0	254.6	143.9	170.7	0.615	2062
276	10.06	35.03	6	835	21.0	70.0	254.6	143.9	170.2	0.612	2055
277	10.06	35.03	6	835	16.0	68.0	254.6	145.6	171.8	0.610	2022
278	10.06	35.03	6	835	26.0	81.0	284.9	194.0	63.6	0.359	1619
279	10.06	35.03	6	835	26.0	90.0	279.4	190.3	63.3	0.341	1585
280	10.06	35.03	6	835	31.0	98.0	265.7	193.7	65.1	0.368	1667
281	10.06	35.03	6	835	31.0	104.0	251.9	191.3	62.3	0.374	1678
282	10.06	35.03	6	835	36.0	113.0	240.9	188.8	66.7	0.393	1740
283	10.06	35.03	6	835	36.0	112.0	240.9	190.3	65.2	0.395	1743
284	10.06	35.03	6	835	31.0	107.0	250.5	190.3	64.9	0.376	1681
285	10.06	35.03	6	835	21.0	81.0	298.7	190.3	65.9	0.327	1520
286	10.06	35.03	6	835	21.0	82.0	300.1	189.3	64.6	0.317	1502
287	10.06	35.03	6	835	16.0	63.0	344.1	189.3	66.2	0.293	1408
288	10.06	35.03	6	835	31.0	69.0	330.3	189.8	92.0	0.367	1666
289	10.06	35.03	6	835	31.0	74.0	333.1	191.3	91.1	0.351	1637
290	10.06	35.03	6	835	36.0	81.0	327.6	191.3	89.9	0.344	1656
291	10.06	35.03	6	835	36.0	83.0	329.0	191.3	89.9	0.337	1642
292	10.06	35.03	6	835	26.0	66.0	349.6	190.3	88.2	0.333	1571
293	10.06	35.03	6	835	26.0	71.0	344.1	189.3	126.2	0.404	1700
294	10.06	35.03	6	835	21.0	62.0	373.0	190.1	124.7	0.372	1606
295	10.06	35.03	6	835	21.0	68.0	363.4	190.8	125.0	0.374	1609
296	10.06	35.03	6	835	16.0	59.0	395.0	191.3	125.0	0.346	1510
297	10.06	35.03	6	835	16.0	60.0	393.7	191.3	125.0	0.345	1509
298	10.06	35.03	6	835	21.0	66.0	415.7	190.8	199.6	0.432	1718
299	10.06	35.03	6	835	21.0	68.0	412.9	190.8	198.0	0.429	1712
300	10.06	35.03	6	835	16.0	60.0	430.8	190.8	197.4	0.413	1640

Table II. Burnout in 3-Rod Clusters

Run No	d_i mm	d_o mm	s mm	L mm	p kg/cm^2	Δt_{sub} °C	$\dot{m}/F$ kg/m^{2}s	$(q/A)_i$ W/cm^2	$(q/A)_o$ W/cm^2	x_{BO}	h_{BO} kJ/kg
301	10.06	35.03	6	835	16.0	70.0	422.6	189.8	197.4	0.400	1616
302	10.06	35.03	6	835	26.0	65.0	375.8	189.6	200.8	0.507	1889
303	10.06	35.03	6	835	26.0	71.0	379.9	188.3	200.8	0.483	1846
304	10.06	35.03	6	835	31.0	84.0	366.1	188.3	200.8	0.486	1877
305	10.06	35.03	6	835	31.0	88.0	366.1	188.3	199.2	0.473	1854
306	10.06	35.03	6	835	36.0	94.0	351.0	186.6	200.0	0.494	1917
307	10.06	35.03	6	835	36.0	96.0	346.9	186.1	200.8	0.499	1925
308	10.06	35.03	6	835	21.0	74.0	385.4	190.8	200.8	0.462	1775
309	10.06	35.03	6	835	21.0	78.0	388.2	190.8	196.9	0.442	1737
310	10.06	35.03	6	835	16.5	67.0	415.7	190.8	198.5	0.420	1659
311	10.06	35.03	6	835	16.5	67.0	415.7	190.8	198.5	0.420	1659
312	10.06	35.03	6	1670	31.0	70.0	382.4	106.0	100.2	0.527	1951
313	10.06	35.03	6	1670	31.0	87.0	366.1	106.6	98.9	0.514	1928
314	10.06	35.03	6	1670	31.0	114.0	310.8	105.8	98.7	0.578	2042
315	10.06	35.03	6	1670	31.0	116.0	317.0	105.5	99.5	0.559	2007
316	10.06	35.03	6	1670	31.0	52.0	395.0	103.3	98.7	0.535	1965
317	10.06	35.03	6	1670	31.0	78.0	351.0	102.9	98.0	0.551	1994
318	10.06	35.03	6	1670	31.0	102.0	324.8	104.0	96.3	0.551	1995
319	10.06	35.03	6	1670	31.0	133.0	286.3	104.0	96.8	0.591	2065
320	10.06	35.03	6	1670	31.0	151.0	275.3	104.9	97.4	0.593	2070
321	10.06	35.03	6	1670	26.0	66.0	201.7	95.9	0	0.401	1695
322	10.06	35.03	6	1670	26.0	67.0	200.3	95.9	0	0.403	1698
323	10.06	35.03	6	1670	31.0	83.0	205.8	98.9	0	0.372	1674
324	10.06	35.03	6	1670	31.0	82.0	203.0	98.9	0	0.382	1693
325	10.06	35.03	6	1670	36.0	96.0	186.2	98.5	0	0.405	1761
326	10.06	35.03	6	1670	36.0	97.0	191.7	98.5	0	0.383	1723
327	10.06	35.03	6	1670	41.0	99.0	184.0	98.1	0	0.406	1789
328	10.06	35.03	6	1670	41.0	110.0	184.7	98.3	0	0.378	1740
329	10.06	35.03	6	1670	21.0	58.0	227.8	98.5	0	0.362	1587
330	10.06	35.03	6	1670	21.0	78.0	212.9	98.5	0	0.352	1568
331	10.06	35.03	6	1670	28.0	73.0	186.2	94.3	0	0.424	1750
332	10.06	35.03	6	1670	31.0	84.0	363.4	151.8	0	0.293	1533
333	10.06	35.03	6	1670	31.0	93.0	366.8	154.3	0	0.275	1501
334	10.06	35.03	6	1670	36.0	98.0	351.0	154.3	0	0.288	1557
335	10.06	35.03	6	1670	36.0	102.0	351.0	155.4	0	0.282	1547
336	10.06	35.03	6	1670	41.0	92.0	353.8	154.5	0	0.301	1609
337	10.06	35.03	6	1670	41.0	90.0	356.5	156.3	0	0.308	1622
338	10.06	35.03	6	1670	32.0	75.0	407.4	156.5	0	0.274	1506
339	10.06	35.03	6	1670	26.0	72.0	424.0	158.7	0	0.266	1448
340	10.06	35.03	6	1670	26.0	72.0	424.0	158.7	0	0.266	1448
341	10.06	35.03	6	1670	21.0	59.0	462.5	158.7	0	0.256	1388
342	10.06	35.03	6	1670	21.0	59.0	457.0	158.7	0	0.261	1397
343	10.06	35.03	6	1670	31.0	68.0	648.3	202.2	0	0.202	1371
344	10.06	35.03	6	1670	31.0	68.0	624.9	196.4	0	0.205	1376
345	10.06	35.03	6	1670	36.0	75.0	594.6	199.7	0	0.215	1430
346	10.06	35.03	6	1670	36.0	78.0	594.6	198.2	0	0.204	1411
347	10.06	35.03	6	1670	41.0	89.0	556.1	200.0	0	0.210	1454
348	10.06	35.03	6	1670	41.0	85.0	558.8	202.2	0	0.223	1476
349	10.06	35.03	6	1670	26.0	88.0	569.9	198.2	0	0.197	1322
350	10.06	35.03	6	1670	26.0	82.0	582.2	197.9	0	0.202	1330
351	10.06	35.03	6	1670	21.0	75.0	678.6	204.7	0	0.172	1229
352	10.06	35.03	6	1670	21.0	75.0	674.5	204.7	0	0.174	1233
353	10.06	35.03	6	1670	31.0	86.0	809.4	248.7	0	0.153	1283
354	10.06	35.03	6	1670	31.0	85.0	812.1	248.7	0	0.154	1285
355	10.06	35.03	6	1670	36.0	100.0	704.8	249.3	0	0.176	1361
356	10.06	35.03	6	1670	36.0	100.0	707.5	249.3	0	0.174	1358
357	10.06	35.03	6	1670	41.0	105.0	688.2	247.4	0	0.169	1385
358	10.06	35.03	6	1670	41.0	106.0	693.7	247.4	0	0.163	1374
359	10.06	35.03	6	1670	26.0	87.0	840.0	249.3	0	0.141	1220
360	10.06	35.03	6	1670	26.0	88.0	842.0	250.7	0	0.138	1214

Table II. Burnout in 3-Rod Clusters

Run	d_i	d_o	s	L	p	Δt_{sub}	$\dot{m}/F$	$(q/A)_i$	$(q/A)_o$	x_{BO}	h_{BO}
No	mm	mm	mm	mm	kg/cm^2	°C	kg/m^{2}s	W/cm^2	W/cm^2		kJ/kg
361	10.06	35.03	6	1670	31.0	65.0	1320.0	299.1	0	0.105	1198
362	10.06	35.03	6	1670	31.0	64.0	1330.0	299.3	0	0.106	1199
363	10.06	35.03	6	1670	31.0	69.0	1185.0	296.2	0	0.124	1231
364	10.06	35.03	6	1670	41.0	80.0	1161.5	298.8	0	0.102	1270
365	10.06	35.03	6	1670	41.0	82.0	1085.0	294.9	0	0.115	1293
366	10.06	35.03	6	1670	31.0	81.0	374.8	105.9	113.3	0.564	2017
367	10.06	35.03	6	1670	31.0	98.0	308.6	106.6	71.2	0.510	1921
368	10.06	35.03	6	1670	31.0	95.0	299.0	106.6	71.2	0.529	1956
369	10.06	35.03	6	1670	31.0	116.0	209.9	105.8	21.7	0.474	1856
370	10.06	35.03	6	1670	31.0	114.0	310.8	105.8	98.7	0.578	2042
371	10.06	35.03	6	1670	31.0	116.0	317.0	105.5	99.5	0.559	2007
372	10.06	35.03	6	1670	31.0	113.0	304.5	105.8	94.0	0.576	2039
373	10.06	35.03	6	1670	31.0	97.0	311.2	105.8	84.3	0.551	1994
374	10.06	35.03	6	1670	31.0	81.0	241.4	106.8	23.8	0.470	1849
375	10.06	35.03	6	1670	31.0	77.0	258.5	105.3	30.9	0.467	1843
376	10.06	35.03	6	1670	31.0	104.0	251.3	105.7	36.5	0.455	1822
377	10.06	35.03	6	1670	31.0	92.0	264.0	105.1	41.7	0.474	1856
378	10.06	35.03	6	1670	31.0	105.0	262.0	105.1	47.3	0.479	1865
379	10.06	35.03	6	1670	31.0	95.0	283.6	104.9	56.2	0.489	1883
380	10.06	35.03	6	1670	31.0	89.0	301.7	104.9	63.7	0.495	1893
381	10.06	35.03	6	1670	31.0	87.0	316.2	104.9	72.1	0.504	1910
382	10.06	35.03	6	1670	31.0	87.0	322.8	104.9	79.4	0.521	1941
383	10.06	35.03	6	1670	31.0	96.0	327.2	105.3	88.5	0.531	1958
384	10.06	35.03	6	1670	31.0	100.0	341.4	104.9	104.7	0.555	2001
385	10.06	35.03	6	1670	31.0	94.0	363.5	104.9	117.6	0.570	2028
386	10.06	35.03	6	1670	31.0	94.0	379.5	104.9	127.2	0.572	2031
387	10.06	35.03	6	1670	31.0	101.0	251.9	102.2	49.6	0.517	1933
388	10.06	35.03	6	1670	31.0	104.0	246.4	101.5	48.8	0.519	1937
389	10.06	35.03	6	1670	31.0	100.0	209.2	100.5	23.7	0.492	1889
390	10.06	35.03	6	1670	31.0	101.0	272.5	99.9	70.7	0.558	2006
391	10.06	35.03	6	1670	31.0	99.0	212.0	102.1	23.7	0.494	1892
392	10.06	35.03	6	1670	31.0	104.0	275.3	100.6	70.1	0.542	1979
393	10.06	35.03	6	1670	21.0	72.0	311.1	100.8	68.8	0.503	1851
394	10.06	35.03	6	1670	21.0	85.0	278.0	101.0	49.5	0.461	1772
395	10.06	35.03	6	1670	21.0	73.0	234.0	99.3	23.7	0.455	1762
396	10.06	35.03	6	1670	21.0	79.0	229.9	98.6	23.7	0.450	1751
397	10.06	35.03	6	1670	21.0	90.0	242.3	104.4	28.6	0.447	1747
398	10.06	35.03	6	1670	21.0	93.0	251.9	104.4	36.0	0.455	1761
399	10.06	35.03	6	1670	21.0	92.0	269.8	104.4	43.3	0.449	1750
400	10.06	35.03	6	1670	21.0	91.0	286.3	104.4	49.1	0.440	1734
401	10.06	35.03	6	1670	21.0	82.0	307.0	104.4	56.1	0.447	1746
402	10.06	35.03	6	1670	21.0	80.0	330.4	104.4	62.2	0.431	1716
403	10.06	35.03	6	1670	21.0	80.0	335.9	104.4	68.0	0.444	1741
404	10.06	35.03	6	1670	21.0	81.0	330.4	104.7	73.3	0.475	1799
405	10.06	35.03	6	1670	21.0	94.0	331.7	104.2	83.7	0.484	1816
406	10.06	35.03	6	1670	21.0	97.0	353.8	104.9	101.7	0.504	1854
407	10.06	35.03	6	1670	21.0	99.0	382.7	104.9	116.6	0.497	1840
408	10.06	35.03	6	1670	21.0	99.0	399.2	104.9	127.6	0.504	1853
409	10.06	35.03	6	1670	21.0	84.0	279.4	101.2	50.0	0.463	1776
410	10.06	35.03	6	1670	41.0	114.0	262.9	100.1	71.4	0.577	2081
411	10.06	35.03	6	1670	41.0	119.0	257.4	99.6	71.2	0.580	2086
412	10.06	35.03	6	1670	41.0	117.0	198.2	99.0	23.5	0.495	1940
413	10.06	35.03	6	1670	41.0	117.0	196.8	99.0	23.5	0.500	1950
414	10.06	35.03	6	1670	41.0	122.0	223.0	98.0	48.4	0.552	2037
415	10.06	35.03	6	1670	41.0	124.0	218.9	98.2	49.2	0.570	2068
416	10.06	35.03	6	1670	43.0	103.0	217.5	104.6	25.4	0.508	1971
417	10.06	35.03	6	1670	43.5	115.0	213.4	104.6	29.5	0.520	1993
418	10.06	35.03	6	1670	42.1	102.0	228.5	104.4	35.8	0.535	2014
419	10.06	35.03	6	1670	42.1	105.0	239.5	103.1	43.2	0.529	2003
420	10.06	35.03	6	1670	42.0	115.0	240.9	103.7	51.7	0.555	2047

Table II. Burnout in 3-Rod Clusters

Run	d_i	d_o	s	L	p	Δt_{sub}	$\dot{m}/F$	$(q/A)_i$	$(q/A)_o$	x_{BO}	h_{BO}
No	mm	mm	mm	mm	kg/cm^2	°C	kg/m^{2}s	W/cm^2	W/cm^2		kJ/kg
421	10.06	35.03	6	1670	43.5	102.0	261.5	104.1	58.7	0.563	2066
422	10.06	35.03	6	1670	42.5	101.0	275.3	102.8	68.1	0.567	2068
423	10.06	35.03	6	1670	43.5	101.0	284.9	102.8	74.9	0.575	2086
424	10.06	35.03	6	1670	43.0	90.0	307.0	102.8	84.3	0.586	2104
425	10.06	35.03	6	1670	43.5	89.0	326.2	102.8	94.8	0.542	2031
426	10.06	35.03	6	1670	41.0	90.0	351.0	104.4	105.6	0.575	2076
427	10.06	35.03	6	1670	42.0	95.0	362.0	104.2	112.5	0.566	2065
428	10.06	35.03	6	1670	43.0	93.0	378.5	104.2	129.4	0.603	2131
429	10.06	35.03	6	1670	42.0	88.0	374.4	102.8	130.1	0.621	2159
430	10.06	35.03	6	1670	26.0	97.0	256.0	100.1	49.2	0.494	1865
431	10.06	35.03	6	1670	26.0	96.0	251.9	100.4	49.0	0.509	1892
432	10.06	35.03	6	1670	36.0	106.0	268.4	101.0	72.0	0.579	2064
433	10.06	35.03	6	1670	36.0	108.0	265.7	99.8	72.0	0.577	2061
434	10.06	35.03	6	1670	24.5	89.0	279.4	100.8	68.8	0.548	1957
435	10.06	35.03	6	1670	26.0	87.0	279.4	100.2	70.1	0.560	1986
436	10.06	35.03	6	1670	36.0	109.0	203.7	100.3	23.5	0.495	1918
437	10.06	35.03	6	1670	36.0	111.0	203.7	99.4	23.5	0.484	1900
438	10.06	35.03	6	1670	26.0	82.0	228.5	98.5	23.4	0.452	1789
439	10.06	35.03	6	1670	26.0	87.0	228.5	99.6	23.4	0.446	1778
440	10.06	35.03	6	1670	36.0	116.0	235.4	98.7	49.1	0.522	1965
441	10.06	35.03	6	1670	36.0	117.0	228.5	96.4	48.5	0.528	1976
442	10.06	35.03	6	1670	31.0	105.0	474.9	159.8	68.1	0.347	1630
443	10.06	35.03	6	1670	31.0	107.0	465.2	159.8	68.1	0.355	1644
444	10.06	35.03	6	1670	31.0	79.0	461.1	162.1	37.8	0.340	1618
445	10.06	35.03	6	1670	31.0	75.0	477.6	162.1	37.6	0.330	1600
446	10.06	35.03	6	1670	31.0	79.0	472.1	161.0	37.5	0.324	1588
447	10.06	35.03	6	1670	31.0	89.0	430.8	160.9	35.4	0.343	1623
448	10.06	35.03	6	1670	31.0	87.0	440.5	158.7	42.9	0.353	1641
449	10.06	35.03	6	1670	31.0	81.0	492.8	158.5	50.9	0.329	1598
450	10.06	35.03	6	1670	31.0	74.0	520.3	158.0	60.4	0.342	1621
451	10.06	35.03	6	1670	31.0	73.0	546.5	157.1	73.9	0.352	1639
452	10.06	35.03	6	1670	31.0	80.0	556.1	158.9	83.0	0.353	1640
453	10.06	35.03	6	1670	31.0	83.0	556.1	158.5	92.9	0.370	1671
454	10.06	35.03	6	1670	31.0	78.0	596.0	158.5	107.4	0.377	1684
455	10.06	35.03	6	1670	31.0	72.0	649.7	158.5	122.8	0.378	1684
456	10.06	35.03	6	1670	31.0	71.0	666.2	158.5	136.3	0.395	1715
457	10.06	35.03	6	1670	31.0	71.0	693.7	158.5	148.1	0.396	1717
458	10.06	35.03	6	1670	41.0	63.0	496.9	158.0	48.0	0.368	1723
459	10.06	35.03	6	1670	41.0	64.0	534.1	159.8	46.2	0.326	1652
460	10.06	35.03	6	1670	41.0	66.0	565.7	160.3	59.5	0.328	1656
461	10.06	35.03	6	1670	41.0	69.0	590.5	159.2	74.2	0.333	1664
462	10.06	35.03	6	1670	41.0	71.0	597.4	158.0	91.9	0.363	1715
463	10.06	35.03	6	1670	41.0	67.0	624.9	159.2	105.6	0.384	1750
464	10.06	35.03	6	1670	41.0	72.0	649.7	158.9	121.4	0.384	1751
465	10.06	35.03	6	1670	41.0	72.0	674.5	160.3	133.1	0.391	1763
466	10.06	35.03	6	1670	41.0	67.0	699.2	160.5	149.0	0.417	1807
467	10.06	35.03	6	1670	41.0	103.0	414.3	157.6	38.2	0.338	1672
468	10.06	35.03	6	1670	41.0	104.0	404.7	159.2	38.1	0.355	1701
469	10.06	35.03	6	1670	41.0	117.0	417.1	156.9	69.5	0.408	1792
470	10.06	35.03	6	1670	40.0	109.0	435.0	157.8	70.1	0.402	1777
471	10.06	35.03	6	1670	21.0	82.0	547.8	160.0	68.1	0.313	1493
472	10.06	35.03	6	1670	21.0	67.0	520.3	157.6	36.4	0.286	1443
473	10.06	35.03	6	1670	26.0	92.0	488.6	160.9	68.1	0.359	1618
474	10.06	35.03	6	1670	26.0	93.0	494.2	160.9	68.1	0.350	1602
475	10.06	35.03	6	1670	36.0	111.	448.7	157.6	68.8	0.368	1697
476	10.06	35.03	6	1670	36.0	114.0	452.2	159.8	68.1	0.360	1683
477	10.06	35.03	6	1670	26.0	72.0	485.9	158.5	37.3	0.315	1538
478	10.06	35.03	6	1670	26.0	77.0	470.8	158.2	37.0	0.318	1542
479	10.06	35.03	6	1670	36.0	92.0	419.8	159.2	36.3	0.353	1670
480	10.06	35.03	6	1670	36.0	94.0	410.2	157.6	36.2	0.357	1677

Table III. Burnout in 7-Rod Clusters

Run	d_i	d_o	s	L	p	Δt_{sub}	$\dot{m}/F$	q/A	x_{BO}	h_{BO}
No	mm	mm	mm	mm	kg/cm^2	°C	kg/m^{2}s	W/cm^2		kJ/kg
1	10.06	49.95	6	1670	31.0	63.6	181.0	89.6	0.562	2013
2	10.06	49.95	6	1670	31.0	63.6	184.5	90.0	0.551	1994
3	10.06	49.95	6	1670	41.0	61.6	192.4	90.9	0.550	2035
4	10.06	49.95	6	1670	41.0	58.6	195.2	90.9	0.548	2030
5	10.06	49.95	6	1670	31.0	71.6	179.6	89.1	0.544	1981
6	10.06	49.95	6	1670	31.0	49.6	191.6	89.2	0.553	1998
7	10.06	49.95	6	1670	21.0	44.0	202.3	88.3	0.504	1853
8	10.06	49.95	6	1670	21.0	27.0	216.5	88.3	0.504	1854
9	10.06	49.95	6	1670	11.0	49.4	225.7	86.1	0.395	1552
10	10.06	49.95	6	1670	11.0	41.4	234.2	86.2	0.394	1551
11	10.06	49.95	6	1670	31.0	71.6	317.3	125.0	0.393	1712
12	10.06	49.95	6	1670	31.0	70.6	318.0	125.0	0.394	1714
13	10.06	49.95	6	1670	41.0	88.6	296.0	125.6	0.405	1788
14	10.06	49.95	6	1670	41.0	84.6	296.0	126.3	0.419	1811
15	10.06	49.95	6	1670	21.0	59.0	356.3	124.4	0.347	1558
16	10.06	49.95	6	1670	21.0	62.0	357.7	124.3	0.338	1541
17	10.06	49.95	6	1670	31.0	126.0	262.6	126.1	0.391	1708
18	10.06	49.95	6	1670	31.0	111.5	283.2	126.5	0.375	1681
19	10.06	49.95	6	1670	31.0	104.7	286.8	127.5	0.388	1703
20	10.06	49.95	6	1670	31.0	86.6	308.1	125.0	0.374	1678
21	10.06	49.95	6	1670	31.0	57.5	360.6	127.9	0.370	1670
22	10.06	49.95	6	1670	31.0	35.6	389.7	125.3	0.377	1683
23	10.06	49.95	6	1670	31.0	66.6	414.5	149.1	0.355	1643
24	10.06	49.95	6	1670	31.0	64.6	403.2	144.9	0.359	1651
25	10.06	49.95	6	1670	41.0	84.6	356.3	144.5	0.387	1756
26	10.06	49.95	6	1670	41.0	80.6	358.4	143.2	0.388	1758
27	10.06	49.95	6	1670	21.0	41.0	496.9	144.1	0.306	1481
28	10.06	49.95	6	1670	21.0	44.0	496.9	143.1	0.296	1462
29	10.06	49.95	6	1670	31.0	81.6	438.7	162.1	0.333	1604
30	10.06	49.95	6	1670	31.0	79.6	437.9	162.3	0.339	1616
31	10.06	49.95	6	1670	31.0	66.6	544.4	170.1	0.285	1519
32	10.06	49.95	6	1670	31.0	70.6	530.9	167.6	0.280	1510
33	10.06	49.95	6	1670	41.0	82.6	462.8	167.6	0.325	1650
34	10.06	49.95	6	1670	41.0	83.5	442.9	162.9	0.331	1661
35	10.06	49.95	6	1670	21.0	64.0	541.6	166.5	0.277	1427
36	10.06	49.95	6	1670	31.0	79.6	675.7	199.0	0.227	1415
37	10.06	49.95	6	1670	31.0	77.6	672.9	198.6	0.233	1425
38	10.06	49.95	6	1670	41.0	107.6	522.4	199.7	0.293	1595
39	10.06	49.95	6	1670	31.0	67.6	881.5	224.5	0.191	1362
40	10.06	49.95	6	1670	41.0	77.6	780.8	226.5	0.227	1483

Table IV. Measured and Predicted Burnout Conditions in 3-Rod Clusters

Run No	d_i mm	d_o mm	L mm	p kg/cm^2	Δt_{sub} °C	$\dot{m}/F$ kg/m^{2}s	Measured Burnout Values			Predicted Burnout Values			Error in q/A %	Error in h_{BO} %
							q/A W/cm^2	x_{BO}	h_{BO} kJ/kg	q/A W/cm^2	x_{BO}	h_{BO} kJ/kg		
52	10.01	40.42	835	22.0	99.9	88.5	128.4	0.345	1563	117.5	0.298	1488	+ 9.3	+ 5.0
68	10.01	40.42	835	21.5	93.0	180.0	193.2	0.209	1303	192.1	0.208	1317	+ 0.6	- 1.0
69	10.01	40.42	835	21.5	96.8	180.0	193.2	0.200	1286	195.4	0.207	1315	- 1.1	- 2.2
83	10.01	40.42	835	19.5	58.3	329.0	250.2	0.160	1190	243.5	0.154	1189	+ 3.5	+ 0.1
85	10.01	40.42	835	20.0	71.8	320.1	249.3	0.138	1154	256.8	0.149	1190	- 2.9	- 3.0
95	10.01	40.42	835	21.5	62.1	338.0	244.8	0.136	1167	252.1	0.148	1204	- 2.9	- 3.1
102	10.01	40.42	835	19.5	65.5	497.3	298.3	0.080	1039	328.0	0.106	1104	- 9.1	- 5.9
121	10.01	40.42	835	20.0	53.2	523.5	306.3	0.101	1085	308.5	0.108	1112	- 0.7	- 2.4
122	10.01	40.42	835	19.5	51.1	544.1	305.1	0.096	1070	316.5	0.105	1092	- 3.6	- 2.0
123	10.01	40.42	835	19.5	65.5	497.1	298.3	0.080	1040	336.0	0.113	1117	- 12.7	- 6.9
187	10.06	35.03	835	21.8	60.3	124.3	101.2	0.325	1523	106.1	0.352	1590	- 4.6	- 4.2
195	10.06	35.03	835	22.0	56.2	217.5	150.4	0.262	1408	149.5	0.263	1423	+ 0.6	- 1.0
196	10.06	35.03	835	20.8	34.3	251.9	151.2	0.257	1388	150.4	0.259	1405	+ 0.5	- 1.2
208	10.06	35.03	835	22.0	71.7	291.8	194.8	0.214	1318	190.9	0.209	1322	+ 2.0	- 0.3
209	10.06	35.03	835	22.0	82.7	279.4	194.8	0.206	1303	194.0	0.207	1319	+ 0.5	- 1.2
341	10.06	35.03	1670	21.0	56.9	462.5	158.7	0.256	1388	149.6	0.237	1366	+ 6.1	+ 1.6
342	10.06	35.03	1670	21.0	56.9	457.0	158.7	0.261	1397	148.5	0.240	1371	+ 6.9	+ 1.9
329	10.06	35.03	1670	21.0	55.9	227.8	98.5	0.362	1587	98.5	0.366	1608	± 0	- 1.2
330	10.06	35.03	1670	21.0	76.5	212.9	98.5	0.352	1568	100.2	0.363	1602	- 1.7	- 2.1
351	10.06	35.03	1670	21.0	73.1	678.6	204.7	0.172	1229	197.7	0.164	1228	+ 3.5	+ 0.1
352	10.06	35.03	1670	21.0	73.1	674.5	204.7	0.174	1233	198.3	0.167	1234	+ 3.2	- 0.1

Table IV. Measured and Predicted Burnout Conditions in 3-Rod Clusters

Run No	d_i mm	d_o mm	L mm	p kg/cm^2	Δt_{sub} ^oC	$\dot{m}/F$ kg/m^{2}s	Measured Burnout Values			Predicted Burnout Values			Error in q/A %	Error in h_{BO} %
							q/A W/cm^2	x_{BO}	h_{BO} kJ/kg	q/A W/cm^2	x_{BO}	h_{BO} kJ/kg		
72	10.01	40.42	835	31.5	119.0	145.5	195.4	0.265	1487	191.3	0.252	1467	+ 2.1	+ 1.4
73	10.01	40.42	835	32.0	116.0	144.5	195.2	0.276	1509	186.2	0.255	1469	+ 4.8	+ 2.7
87	10.01	40.42	835	28.5	95.0	242.0	249.3	0.190	1329	248.6	0.201	1354	+ 0.3	- 1.8
89	10.01	40.42	835	31.0	102.0	223.0	250.4	0.212	1389	246.0	0.206	1382	+ 2.0	+ 0.5
104	10.01	40.42	835	27.5	76.0	379.0	300.1	0.136	1223	306.0	0.156	1269	- 2.0	- 3.6
105	10.01	40.42	835	32.5	86.0	331.0	300.8	0.160	1307	300.4	0.160	1303	+ 0.1	+ 0.3
106	10.01	40.42	835	31.0	88.0	351.7	301.4	0.134	1248	314.0	0.151	1263	- 4.0	- 1.2
116	10.01	40.42	835	30.5	87.0	359.2	302.6	0.130	1238	317.5	0.150	1280	- 4.7	- 3.3
117	10.01	40.42	835	29.5	82.0	376.4	302.0	0.125	1221	314.7	0.149	1267	- 4.0	- 3.6
119	10.01	40.42	835	27.6	75.0	372.1	303.2	0.148	1244	298.7	0.156	1270	+ 2.3	- 2.0
124	10.01	40.42	835	27.5	76.0	388.8	300.1	0.127	1208	308.3	0.150	1259	- 2.7	- 4.0
125	10.01	40.42	835	32.5	89.0	338.3	300.8	0.151	1280	309.0	0.155	1294	- 2.6	- 1.1
126	10.01	40.42	835	27.5	73.0	382.0	303.2	0.124	1232	300.0	0.155	1268	+ 1.1	- 2.8
182	10.06	35.03	835	32.5	104.0	91.9	103.6	0.425	1778	102.6	0.407	1749	+ 1.0	+ 1.7
183	10.06	35.03	835	29.0	96.0	101.9	103.2	0.371	1659	106.7	0.395	1704	- 4.5	- 2.6
184	10.06	35.03	835	28.0	92.0	104.5	102.1	0.358	1629	107.0	0.395	1703	- 4.6	- 4.3
189	10.06	35.03	835	30.5	83.0	105.4	100.0	0.364	1657	106.0	0.395	1722	- 5.6	- 3.8
190	10.06	35.03	835	31.8	89.0	99.2	100.0	0.387	1706	103.5	0.407	1734	- 3.4	- 1.6
199	10.06	35.03	835	31.0	88.0	181.7	151.9	0.283	1716	156.5	0.298	1545	- 2.5	- 1.7
200	10.06	35.03	835	31.0	83.0	185.8	151.7	0.284	1516	156.1	0.299	1548	- 2.8	- 2.1
204	10.06	35.03	835	31.0	91.0	181.7	152.6	0.279	1508	158.1	0.296	1542	- 3.5	- 2.2
211	10.06	35.03	835	28.0	83.0	273.9	196.3	0.222	1383	200.8	0.249	1437	- 2.2	- 3.8
212	10.06	35.03	835	31.0	81.0	273.9	196.3	0.227	1416	204.0	0.244	1449	- 3.8	- 2.5
213	10.06	35.03	835	32.5	96.0	245.0	195.7	0.242	1453	202.7	0.249	1458	- 3.5	- 0.4

Table IV. Measured and Predicted Burnout Conditions in 3-Rod Clusters

Run No	d_i mm	d_o mm	L mm	p kg/cm^2	Δt_{sub} °C	$\dot{m}/F$ kg/m^{2}s	Measured Burnout Values			Predicted Burnout Values			Error in q/A %	Error in h_{BO} %
							q/A W/cm^2	x_{BO}	h_{BO} kJ/kg	q/A W/cm^2	x_{BO}	h_{BO} kJ/kg		
216	10.06	35.03	835	30.0	100.0	249.1	195.7	0.224	1403	205.0	0.247	1455	- 4.5	- 3.6
222	10.06	35.03	835	31.0	111.0	301.0	234.0	0.193	1355	244.8	0.214	1394	- 4.4	- 2.8
223	10.06	35.03	835	31.0	117.0	297.0	234.0	0.186	1341	246.2	0.208	1384	- 5.0	- 3.1
224	10.06	35.03	835	31.0	117.0	301.0	234.0	0.179	1330	248.6	0.208	1384	- 5.9	- 3.9
225	10.06	35.03	835	31.0	110.0	325.0	240.9	0.174	1320	256.0	0.201	1370	- 5.9	- 3.6
226	10.06	35.03	835	31.0	104.0	331.0	242.5	0.182	1336	255.0	0.201	1371	- 4.9	- 2.6
227	10.06	35.03	835	31.0	184.0	213.1	234.1	0.223	1407	239.2	0.227	1418	- 2.1	- 0.8
228	10.06	35.03	835	31.0	171.0	240.2	240.0	0.191	1352	253.0	0.218	1402	- 5.1	- 3.6
229	10.06	35.03	835	31.0	154.0	261.1	242.1	0.186	1342	255.2	0.210	1389	- 5.1	- 3.4
230	10.06	35.03	835	31.0	140.0	264.3	242.1	0.211	1387	246.3	0.216	1393	- 1.6	- 0.5
231	10.06	35.03	835	31.0	126.0	285.0	232.2	0.194	1356	245.8	0.214	1385	- 5.5	- 2.1
232	10.06	35.03	835	31.0	121.0	287.3	240.2	0.206	1378	246.0	0.213	1382	- 2.3	- 0.3
233	10.06	35.03	835	31.0	63.0	406.1	245.2	0.202	1371	243.1	0.200	1370	+ 0.9	+ 0.1
234	10.06	35.03	835	31.0	57.0	420.0	245.2	0.205	1376	240.0	0.198	1369	+ 2.2	+ 0.5
235	10.06	35.03	835	31.0	53.0	424.1	242.8	0.208	1382	238.3	0.201	1372	- 1.9	+ 0.7
236	10.06	35.03	835	31.0	101.0	468.5	304.0	0.139	1258	312.0	0.150	1281	- 2.6	- 1.8
237	10.06	35.03	835	29.5	92.0	497.2	303.0	0.136	1240	308.0	0.147	1271	- 1.7	- 2.4
238	10.06	35.03	835	31.0	93.0	492.1	297.9	0.131	1243	310.3	0.146	1273	- 4.0	- 2.4
323	10.06	35.03	1670	31.0	83.0	205.8	98.9	0.372	1674	104.0	0.401	1740	- 4.9	- 3.8
324	10.06	35.03	1670	31.0	82.0	203.0	98.9	0.382	1693	102.0	0.401	1729	- 3.1	- 1.5
331	10.06	35.03	1670	28.0	73.0	186.2	94.3	0.424	1750	94.0	0.435	1775	+ 0.3	- 1.4
332	10.06	35.03	1670	31.0	84.0	363.4	151.8	0.293	1533	152.5	0.296	1542	- 0.5	- 0.6
333	10.06	35.03	1670	31.0	93.0	366.8	154.3	0.275	1501	156.5	0.283	1518	- 1.5	- 1.1
343	10.06	35.03	1670	31.0	68.0	648.3	202.2	0.202	1371	200.8	0.205	1381	+ 0.7	- 0.7

Table IV. Measured and Predicted Burnout Conditions in 3-Rod Clusters

Run No	d_i mm	d_o mm	L mm	p kg/cm^2	Δt_{sub} ^oC	$\dot{m}/F$ kg/m^2s	Measured Burnout Values			Predicted Burnout Values			Error in q/A %	Error in h_{BO} %
							q/A W/cm^2	x_{BO}	h_{BO} kJ/kg	q/A W/cm^2	x_{BO}	h_{BO} kJ/kg		
344	10.06	35.03	1670	31.0	68.0	624.9	196.4	0.205	1376	197.6	0.208	1384	- 0.6	- 0.6
353	10.06	35.03	1670	31.0	86.0	809.7	248.7	0.153	1283	249.1	0.154	1287	- 0.2	- 0.2
354	10.06	35.03	1670	31.0	85.0	812.1	248.7	0.154	1285	248.3	0.153	1287	+ 0.2	- 0.2
361	10.06	35.03	1670	31.0	65.0	1320.0	299.1	0.105	1198	294.4	0.103	1196	+ 1.6	+ 0.2
362	10.06	35.03	1670	31.0	64.0	1330.0	299.3	0.106	1199	294.2	0.103	1197	+ 1.7	+ 0.2
363	10.06	35.03	1670	31.0	69.0	1185.0	296.2	0.124	1231	283.0	0.112	1213	+ 4.6	+ 1.8

Table V. Measured and Predicted Burnout Conditions in a 7-Rod Cluster

Run No	d_i mm	d_o mm	L mm	p kg/cm^2	Δt_{sub} °C	$\dot{m}/F$ kg/m^{2}s	Measured Burnout Values			Predicted Burnout Values			Error in q/A %	Error in h_{BO} %
							q/A W/cm^2	x_{BO}	h_{BO} kJ/kg	q/A W/cm^2	x_{BO}	h_{BO} kJ/kg		
7	10.06	49.95	1670	21.0	41.3	202.3	88.3	0.504	1853	88.5	0.508	1875	- 0.2	- 1.2
8	10.06	49.95	1670	21.0	23.8	216.5	88.3	0.504	1854	88.7	0.510	1879	- 0.4	- 1.3
16	10.06	49.95	1670	21.0	60.0	357.7	124.3	0.338	1541	128.4	0.357	1591	- 3.2	- 2.5
27	10.06	49.95	1670	21.0	38.4	496.9	144.1	0.306	1481	144.0	0.308	1499	+ 0.1	- 1.2
28	10.06	49.95	1670	21.0	41.3	496.9	143.1	0.296	1462	144.6	0.304	1492	- 1.0	- 2.0
35	10.06	49.95	1670	21.0	62.1	541.6	166.5	0.277	1427	162.1	0.268	1423	+ 2.7	+ 0.3
1	10.06	49.95	1670	31.0	63.6	181.0	89.6	0.562	2013	91.8	0.570	2032	- 2.4	- 0.9
2	10.06	49.95	1670	31.0	63.6	184.5	90.0	0.551	1994	91.4	0.555	2106	- 1.2	- 5.3
5	10.06	49.95	1670	31.0	71.6	179.6	89.1	0.554	1981	92.4	0.562	2017	- 3.6	- 1.8
6	10.06	49.95	1670	31.0	49.6	191.6	89.2	0.553	1998	92.3	0.565	2022	- 3.4	- 1.2
11	10.06	49.95	1670	31.0	71.6	317.3	125.0	0.393	1712	127.1	0.398	1724	- 1.6	- 0.7
12	10.06	49.95	1670	31.0	70.6	318.0	125.0	0.394	1714	128.1	0.403	1733	- 2.3	- 1.1
17	10.06	49.95	1670	31.0	126.0	262.6	126.1	0.391	1708	132.3	0.403	1734	- 4.6	- 1.5
18	10.06	49.95	1670	31.0	111.5	283.2	126.5	0.375	1681	132.5	0.397	1722	- 4.5	- 2.4
19	10.06	49.95	1670	31.0	104.7	286.8	127.5	0.388	1703	132.0	0.402	1732	- 3.4	- 1.7
20	10.06	49.95	1670	31.0	86.6	308.1	125.0	0.374	1678	128.0	0.406	1739	- 2.3	- 3.5
21	10.06	49.95	1670	31.0	57.5	360.6	127.9	0.370	1670	134.6	0.388	1705	- 5.0	- 2.0
22	10.06	49.95	1670	31.0	35.6	389.7	125.3	0.377	1683	132.7	0.388	1707	- 5.6	- 1.4
23	10.06	49.95	1670	31.0	66.6	414.5	149.1	0.355	1643	150.8	0.355	1647	- 1.1	- 0.3
24	10.06	49.95	1670	31.0	64.6	403.2	144.9	0.359	1651	144.6	0.353	1646	+ 0.2	+ 0.4
29	10.06	49.95	1670	31.0	81.6	438.7	162.1	0.333	1604	163.5	0.332	1606	- 0.9	- 0.1

Table V. Measured and Predicted Burnout Conditions in a 7-Rod Cluster

Run No	d_i mm	d_o mm	L mm	p kg/cm^2	Δt_{sub} ^oC	$\dot{m}/F$ kg/m^2s	Measured Burnout Values			Predicted Burnout Values			Error in q/A %	Error in h_{BO} %
							q/A W/cm^2	x_{BO}	h_{BO} kJ/kg	q/A W/cm^2	x_{BO}	h_{BO} kJ/kg		
30	10.06	49.95	1670	31.0	79.6	437.9	162.3	0.339	1616	159.3	0.327	1599	+ 1.9	+ 1.0
31	10.06	49.95	1670	31.0	66.6	544.4	170.1	0.285	1519	175.2	0.296	1543	- 2.9	- 1.6
32	10.06	49.95	1670	31.0	70.6	530.9	167.6	0.280	1510	176.7	0.303	1554	- 5.1	- 2.8
36	10.06	49.95	1670	31.0	79.6	675.7	199.0	0.227	1415	208.2	0.246	1453	- 4.4	- 2.6
37	10.06	49.95	1670	31.0	77.6	672.9	198.6	0.233	1425	199.0	0.259	1475	- 0.2	- 3.4
39	10.06	49.95	1670	31.0	67.6	881.5	224.5	0.191	1362	230.8	0.206	1382	- 2.7	- 1.4

Table VI. Measured and Predicted Burnout Conditions in Annuli (Data from References 5 and 7)

Run No	d_i mm	d_o mm	L mm	p kg/cm^2	Δt_{sub} °C	$\dot{m}/F$ kg/m^{2}s	Measured Burnout Values			Predicted Burnout Values			Error in q/A %	Error in h_{BO} %
							q/A W/cm^2	x_{BO}	h_{BO} kJ/kg	q/A W/cm^2	x_{BO}	h_{BO} kJ/kg		
260	9.92	17.42	608	21.5	159.8	89.5	100.4	0.333	1550	100.5	0.336	1557	- 0.1	- 0.5
271	9.92	17.42	608	18.8	166.0	89.8	103.3	0.334	1529	102.5	0.330	1521	+ 0.8	+ 0.5
280	9.92	17.42	608	19.0	168.1	160.5	158.1	0.227	1328	160.4	0.238	1349	- 1.4	- 1.6
290	9.92	17.42	608	22.0	175.6	154.4	157.3	0.234	1369	158.5	0.239	1378	- 0.8	- 0.7
291	9.92	17.42	608	20.0	170.7	159.2	157.1	0.224	1332	160.5	0.238	1358	- 2.1	- 1.9
306	9.92	17.42	608	21.0	164.5	217.0	199.9	0.197	1291	199.5	0.200	1296	+ 0.2	- 0.3
312	9.92	17.42	608	20.8	162.6	224.2	201.9	0.188	1272	203.0	0.193	1280	- 0.5	- 0.6
316	9.92	17.42	608	20.0	160.1	231.0	203.8	0.183	1254	206.5	0.191	1268	- 1.3	- 1.1
318	9.92	17.42	608	20.7	162.6	230.5	204.1	0.180	1256	207.4	0.188	1272	- 1.6	- 1.3
329	9.92	17.42	608	21.0	153.8	292.5	247.9	0.176	1250	240.9	0.161	1223	+ 2.9	+ 2.2
337	9.92	17.42	608	20.5	155.1	294.5	247.2	0.167	1229	243.3	0.160	1215	+ 1.6	+ 1.2
343	9.92	17.42	608	19.0	147.5	308.0	246.4	0.159	1199	245.2	0.157	1195	+ 0.5	+ 0.3
357	9.92	17.42	608	21.5	144.9	385.0	297.9	0.148	1205	286.0	0.130	1171	+ 4.2	+ 2.9
358	9.92	17.42	608	20.0	140.7	406.0	299.9	0.137	1166	292.2	0.125	1145	+ 2.6	+ 1.8
365	9.92	17.42	608	20.0	139.1	406.0	296.5	0.135	1163	290.0	0.126	1145	+ 2.2	+ 1.6
369	9.92	17.42	608	21.0	136.8	445.0	297.4	0.101	1110	307.0	0.115	1137	- 3.1	- 2.4
370	9.92	17.42	608	21.0	136.8	419.0	297.9	0.128	1160	294.3	0.123	1151	+ 1.2	+ 0.8
373	9.92	17.42	608	21.0	140.1	418.5	303.2	0.129	1163	298.1	0.122	1149	+ 1.7	+ 1.2
1127	10.05	17.45	1216	21.5	170.8	177.4	103.6	0.356	1594	101.0	0.336	1558	+ 2.6	+ 2.4
1137	10.05	17.45	1216	19.0	164.5	183.6	105.4	0.354	1569	102.4	0.332	1529	+ 2.9	+ 2.7
1147	10.05	17.45	1216	22.5	158.3	301.2	151.9	0.282	1464	143.3	0.245	1395	+ 6.0	+ 4.9

Table VI. Measured and Predicted Burnout Conditions in Annuli (Data from References 5 and 7)

Run No	d_i mm	d_o mm	L mm	p kg/cm^2	Δt_{sub} °C	$\dot{m}/F$ kg/m^2s	Measured Burnout Values			Predicted Burnout Values			Error in q/A %	Error in h_{BO} %
							q/A W/cm^2	x_{BO}	h_{BO} kJ/kg	q/A W/cm^2	x_{BO}	h_{BO} kJ/kg		
1155	10.05	17.45	1216	21.0	156.4	297.5	151.1	0.290	1465	141.4	0.248	1386	+ 6.8	+ 5.7
1156	10.05	17.45	1216	19.0	149.2	315.7	152.6	0.273	1415	144.7	0.241	1355	+ 5.5	+ 4.1
1164	10.05	17.45	1216	19.5	124.9	578.0	200.7	0.154	1195	202.6	0.158	1203	- 0.9	- 0.7
1168	10.05	17.45	1216	18.5	124.5	582.4	200.6	0.152	1179	203.5	0.157	1190	- 1.4	- 0.9
1548	9.96	24.95	1216	21.0	161.7	140.2	152.6	0.164	1228	159.5	0.189	1275	- 4.3	- 3.7
1552	9.96	24.95	1216	21.5	167.9	136.3	155.3	0.175	1254	159.2	0.190	1282	- 2.4	- 2.3
1554	9.96	24.95	1216	20.0	160.9	139.2	154.7	0.176	1240	158.2	0.190	1267	- 2.3	- 2.1
1567	9.96	24.95	1216	21.0	110.7	252.2	205.8	0.147	1196	207.1	0.146	1195	- 0.6	+ 0.1
1571	9.96	24.95	1216	21.5	118.8	244.9	209.2	0.143	1195	210.0	0.146	1200	- 0.5	- 0.4
1575	9.96	24.95	1216	21.5	121.2	228.8	203.1	0.154	1216	201.6	0.152	1212	+ 0.7	+ 0.3
258	9.92	17.42	608	30.5	175.3	82.4	100.8	0.374	1672	99.5	0.351	1664	+ 1 3	+ 0.9
259	9.92	17.42	608	27.5	169.5	88.0	100.8	0.342	1608	105.0	0.372	1662	- 4.0	- 3.4
276	9.92	17.42	608	30.0	193.1	136.3	156.8	0.284	1516	153.2	0.269	1483	+ 2.4	+ 2.1
285	9.92	17.42	608	31.2	193.1	136.2	156.0	0.279	1511	156.8	0.283	1519	- 0.5	- 0.5
301	9.92	17.42	608	32.2	185.8	191.5	200.8	0.230	1427	203.0	0.239	1443	- 1.2	- 1.2
302	9.92	17.42	608	28.5	179.0	196.0	199.4	0.224	1396	197.4	0.236	1418	+ 1.0	- 1.6
308	9.92	17.42	608	31.0	183.0	198.0	203.4	0.227	1418	199.4	0.235	1433	+ 2.0	- 1.0
325	9.92	17.42	608	30.5	170.8	261.5	249.0	0.206	1380	245.0	0.197	1362	+ 1.6	+ 1.3
332	9.92	17.42	608	31.7	181.3	257.0	246.4	0.183	1342	252.0	0.198	1367	- 2.2	- 1.8
333	9.92	17.42	608	29.2	173.7	261.0	247.1	0.195	1351	247.1	0.194	1350	0	± 0
350	9.92	17.42	608	28.7	157.0	355.5	299.9	0.176	1308	292.2	0.162	1282	+ 2.6	+ 2.0
352	9.92	17.42	608	30.2	161.3	353.0	299.9	0.164	1301	297.3	0.161	1303	- 0.9	- 0.1
353	9.92	17.42	608	30.4	161.7	340.5	297.4	0.179	1313	292.5	0.164	1304	+ 1.7	+ 0.7
354	9.92	17.42	608	28.5	158.1	350.0	298.1	0.172	1316	290.2	0.163	1285	+ 2.7	+ 2.4
360	9.92	17.42	608	30.5	159.5	344.0	297.0	0.177	1322	290.2	0.161	1290	+ 2.3	+ 2.5

Table VI. Measured and Predicted Burnout Conditions in Annuli (Data from References 5 and 7)

Run No	d_i mm	d_o mm	L mm	p kg/cm^2	Δt_{sub} °C	$\dot{m}/F$ kg/m^{2}s	Measured Burnout Values			Predicted Burnout Values			Error in q/A %	Error in h_{BO} %
							q/A W/cm^2	x_{BO}	h_{BO} kJ/kg	q/A W/cm^2	x_{BO}	h_{BO} kJ/kg		
361	9.92	17.42	608	29.5	157.3	351.5	297.0	0.174	1307	290.5	0.163	1288	+ 2.2	+ 1.5
366	9.92	17.42	608	31.5	162.1	375.5	297.9	0.119	1226	313.7	0.148	1278	- 5.0	- 4.1
367	9.92	17.42	608	28.0	155.5	392.5	299.0	0.124	1213	311.3	0.147	1254	- 4.0	- 3.3
368	9.92	17.42	608	29.0	157.3	383.0	299.0	0.134	1234	308.2	0.150	1263	- 3.0	- 2.3
371	9.92	17.42	608	30.0	157.9	368.0	299.7	0.147	1269	301.2	0.152	1277	- 1.2	- 0.6
1134	10.05	17.42	1216	31.5	191.8	166.0	104.9	0.382	1700	105.0	0.370	1680	- 0.1	+ 1.2
1143	10.05	17.42	1216	30.5	174.7	274.8	150.8	0.315	1567	143.5	0.273	1496	+ 4.5	+ 4.7
1144	10.05	17.42	1216	28.0	170.0	288.7	151.1	0.296	1520	148.2	0.274	1478	+ 2.0	+ 2.8
1151	10.05	17.42	1216	32.0	178.8	268.5	151.1	0.315	1578	145.2	0.278	1516	+ 4.1	+ 4.1
1152	10.05	17.42	1216	29.0	173.2	274.2	151.3	0.323	1578	143.7	0.281	1503	+ 5.1	+ 5.0
1162	10.05	17.42	1216	31.0	149.6	469.2	199.8	0.202	1379	200.0	0.203	1378	- 0.1	± 0
1166	10.05	17.42	1216	28.5	147.2	481.7	199.7	0.202	1357	201.0	0.204	1361	- 0.7	- 0.3
1544	9.96	24.95	1216	31.0	183.8	113.7	152.3	0.239	1440	149.3	0.225	1411	+ 2.0	+ 2.1
1545	9.96	24.95	1216	30.5	180.3	112.2	152.6	0.260	1475	145.0	0.229	1419	+ 5.3	+ 4.0
1550	9.96	24.95	1216	31.0	187.3	111.0	154.7	0.260	1478	147.4	0.227	1419	+ 5.5	+ 4.2
1555	9.96	24.95	1216	29.0	177.4	118.8	151.6	0.230	1410	149.8	0.225	1401	+ 1.2	+ 0.6
1565	9.96	24.95	1216	31.0	135.4	207.4	207.2	0.179	1332	208.6	0.186	1345	- 0.6	- 1.0
1566	9.96	24.95	1216	31.0	130.3	208.4	205.8	0.186	1345	204.7	0.186	1345	+ 0.5	± 0
1570	9.96	24.95	1216	31.0	145.6	194.7	209.8	0.194	1359	207.4	0.187	1347	+ 1.2	+ 0.9

Table VII. Measured and Predicted Burnout Conditions in an Annulus (Data from Reference 8)

Run No	d_i mm	d_o mm	L mm	p kg/cm^2	Δt_{sub} ^oC	$\dot{m}/F$ kg/m^{2}s	Measured Burnout Values			Predicted Burnout Values			Error in q/A %	Error in h_{BO} %
							q/A W/cm^2	x_{BO}	h_{BO} kJ/kg	q/A W/cm^2	x_{BO}	h_{BO} kJ/kg		
1	13.9	34.5	4220	31.0	6.5	452.1	100.9	0.278	1510	100.5	0.277	1508	+ 0.39	+ 0.13
2	13.9	34.5	4220	31.0	6.5	458.2	100.9	0.276	1506	100.6	0.277	1504	+ 0.30	+ 0.13
3	13.9	34.5	4220	31.0	6.5	452.0	100.9	0.278	1510	100.5	0.277	1508	+ 0.39	+ 0.13
4	13.9	34.5	4220	31.0	6.5	687.8	127.2	0.228	1429	121.8	0.218	1400	+ 4.43	+ 2.07
5	13.9	34.5	4220	31.0	5.5	1065.0	149.5	0.170	1318	150.0	0.169	1315	- 0.33	+ 2.28
6	13.9	34.5	4220	31.0	6.5	1590.0	168.0	0.123	1233	176.3	0.130	1244	- 4.70	- 0.89
7	13.9	34.5	4220	31.0	6.5	1589.0	168.0	0.123	1233	176.3	0.130	1244	- 4.70	- 0.89
8	13.9	34.5	4220	31.0	46.5	358.0	101.5	0.257	1473	105.3	0.270	1495	- 3.60	- 1.47
9	13.9	34.5	4220	31.0	53.5	482.1	126.0	0.209	1387	130.2	0.220	1406	- 2.90	- 1.35
10	13.9	34.5	4220	31.0	48.5	604.9	149.0	0.200	1371	146.3	0.196	1374	+ 1.85	- 0.22
11	13.9	34.5	4220	31.0	58.5	688.0	167.5	0.172	1321	169.3	0.172	1321	- 1.07	0
12	13.9	34.5	4220	31.0	65.5	616.0	167.5	0.192	1356	171.2	0.169	1326	- 2.16	+ 2.26
13	13.9	34.5	4220	21.0	7.0	486.9	101.5	0.245	1379	103.6	0.249	1380	- 2.03	- 0.07
14	13.9	34.5	4220	21.0	7.0	757.1	126.7	0.193	1281	125.0	0.189	1274	+ 1.36	+ 0.55
15	13.9	34.5	4220	21.0	4.0	1200.1	149.0	0.146	1191	147.0	0.142	1183	+ 1.36	+ 0.67
16	13.9	34.5	4220	21.0	3.0	1750.0	162.5	0.108	1121	163.5	0.109	1122	- 1.01	- 0.09

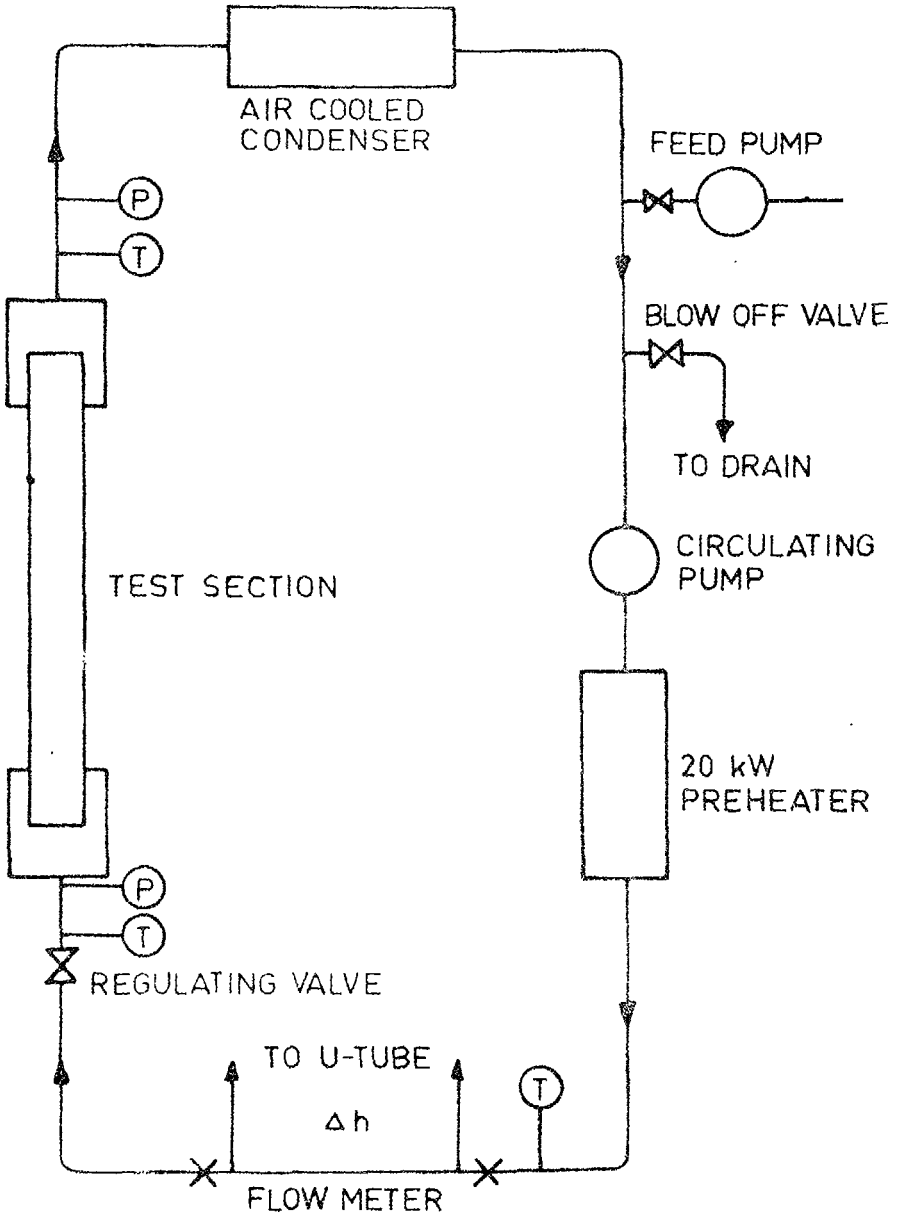

Fig. 1. Flow diagram.

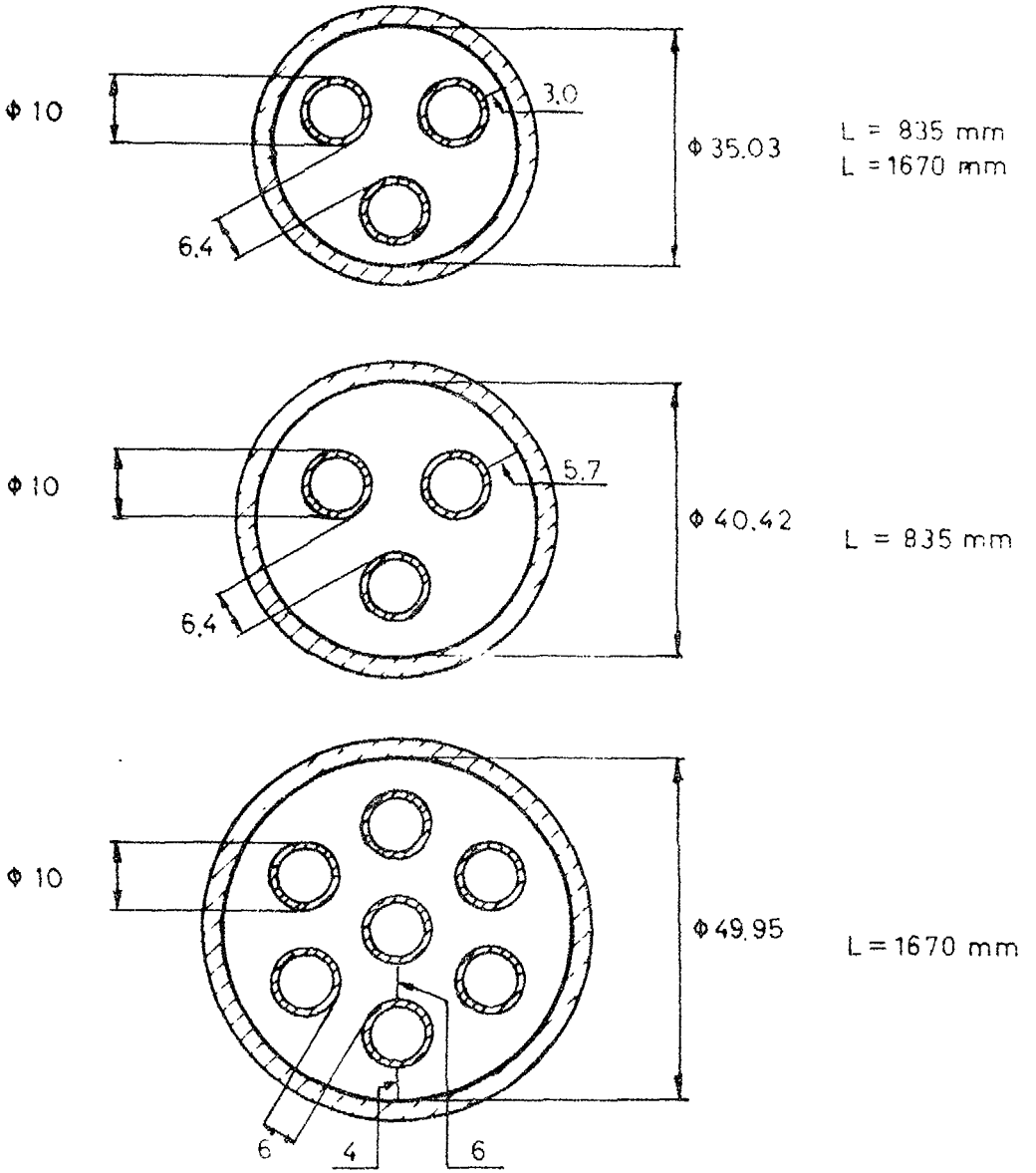

Fig. 2. Rod cluster cross sections.

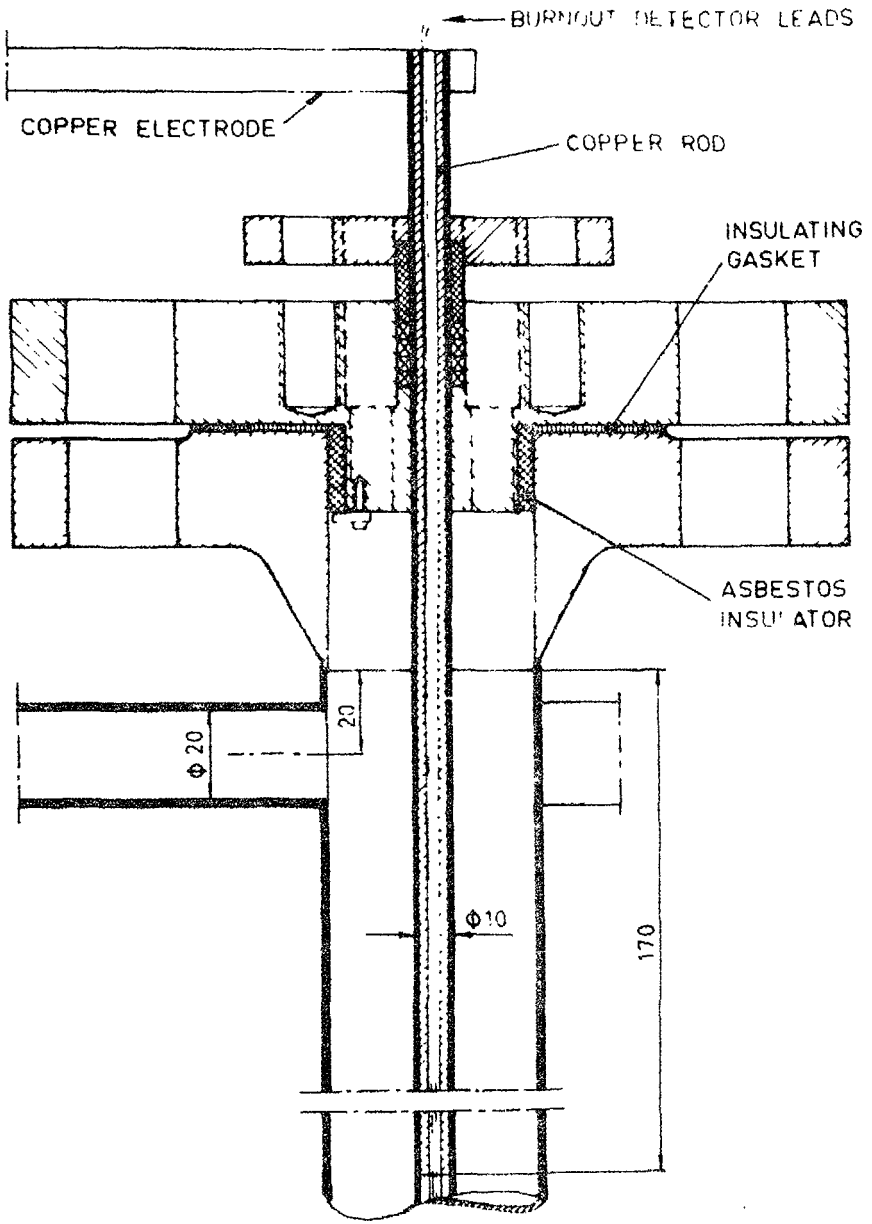

Fig. 3. End of test section.

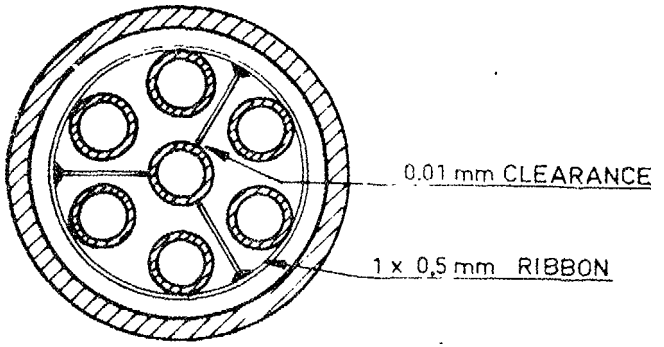

Fig. 4. Rod support.

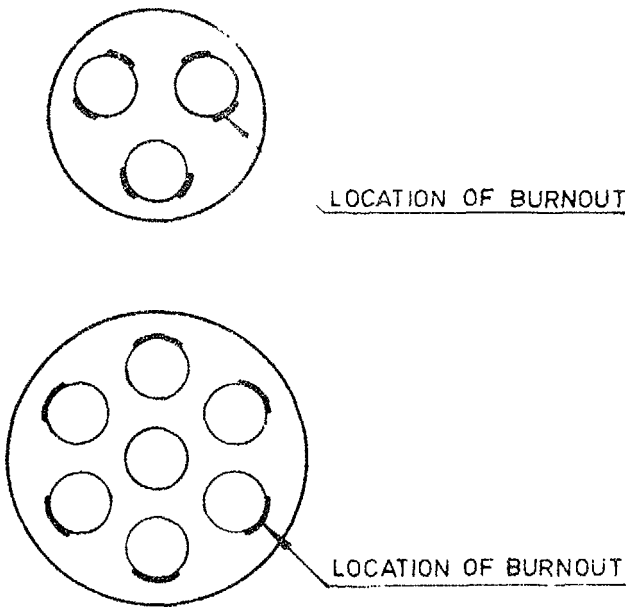

Fig. 5. Circumferential location of burnout.

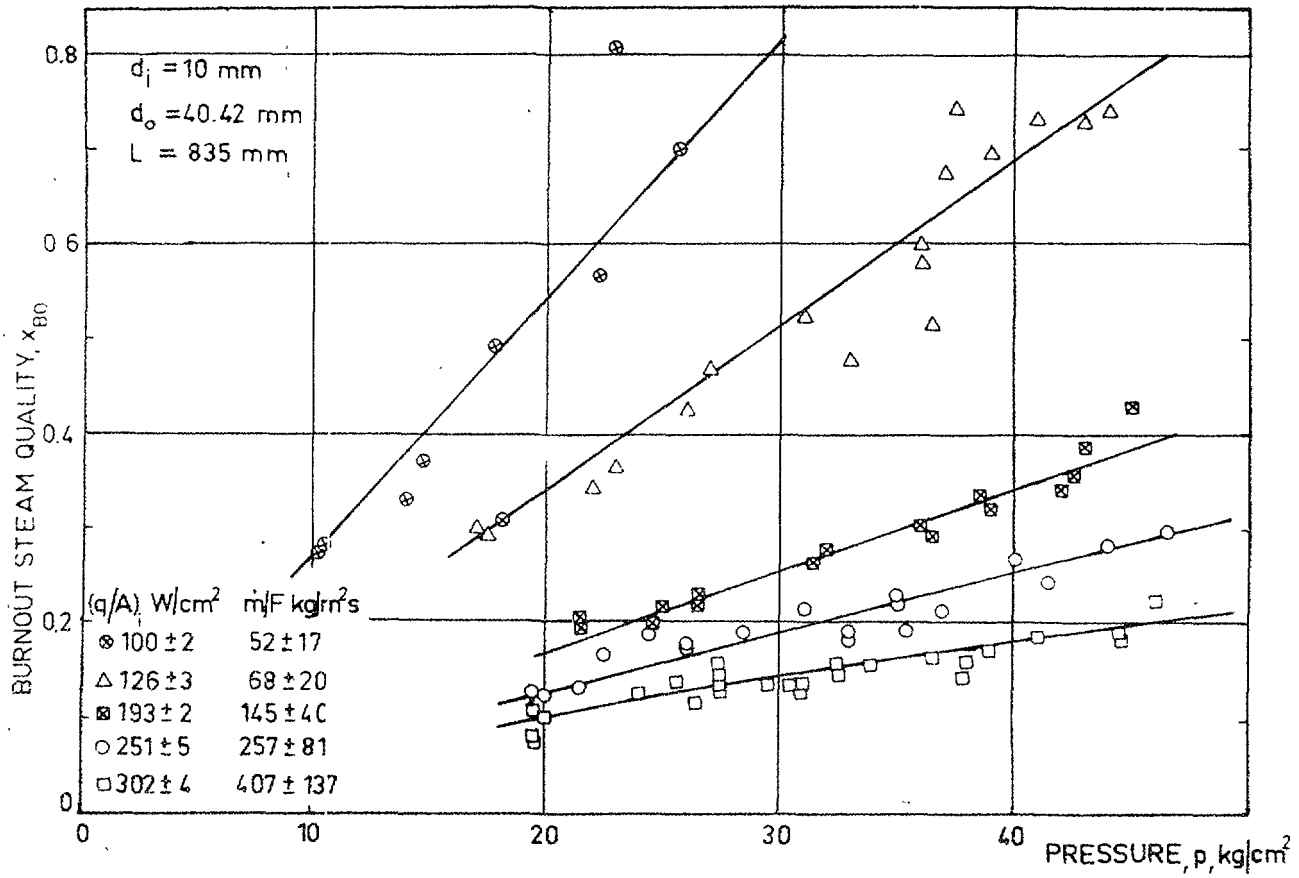

Fig. 6. Measured burnout conditions for internal heating.

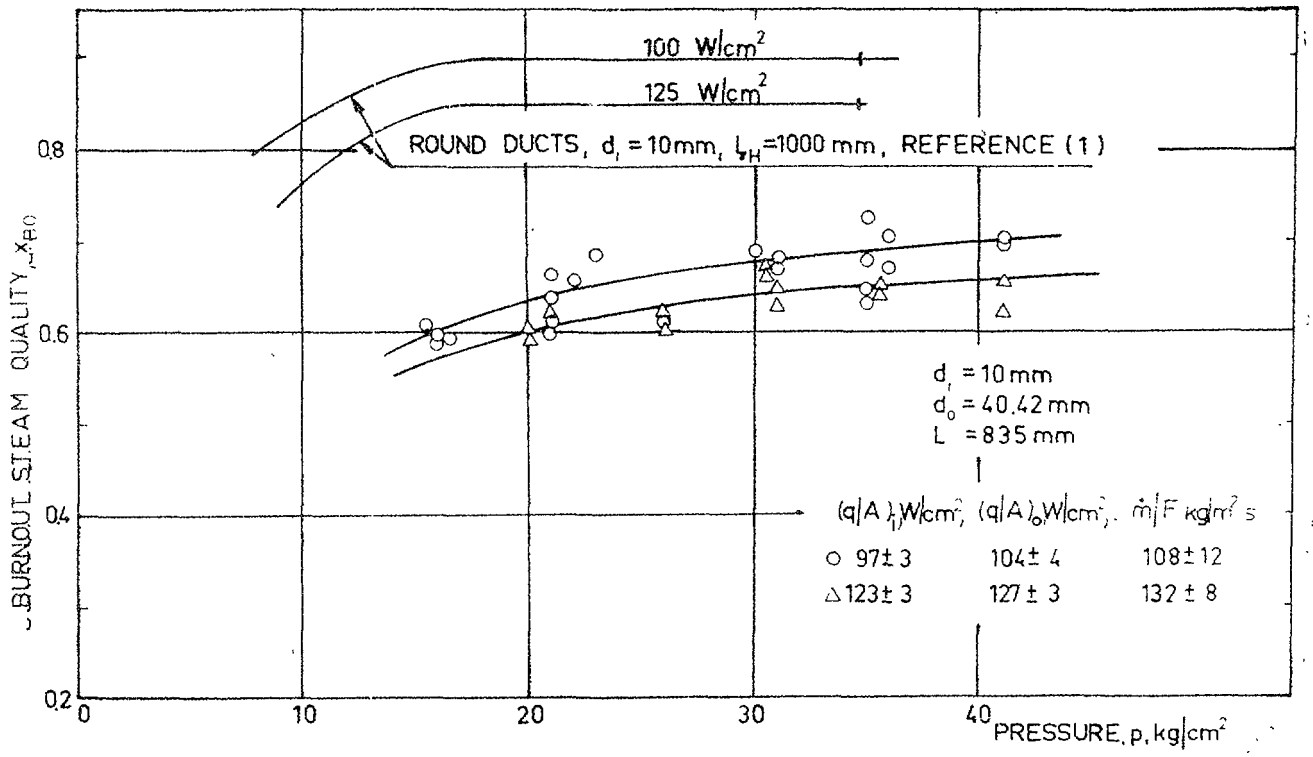

Fig. 7. Measured burnout conditions for total heating.

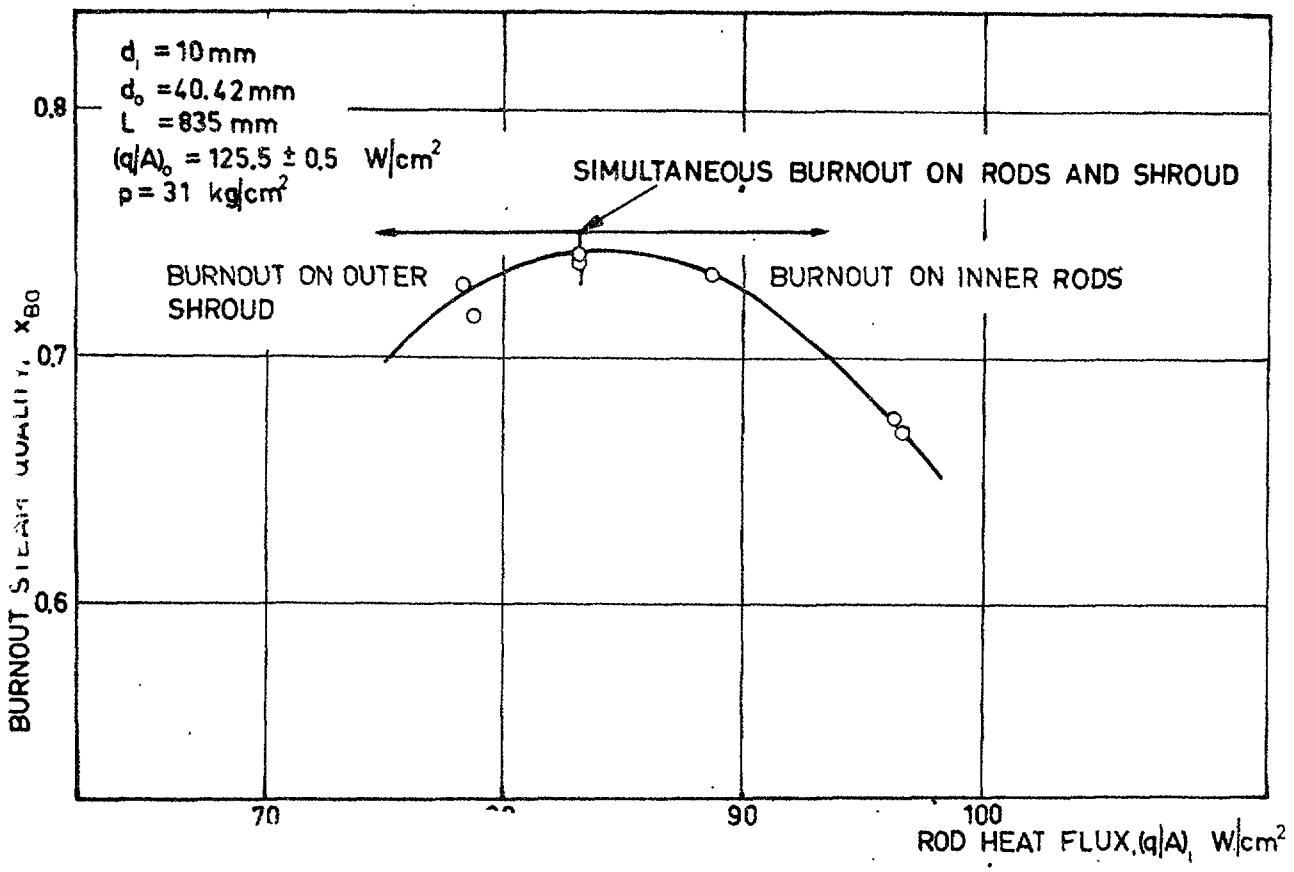

Fig. 8. Burnout conditions for non-uniform heating.

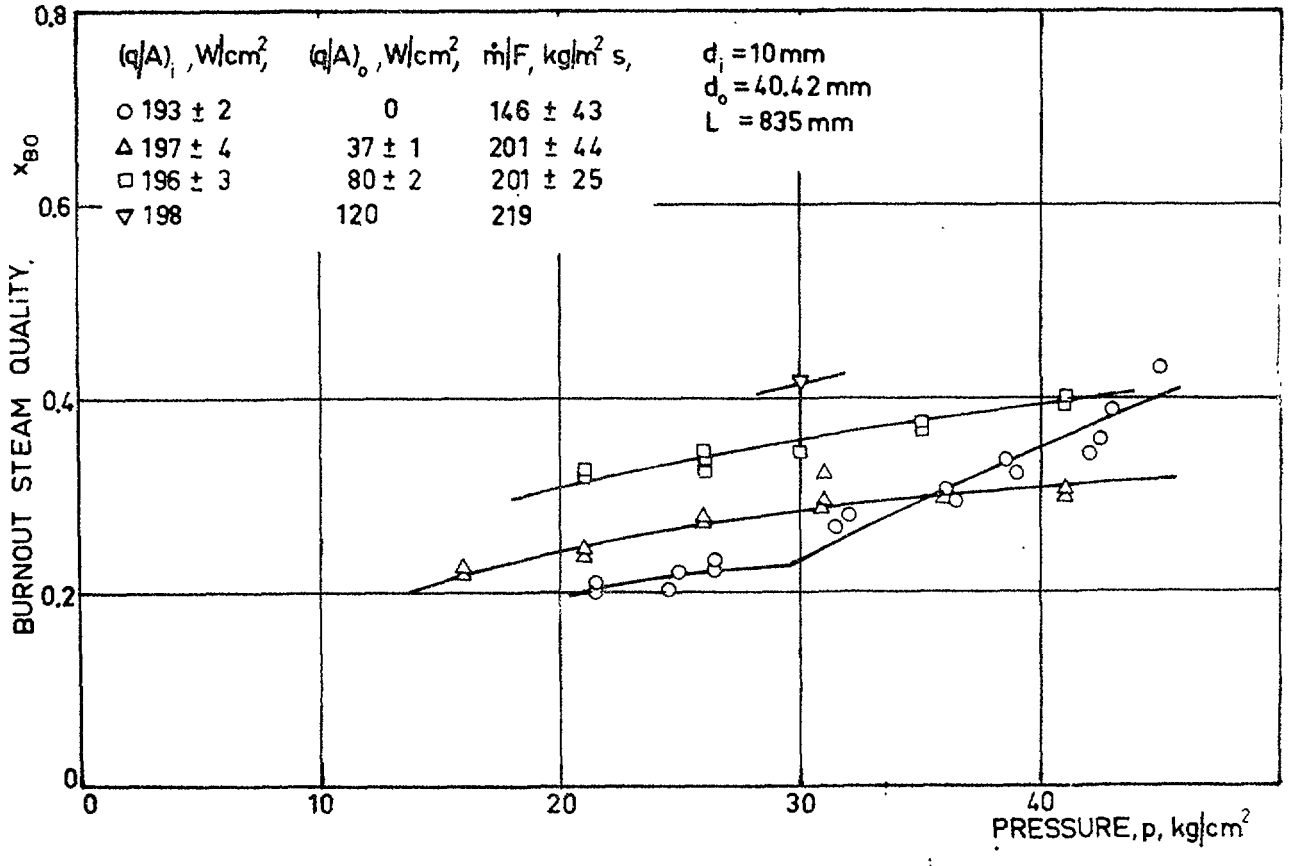

Fig. 9. Effect of outer surface heat flux.

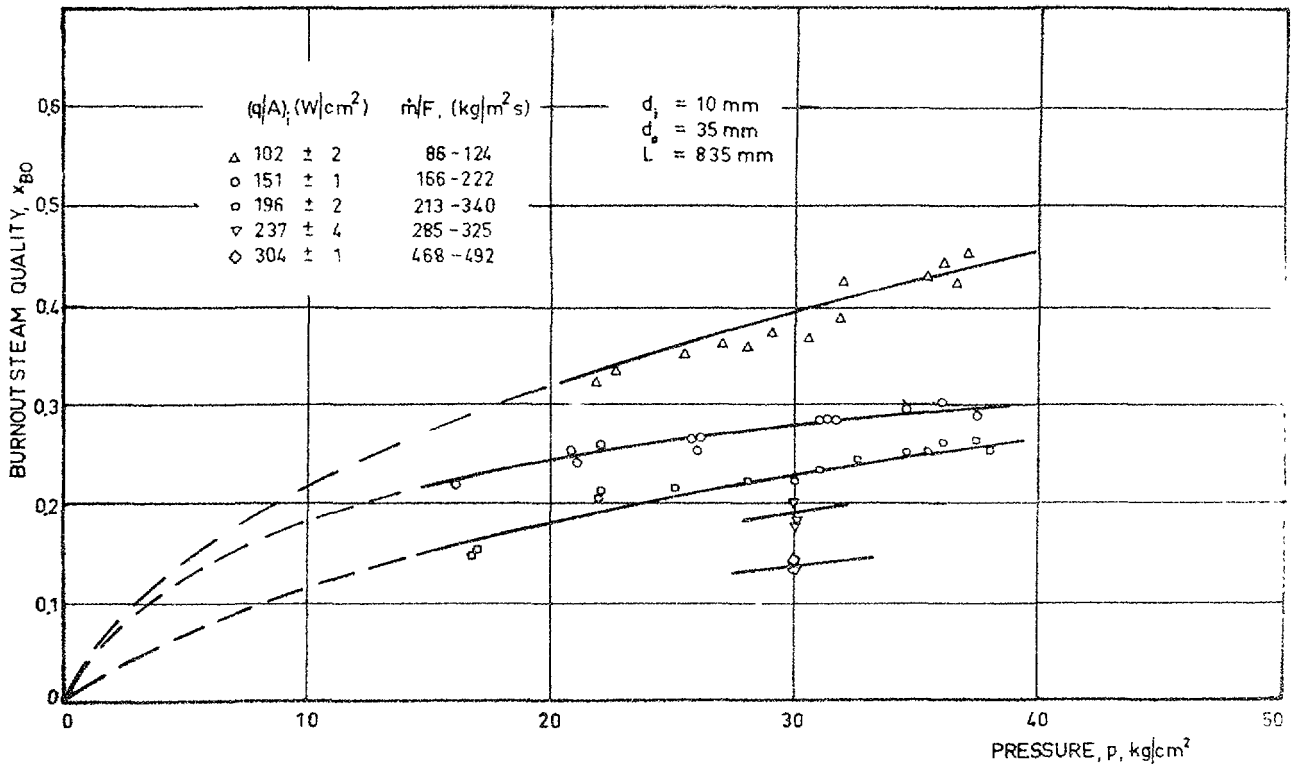

Fig. 10. Measured burnout cinditions for internal heating of 3-rod cluster.

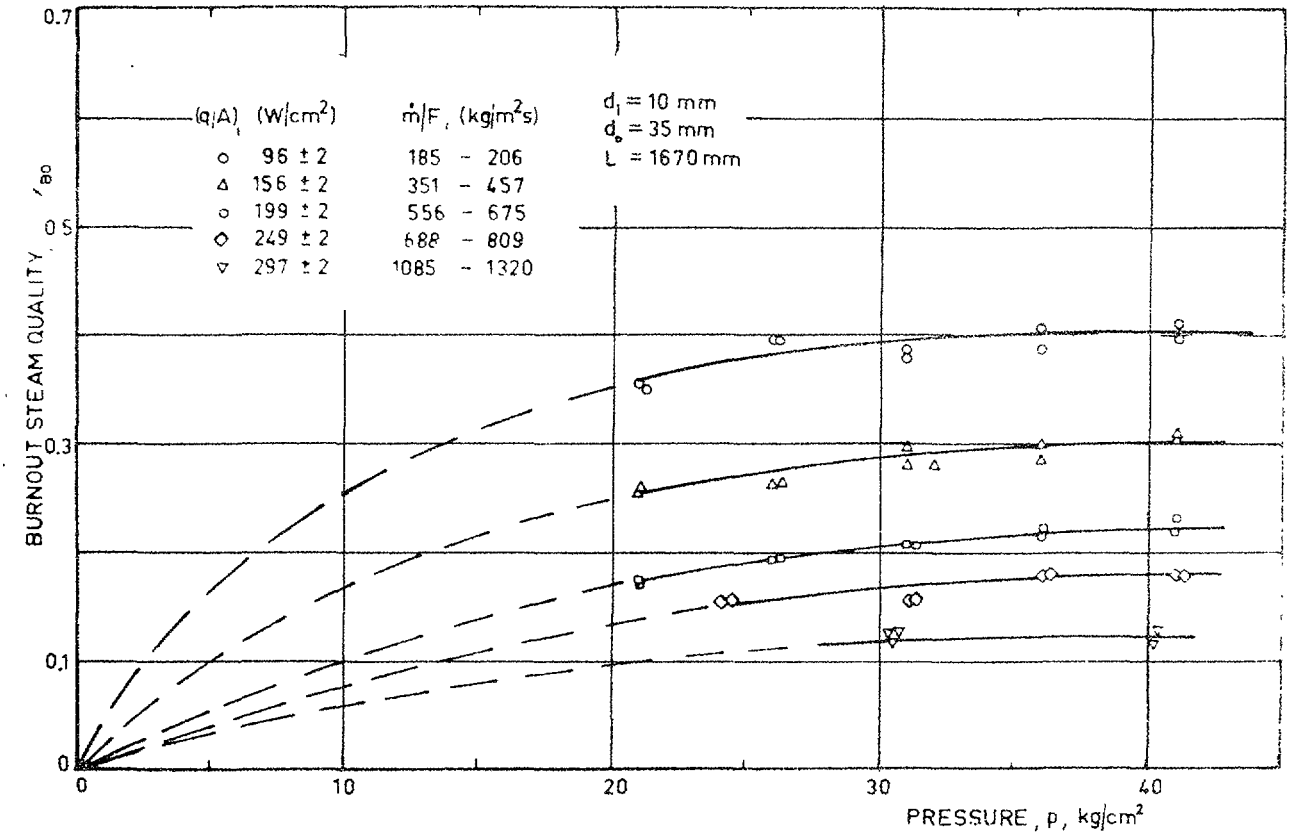

Fig. 11. Measured burnout conditions for internal heating of 3-rod cluster.

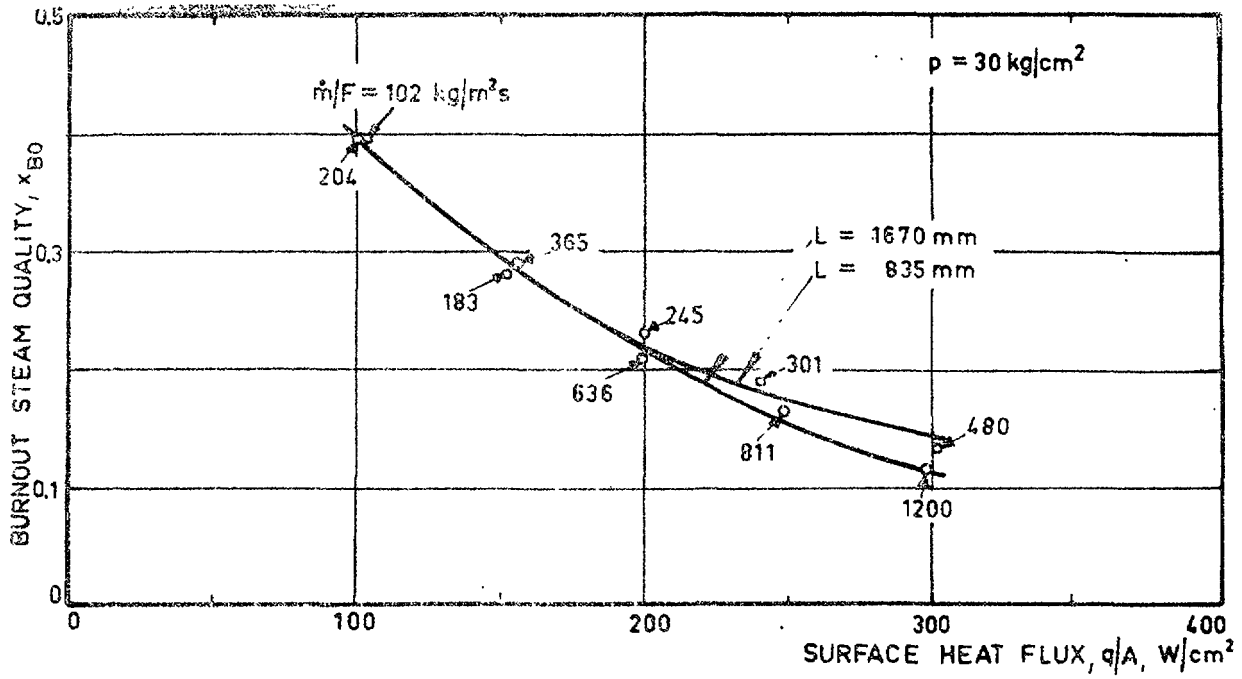

Fig. 12. Burnout steam quality versus surface heat flux.

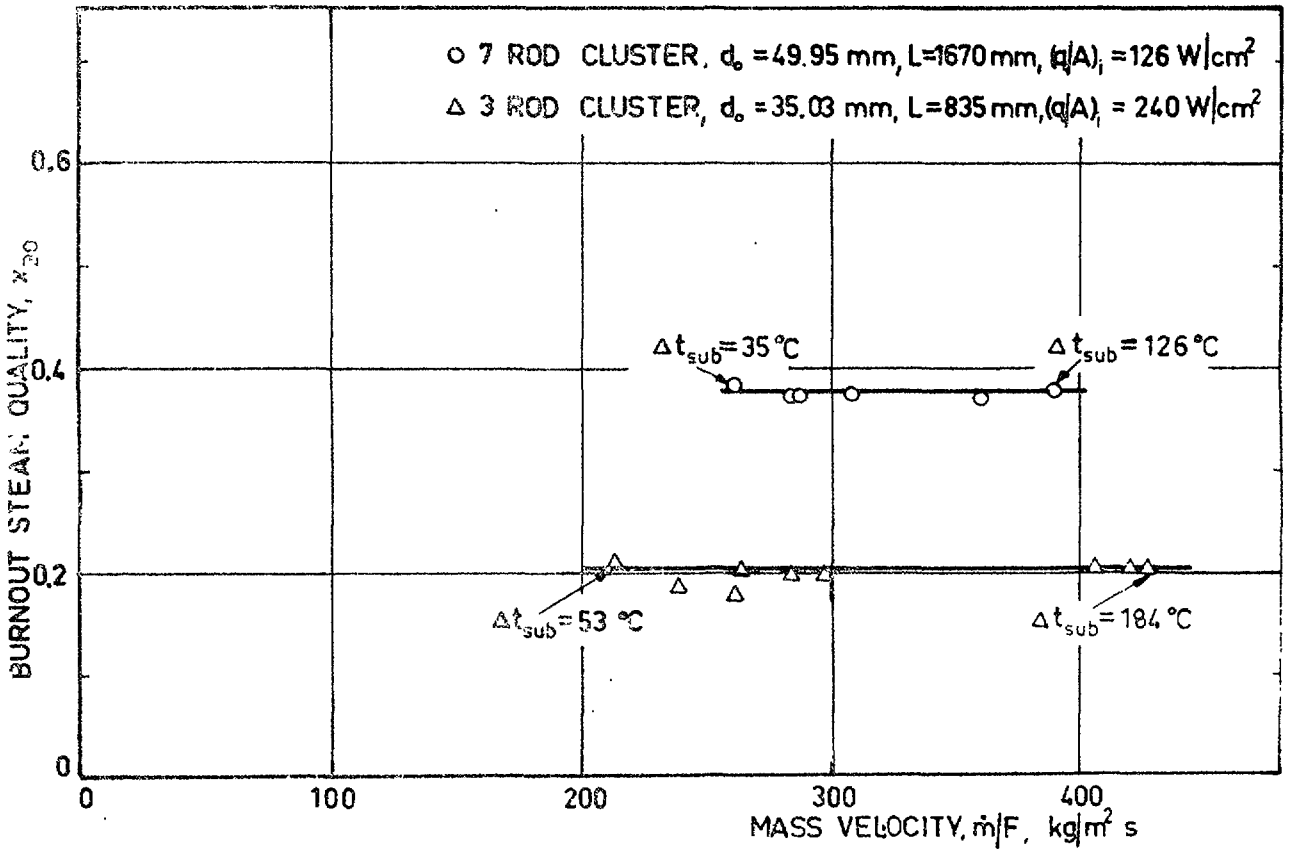

Fig. 13. Effect of mass velocity.

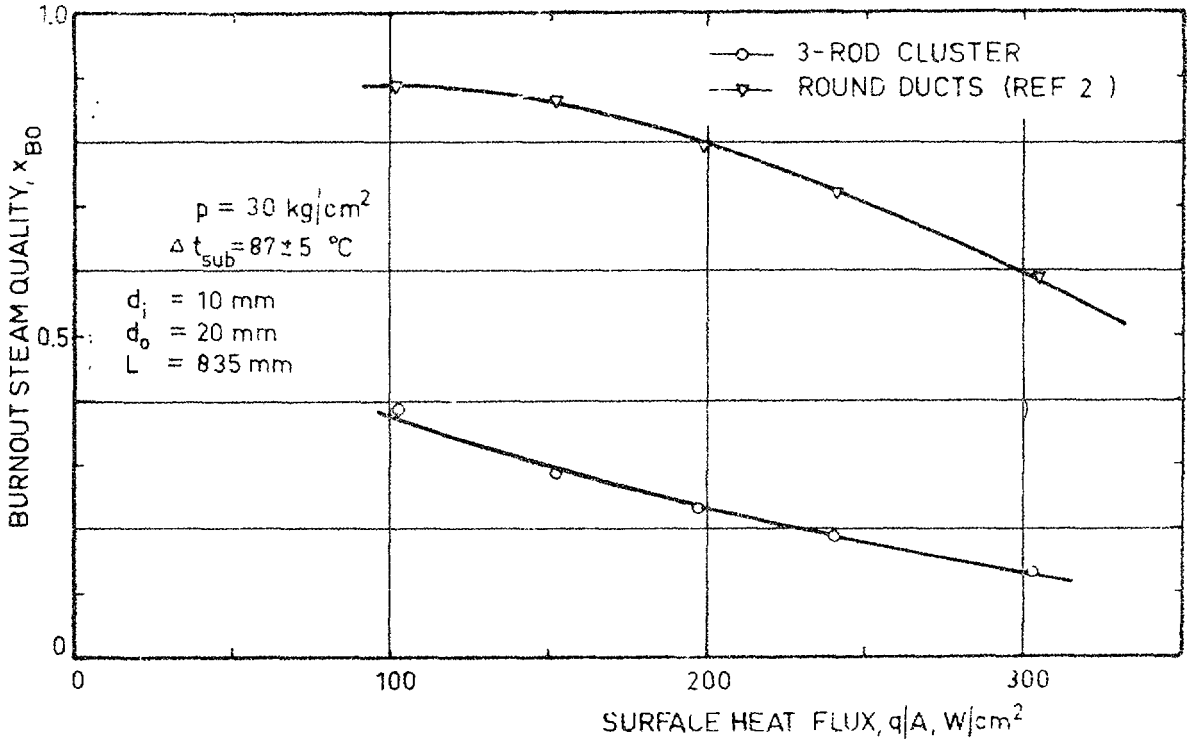

Fig. 14. Burnout conditions for 3-rod cluster compared with round duct results.

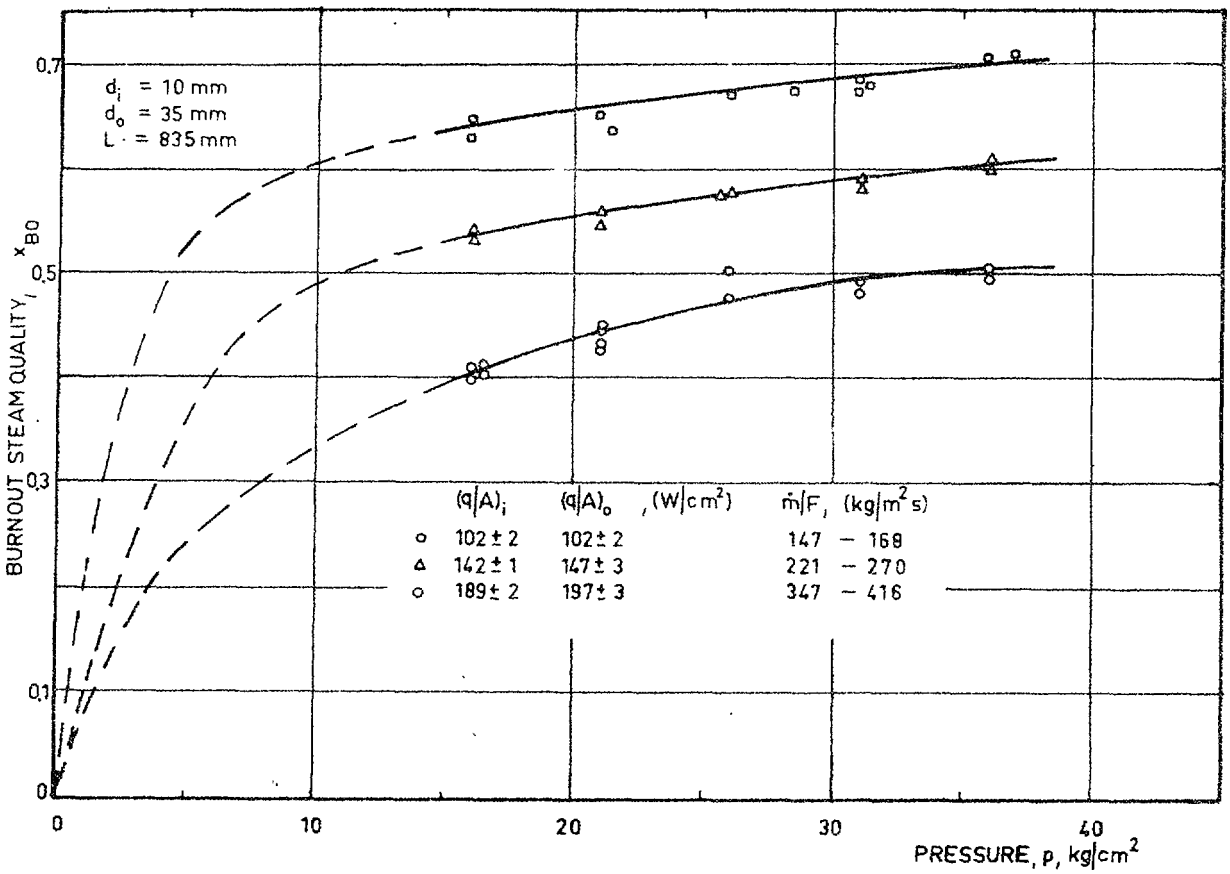

Fig. 15. Measured burnout conditions for total heating of 3-rod cluster.

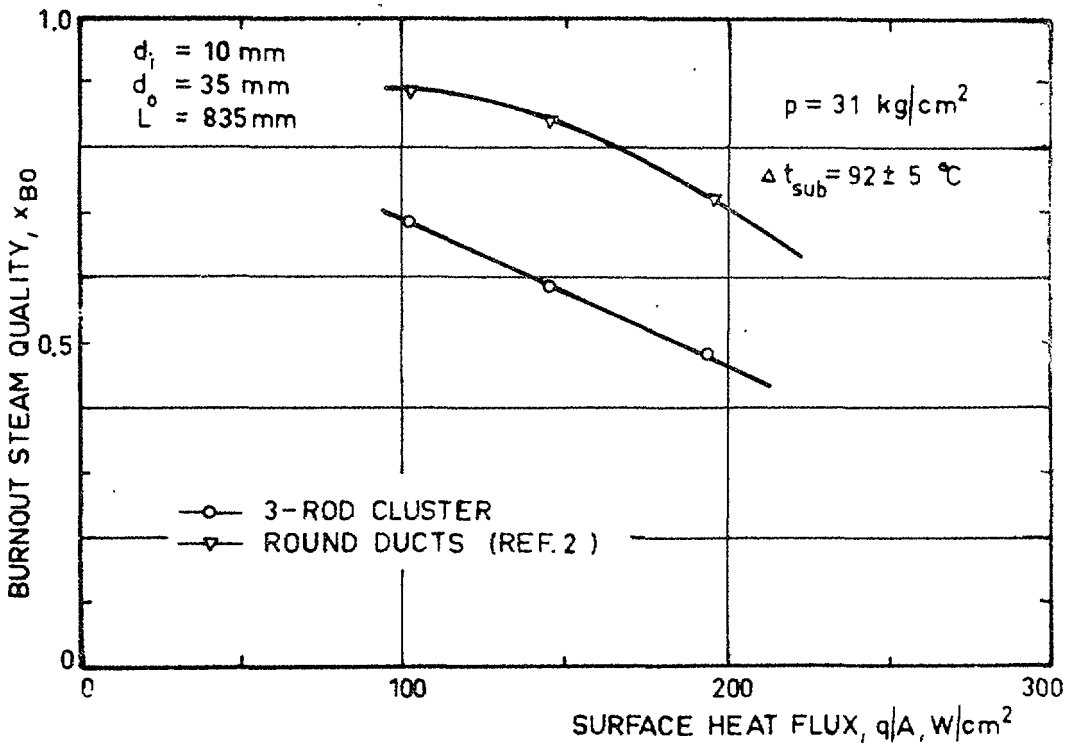

Fig. 16. Burnout conditions for totally heated 3-rod cluster compared with round duct results.

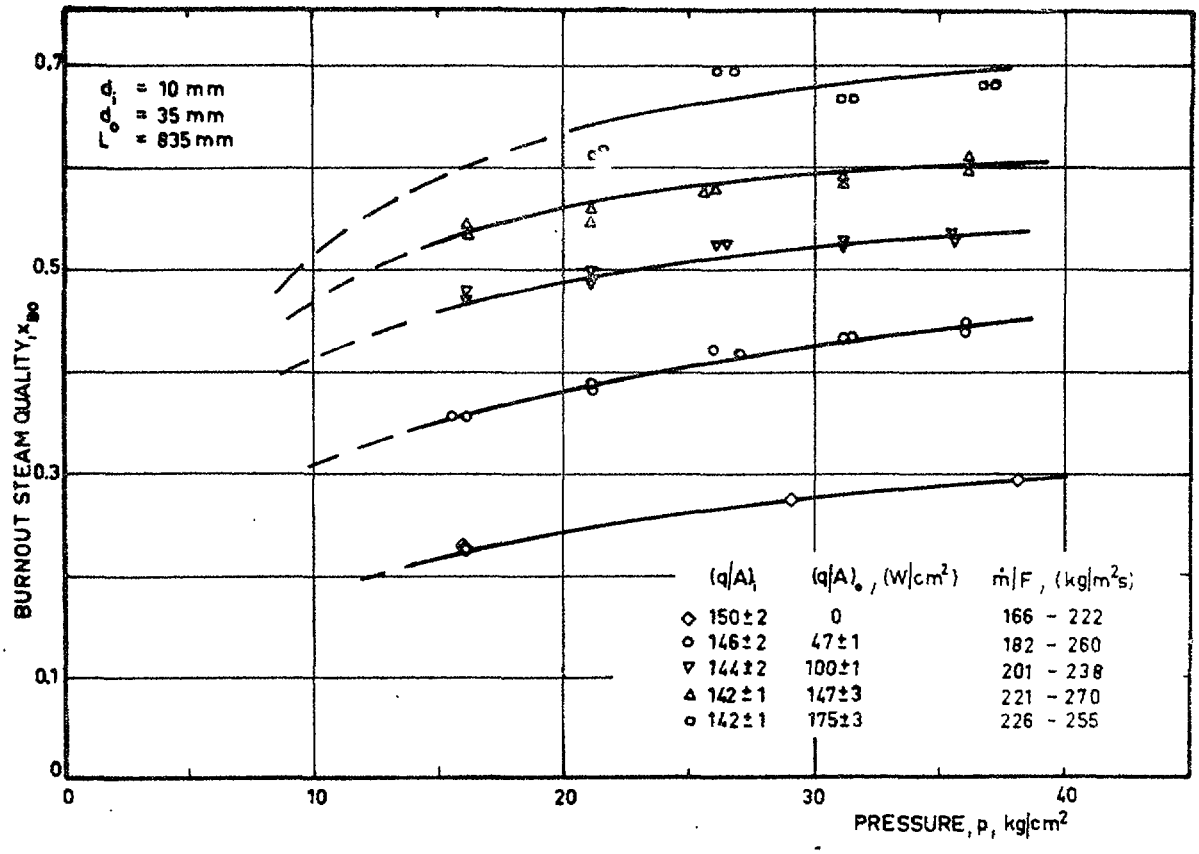

Fig. 17. Measured burnout conditions for dual nonuniform heating of 3-rod cluster.

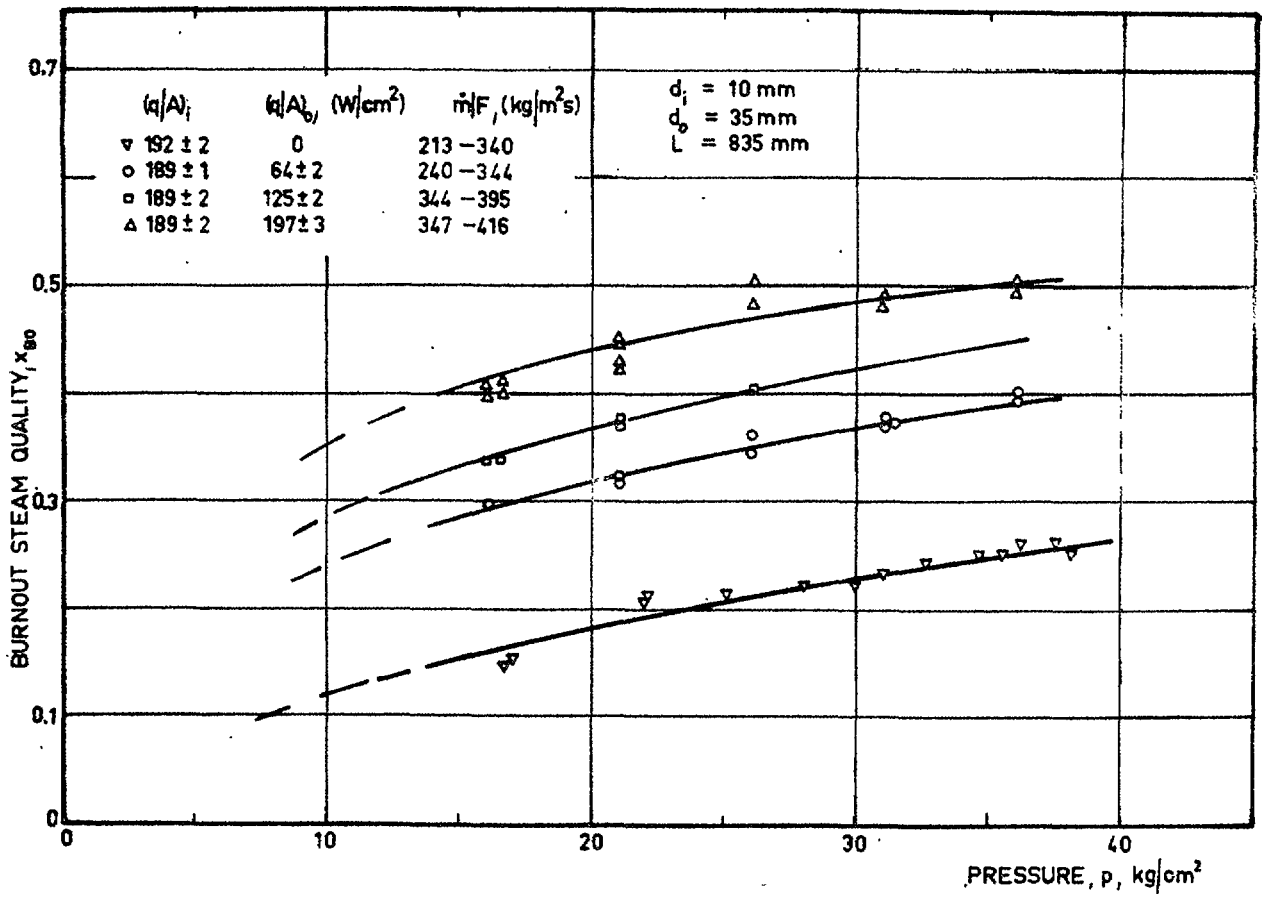

Fig. 18. Measured burnout conditions for dual nonuniform heating of 3-rod cluster.

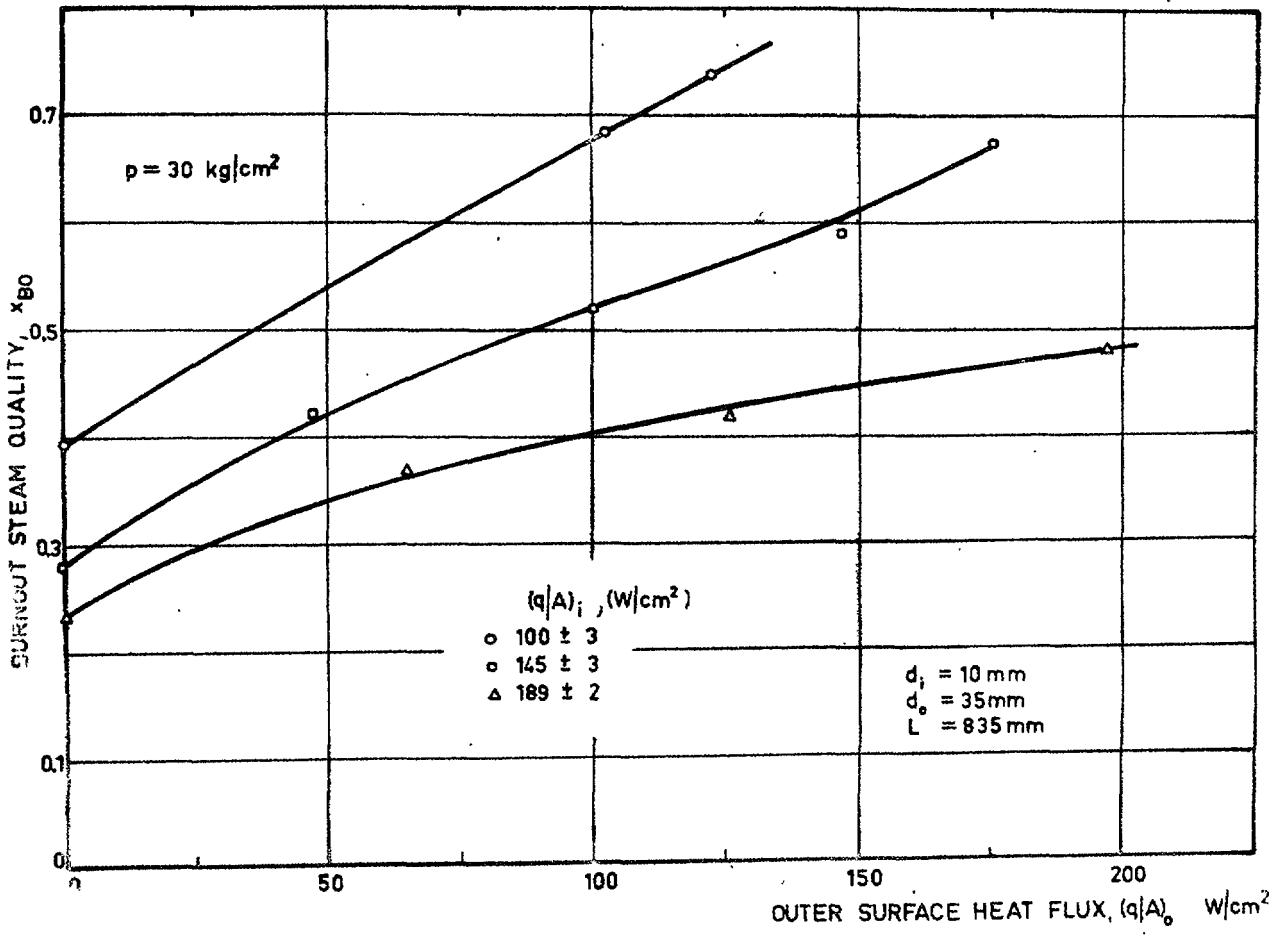

Fig. 19. Effect of outer surface heat flux.

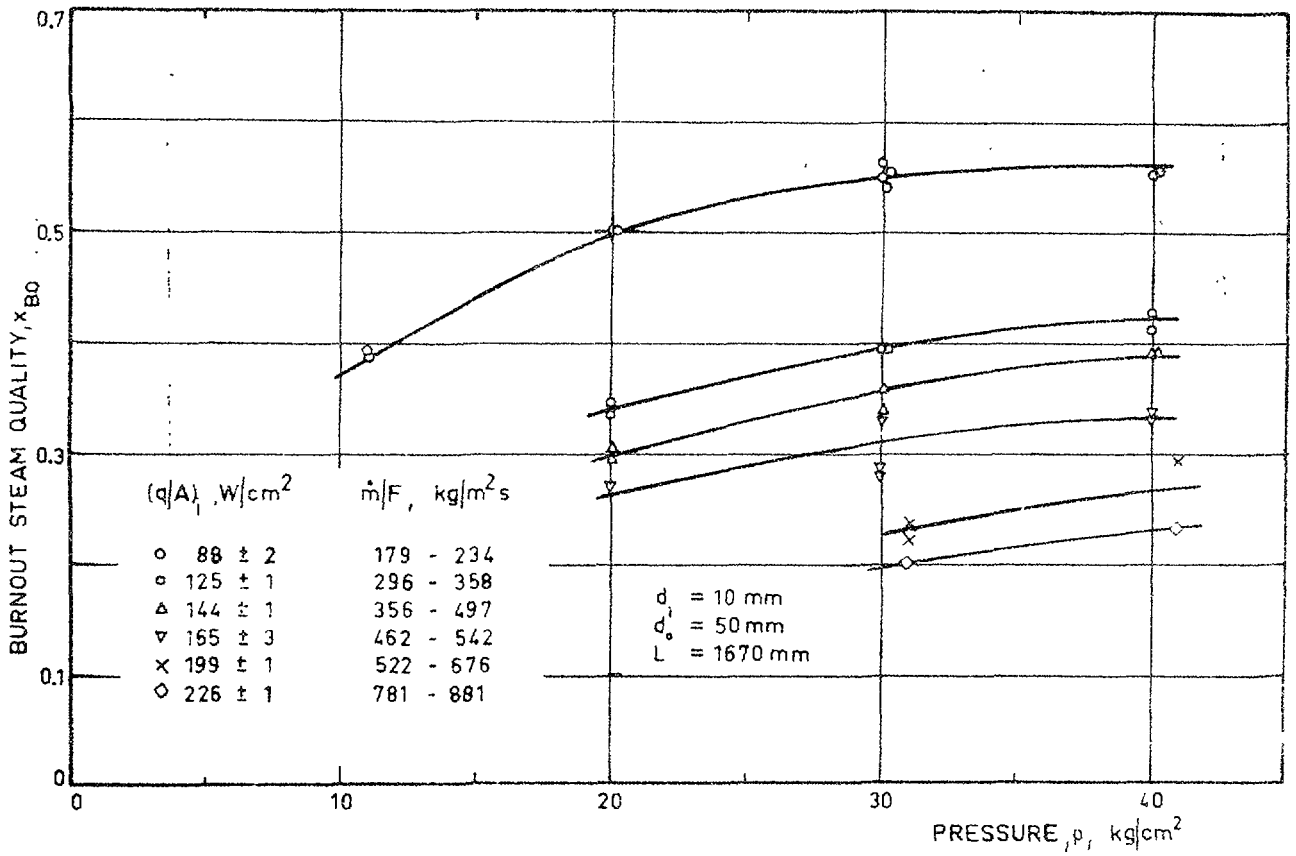

Fig. 20. Measured burnout conditions for 7-rod cluster.

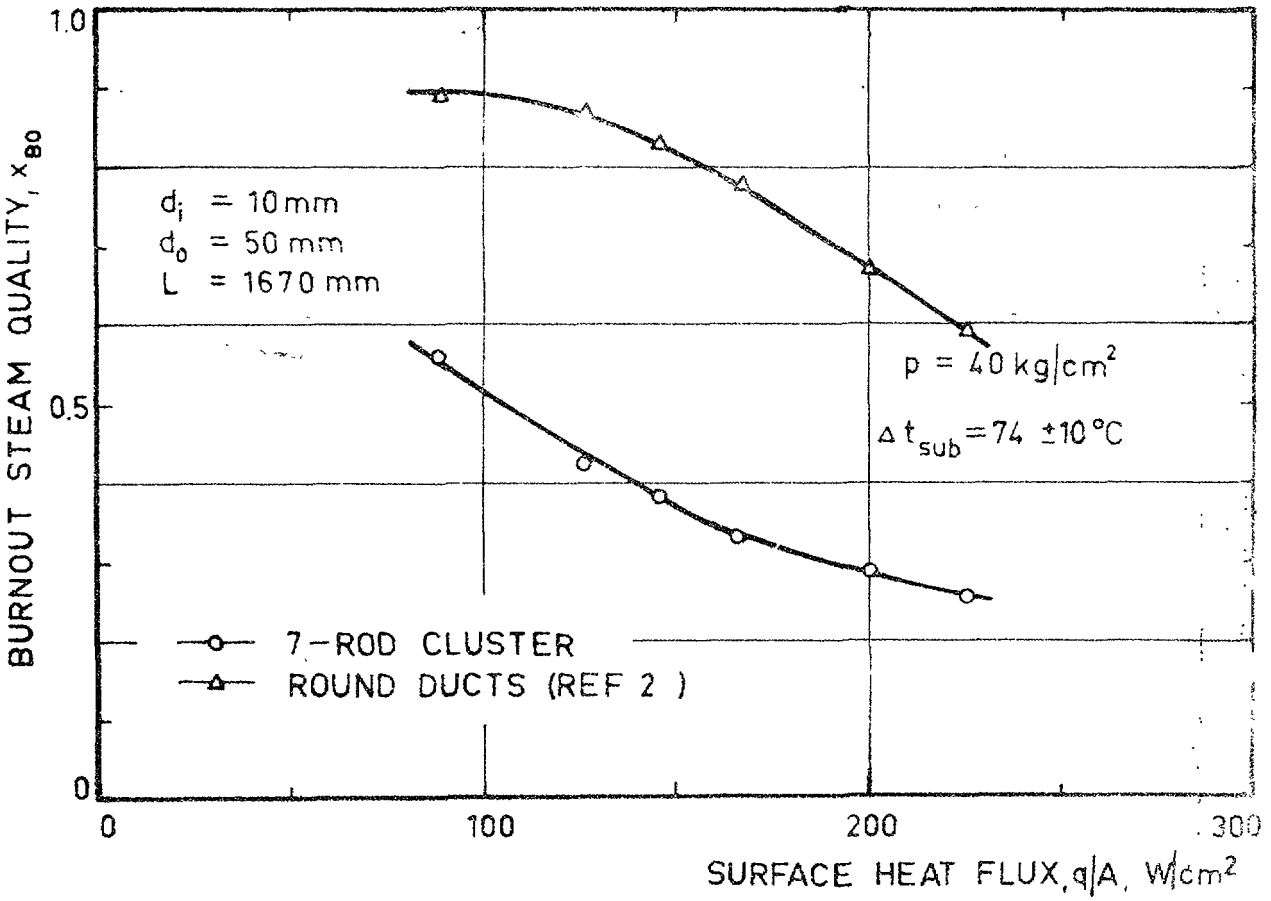

Fig. 21. Burnout conditions for 7-rod cluster compared with round duct results.

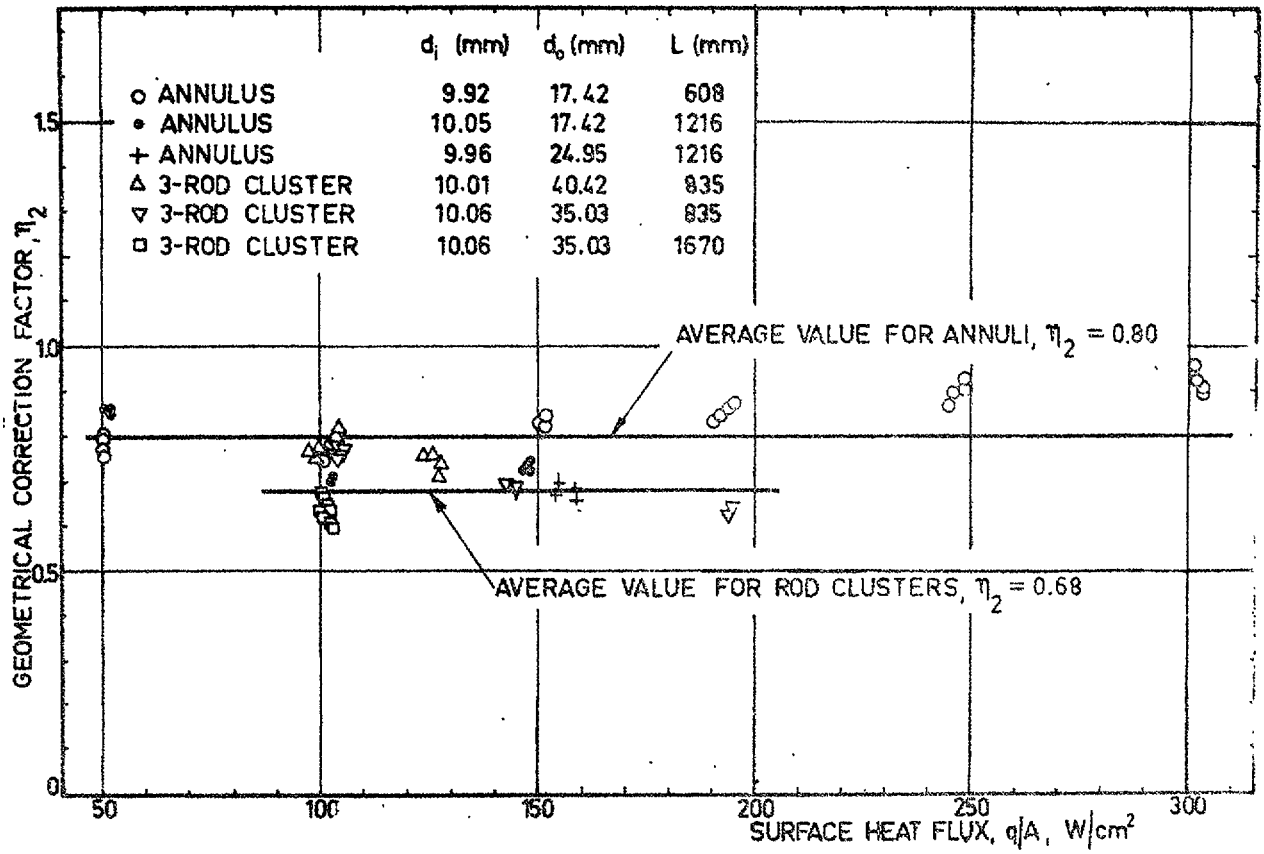

Fig. 22 Geometrical correction factor versus surface heat flux.

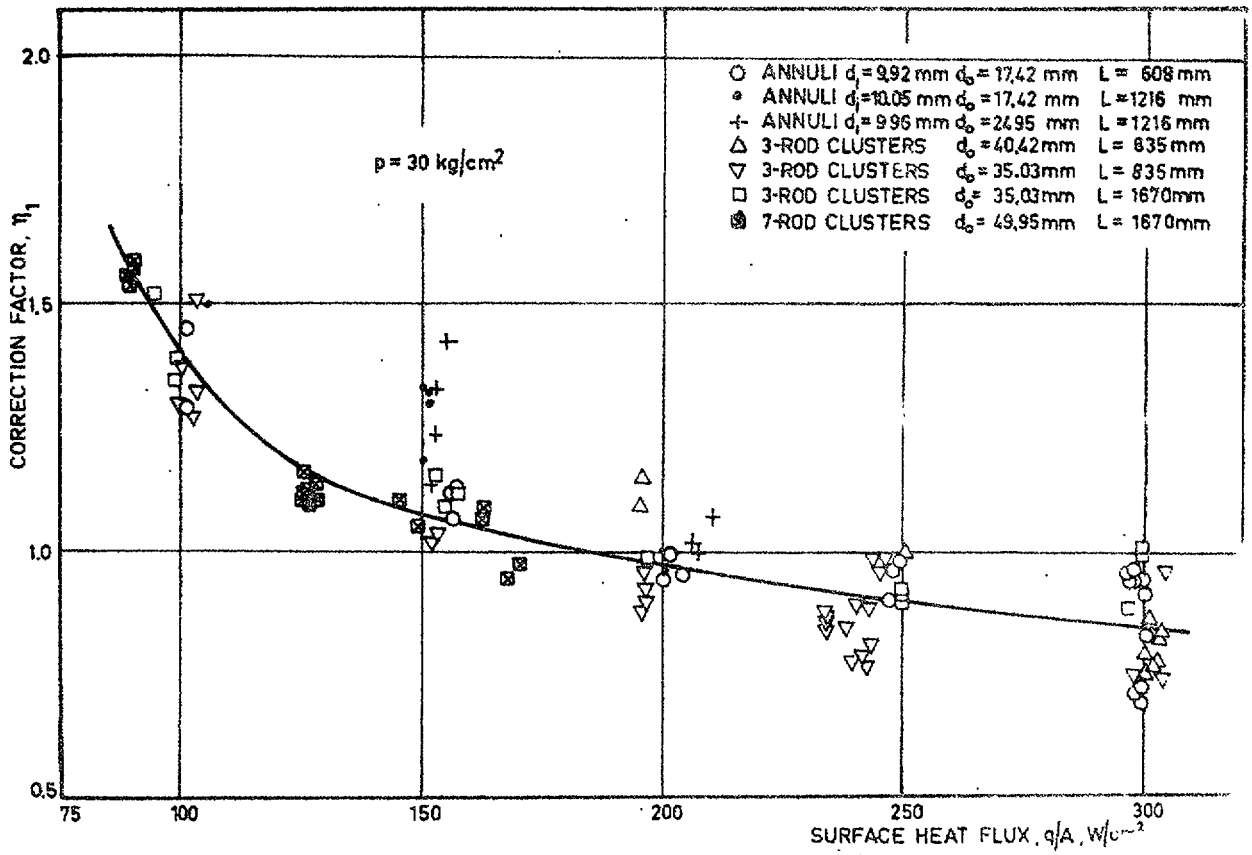

Fig. 23. Correction factor, η_1, for burnout correlation.

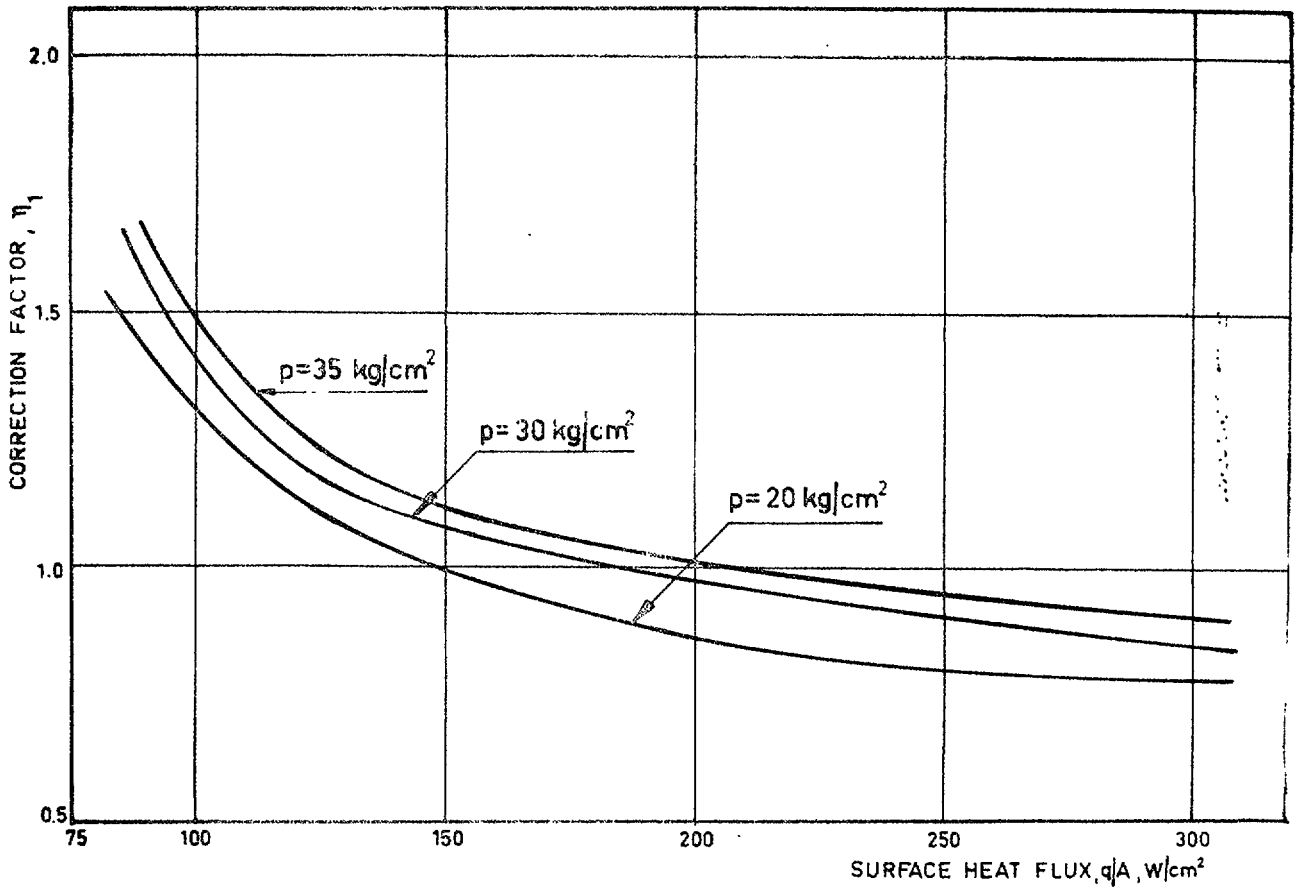

Fig. 24. Correction factor, η_1, for burnout correlation.

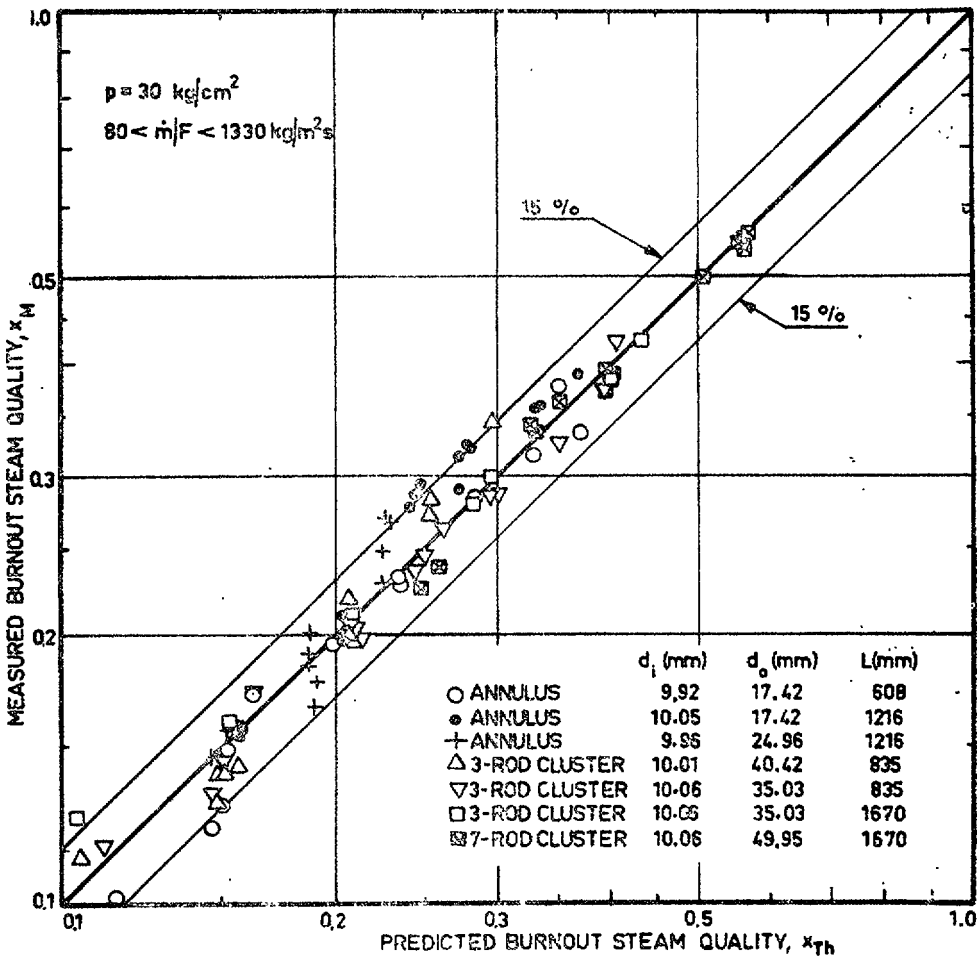

Fig. 25. Comparison between measured and predicted burnout steam qualities.

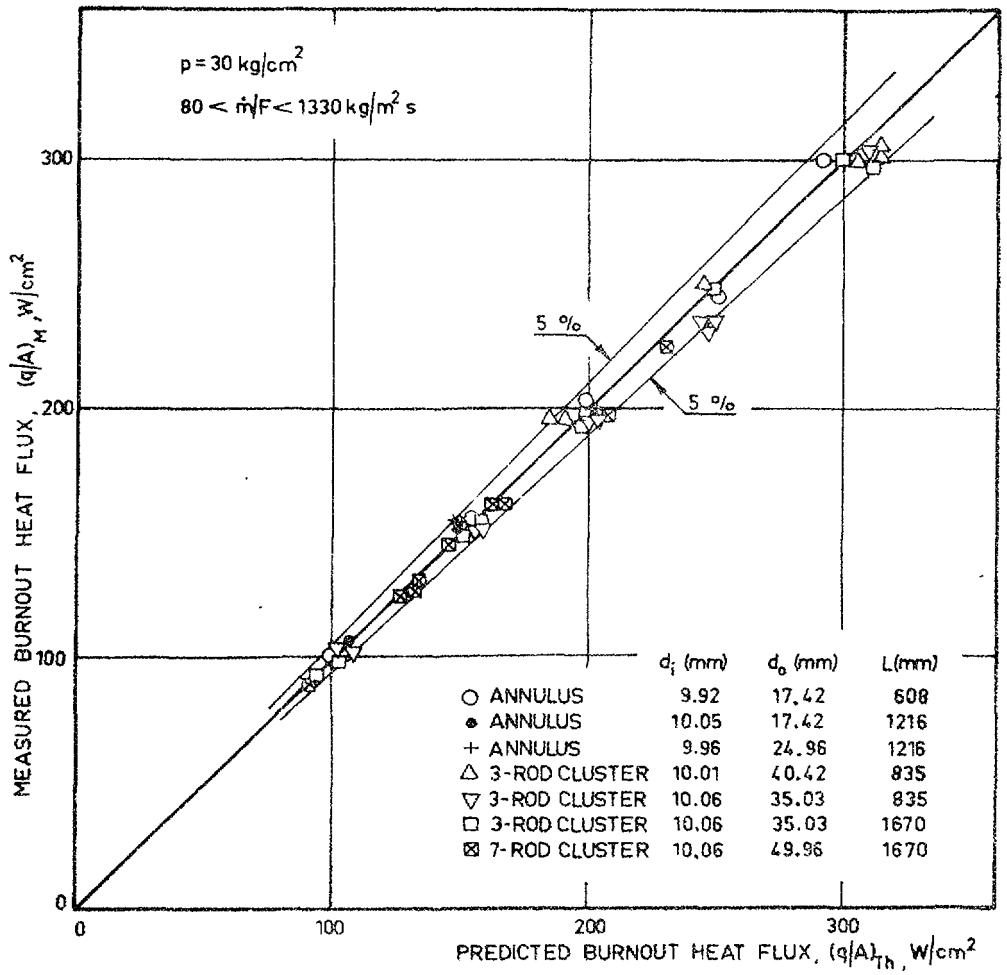

Fig. 26. Comparison between measured and predicted burnout heat fluxes.

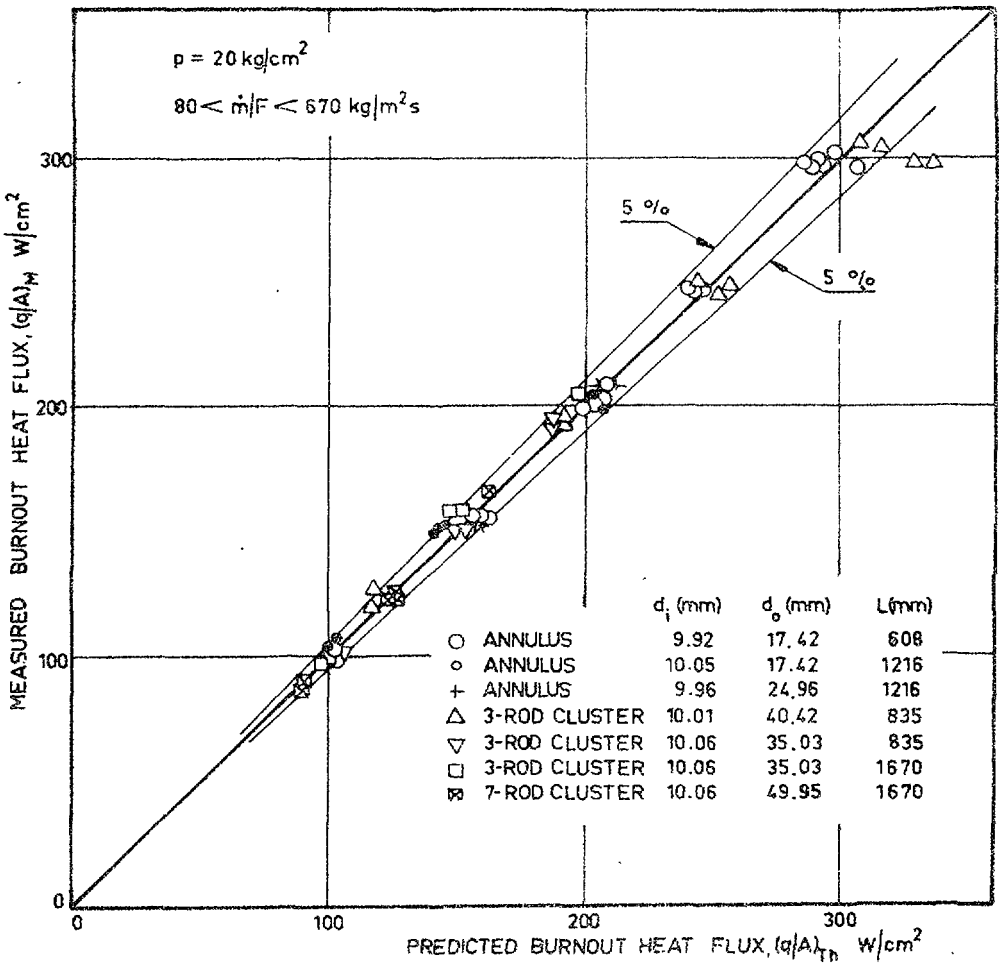

Fig. 27. Comparison between measured and predicted burnout heat fluxes.

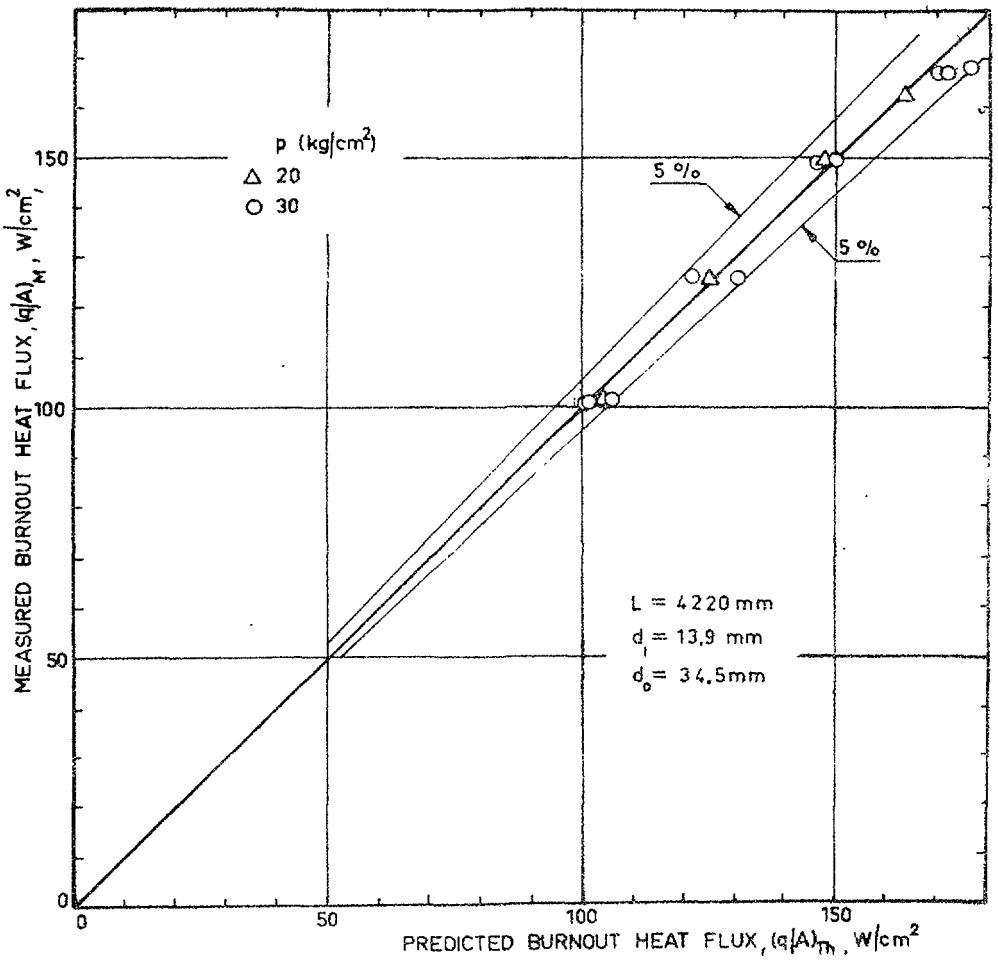

Fig. 28. Comparison between measured and predicted burnout heat fluxes in an annulus. (Data from reference 8).

LIST OF PUBLISHED AE-REPORTS

1—80. (See the back cover earlier reports.)

81. The resonance integral of niobium. By E. Hellstrand and G. Lundgren. 1962. 14 p. Sw. cr. 6:—.

82. Some chemical group separations of radioactive trace elements. By K. Samsahl. 1962. 18 p. Sw. cr. 6:—.

83. Void measurement by the (γ, n) reactions. By S. Z. Rouhani. 1962. 17 p. Sw. cr. 6,:—.

84. Investigation of the pulse height distribution of boron trifluoride proportional counters. By I. Ö. Andersson and S. Malmskog. 1962. 16 p. Sw. cr. 6,:—.

85. An experimental study of pressure gradients for flow of boiling water in vertical round ducts. (Part 3). By K. M. Becker, G. Hernborg and M. Bode. 1962. 29 p. Sw. cr. 6:—.

86. An experimental study of pressure gradients for flow of boiling water in vertical round ducts. (Part 4). By K. M. Becker, G. Hernborg and M. Bode. 1962. 19 p. Sw. cr 6:—.

87. Measurements of burnout conditions for flow of boiling water in vertical round ducts. By K. M. Becker. 1962. 38 p. Sw. cr. 6:—.

88. Cross sections for neutron inelastic scattering and (n, 2n) processes. By M. Leimdörfer, E. Bock and L. Arkeryd. 1962. 225 p. Sw. cr. 10:—.

89. On the solution of the neutron transport equation. By S. Depken. 1962. 43 p. Sw. cr. 6:—.

90. Swedish studies on irradiation effects in structural materials. By M. Grounes and H. P. Myers. 1962. 11 p. Sw. cr. 6:—.

91. The energy variation of the sensitivity of a polyethylene moderated BF_3 proportional counter. By R. Fräki, M. Leimdörfer and S. Malmskog. 1962. 12. Sw. cr. 6:—.

92. The backscattering of gamma radiation from plane concrete walls. By M. Leimdörfer. 1962. 20 p. Sw. cr. 6:—.

93. The backscattering of gamma radiation from spherical concrete walls. By M. Leimdörfer. 1962. 16 p. Sw. cr. 6:—.

94. Multiple scattering of gamma radiation in a spherical concrete wall room. By m. Leimdörfer. 1962. 18 p. Sw. cr. 6:—.

95. The paramagnetism of Mn dissolved in α and β brasses. By H. P. Myers and R. Westin. 1962. 13 p. Sw. cr. 6:—.

96. Isomorphic substitutions of calcium by strontium in calcium hydroxyapatite. By H. Christensen. 1962. 9 p. Sw. cr. 6:—.

97. A fast time-to-pulse height converter. By O. Aspelund. 1962. 21 p. Sw. cr. 6:—.

98. Neutron streaming in D_2O pipes. By J. Braun and K. Randén. 1962 41 p. Sw. cr. 6:—.

99. The effective resonance integral of thorium oxide rods. By J. Weitman. 1962. 41 p. Sw. cr. 6:—.

100. Measurements of burnout conditions for flow of boiling water in vertical annuli. By K. M. Becker and G. Hernborg. 1962. 41 p. Sw. cr. 6:—.

101. Solid angle computations for a circular radiator and a circular detector. By J. Konijn and B. Tollander. 1963. 6 p. Sw. cr. 8:—.

102. A selective neutron detector in the keV region utilizing the $^{19}F(n, \gamma)^{20}F$ reaction. By J. Konijn. 1963. 21 p. Sw. cr. 8:—.

103. Anion-exchange studies of radioactive trace elements in sulphuric acid solutions. By K. Samsahl. 1963. 12 p. Sw. cr. 8:—.

104. Problems in pressure vessel design and manufacture. By O. Hellström and R. Nilson. 1963. 44 p. Sw. cr. 8:—.

105. Flame photometric determination of lithium contents down to 10^{-3} ppm in water samples. By G. Jönsson. 1963. 9 p. Sw. cr. 8:—.

106. Measurements of void fractions for flow of boiling heavy water in a vertical round duct. By S. Z. Rouhani and K. M. Becker. 1963. 2nd rev. ed. 32 p. Sw. cr. 8:—.

107. Measurements of convective heat transfer from a horizontal cylinder rotating in a pool of water. K. M. Becker. 1963. 20 p. Sw. cr. 8:—.

108. Two-group analysis of xenon stability in slab geometry by modal expansion. O. Norinder. 1963. 50 p. Sw. cr. 8:—.

109. The properties of $CaSO_4Mn$ thermoluminescence dosimeters. B. Bjärngard. 1963. 27 p. Sw. cr. 8:—.

110. Semianalytical and seminumerical calculations of optimum material distributions. By C. I. G. Andersson. 1963. 26 p. Sw. cr. 8:—.

111. The paramagnetism of small amounts of Mn dissolved in Cu-Al and Cu-Ge alloys. By H. P. Myers and R. Westin. 1963. 7 p. Sw. cr. 8:—.

112. Determination of the absolute disintegration rate of Cs^{137}-sources by the tracer method. S. Hellström and D. Brune. 1963. 17 p. Sw. cr. 8:—.

113. An analysis of burnout conditions for flow of boiling water in vertical round ducts. By K. M. Becker and P. Persson. 1963. 28 p. Sw. cr 8:—.

114. Measurements of burnout conditions for flow of boiling water in vertical round ducts (Part 2). By K. M. Becker, et al. 1963. 29 p. Sw. cr. 8:—.

115. Cross section measurements of the $^{58}Ni(n, p)^{58}Co$ and $^{29}Si(n,\alpha_m)^{26}Mg$ reactions in the energy range 2.2 to 3.8 MeV. By J. Konijn and A. Lauber 1963. 30 p. Sw. cr. 8:—.

116. Calculations of total and differential solid angles for a proton recoil solid state detector. By J. Konijn, A. Lauber and B. Tollander. 1963. 31 p. Sw. cr. 8:—.

117. Neutron cross sections for aluminium. By L. Forsberg. 1963. 32 p. Sw. cr. 8:—.

118. Measurements of small exposures of gamma radiation with $CaSO_4$:Mn radiothermoluminescence. By B. Bjärngard. 1963. 18 p. Sw. cr. 8:—.

119. Measurement of gamma radioactivity in a group of control subjects from the Stockholm area during 1959—1963. By I. Ö. Andersson, I. Nilsson and Eckerstig. 1963. 19 p. Sw. cr. 8:—.

120. The thermox process. By O. Tjälldin. 1963. 38 p. Sw. cr. 8:—.

121. The transistor as low level switch. By A. Lydén. 1963. 47 p. Sw. cr. 8:—.

122. The planning of a small pilot plant for development work on aqueous reprocessing of nuclear fuels. By T. U. Sjöborg, E. Haeffner and Hultgren. 1963. 20 p. Sw. cr. 8:—.

123. The neutron spectrum in a uranium tube. By E. Johansson, E. Jonsson, M. Lindberg and J. Mednis. 1963. 36 p. Sw. cr. 8:—.

124. Simultaneous determination of 30 trace elements in cancerous and noncancerous human tissue samples with gamma-ray spectrometry. K. Samsahl, D. Brune and P. O. Wester. 1963. 23 p. Sw. cr. 8:—.

125. Measurement of the slowing-down and thermalization time of neutrons in water. By E. Möller and N. G. Sjöstrand. 1963. 42 p. Sw. cr. 8:—.

126. Report on the personnel dosimetry at AB Atomenergi during 1962. By K-A. Edvardsson and S. Hagsgård. 1963. 12 p. Sw. cr. 8:—.

127. A gas target with a tritium gas handling system. By B. Holmqvist and T. Wiedling. 1963. 12 p. Sw. cr. 8:—.

128. Optimization in activation analysis by means of epithermal neutrons. Determination of molybdenum in steel. By D. Brune and K. Jirlow. 1963. 11 p. Sw. cr. 8:—.

129. The P_1-approximation for the distribution of neutrons from a pulsed source in hydrogen. By A. Claesson. 1963. 18 p. Sw. cr. 8:—.

130. Dislocation arrangements in deformed and neutron irradiated zirconium and zircaloy-2. By R. B. Roy. 1963 18 p. Sw. cr. 8:—.

131. Measurements of hydrodynamic instabilities, flow oscillations and burnout in a natural circulation loop. By K. M. Becker, R. P. Mathisen, O. Eklind and B. Norman. 1964. 21 p. Sw. cr. 8:—.

132. A neutron rem counter. By I. Ö. Andersson and J. Braun. 1964. 14 p. Sw. cr. 8:—.

133. Studies of water by scattering of slow neutrons. By K. Sköld, E. Pilcher and K. E. Larsson. 1964. 17 p. Sw. cr. 8:—.

134. The amounts of As, Au, Br, Cu, Fe, Mo, Se, and Zn in normal and uraemic human whole blood. A comparison by means of neutron activation analysis. By D. Brune, K. Samsahl and P. O. Wester. 1964. 10 p. Sw. cr. 8:—.

135. A Monte Carlo method for the analysis of gamma radiation transport from distributed sources in laminated shields. By M. Leimdörfer. 1964. 28 p. Sw. cr. 8:—.

136. Ejection of uranium atoms from UO_2 by fission fragments. By G. Nilsson. 1964. 38 p. Sw. cr. 8:—.

137. Personnel neutron monitoring at AB Atomenergi. By S. Hagsgård and C-O. Widell. 1964. 11 p. Sw. cr. 8:—.

138. Radiation induced precipitation in iron. By B. Solly. 1964. 8 p. Sw. cr. 8:—.

139. Angular distributions of neutrons from (p, n)-reactions in some mirror nuclei. By L. G. Strömberg, T. Wiedling and B. Holmqvist. 1964. 28 p. Sw. cr. 8:.

140. An extended Greuling-Goertzel approximation with a P_n-approximation in the angular dependence. By R. Håkansson. 1964. 21 p. Sw. cr. 8:—.

141. Heat transfer and pressure drop with rough surfaces, a literature survey. By A. Bhattachayya. 1964. 78 p. Sw. cr. 8:—.

142. Radiolysis of aqueous benzene solutions. By. H. Christensen. 1964. 40 p. Sw. cr. 8:—.

143. Cross section measurements for some elements suited as thermal spectrum indicators: Cd, Sm, Gd and Lu. By E. Sokolowski, H. Pekarek and E. Jonsson. 1964. 27 p. Sw. cr. 8:—.

144. A direction sensitive fast neutron monitor. By B. Antolkovic, B. Holmqvist and T. Wiedling. 1964. 14 p. Sw. cr. 8:—.

145. A user's manual for the NRN shield design method. By L. Hjärne. 1964. 107 p. Sw. cr. 10:—.

146. Concentration of 24 trace elements in human heart tissue determined by neutron activation analysis. By P. O. Wester. 1964. 33 p. Sw. cr. 8:—.

147. Report on the personnel Dosimetry at AB Atomenergi during 1963. By K.-A. Edvardsson and S. Hagsgård. 1964. 16 p. Sw. cr. 8:—.

148. A calculation of the angular moments of the kernel for a monatomic gas scatterer. By R. Håkansson. 1964. 16 p. Sw. cr. 8:—.

149. An anion-exchange method for the separation of P-32 activity in neutron-irradited biological material. By K. Samsahl. 1964. 10 p. Sw. cr. 8:—.

150. Inelastic neutron scattering cross sections of Cu^{63} and Cu^{65} in the energy region 0.7 to 1.4 MeV. By B. Holmqvist and T. Wiedling. 1964. 30 p. Sw. cr. 8:—.

151. Determination of magnesium in needle biopsy samples of muscle tissue by means of neutran activation analysis. By D. Brune and H. E. Sjöberg. 1964. 8 p. Sw. cr. 8:—.

152. Absolute E1 transition probabilities in the dofermed nuclei Yb^{177} and Hf^{179}. By Sven G. Malmskog. 1964. 21 p. Sw. cr. 8:—.

153. Measurements of burnout conditions for flow of boiling water in vertical 3-rod and 7-rod clusters. By K. M. Becker, G. Hernborg and J. E. Flinta. 1964. Sw. cr. 8:—.

Förteckning över publicerade AES-rapporter

1. Analys medelst gamma-spektrometri. Av D. Brune. 1961. 10 s. Kr 6:—.
2. Beströlningsförändringar och neutronatmosfär i reaktortrycktankar — några synpunkter. Av M. Grounes. 1962. 33 s. Kr 6:—.
3. Studium av sträckgränsen i mjukt stål. G. Östberg, R. Attermo. 1963. 17 s. Kr 6:—.
4. Teknisk upphandling inom reaktorområdet. Erik Jonson. 1963. 64 s. Kr. 8:—.

Additional copies available at the library of AB Atomenergi, Studsvik, Nyköping, Sweden. Transparent microcards of the reports are obtainable through the International Documentation Center, Tumba, Sweden.

EOS-tryckerierna, Stockholm 1964